MANEESH KUMAR SINGH

Dissecando o mecanismo de sinalização intracelular de cálcio e a caracterização do gene Pf1468 no parasita da malária humana *P. falciparum*

Tese apresentada ao Programa de Pós-Graduação em Biologia da Relação Patógeno-Hospedeiro do Instituto de Ciências Biomédicas da Universidade de São Paulo, para obtenção do Titulo de Doutor em Ciências.

São Paulo
2018

MANEESH KUMAR SINGH

Dissecting intracellular calcium signaling mechanism and characterization of Pf1468 gene in human malaria parasite *P. falciparum*

Tese apresentada ao Programa de Pós-Graduação em Biologia da Relação Patógeno-Hospedeiro do Instituto de Ciências Biomédicas da Universidade de São Paulo, para obtenção do Titulo de Doutor em Ciências.

Área de Concentração: Biologia da Relação Patógeno-Hospedeiro

Orientadora: Profª Drª Célia Regina da Silva Garcia

Versão original

São Paulo

2018

CATALOGAÇÃO NA PUBLICAÇÃO (CIP)
Serviço de Biblioteca e informação Biomédica
do Instituto de Ciências Biomédicas da Universidade de São Paulo

Ficha Catalográfica elaborada pelo(a) autor(a)

Singh, Maneesh Kumar

Dissecting intracellular calcium signaling mechanism and characterization of Pf1468 gene in human malaria parasite *P. falciparum* / Maneesh Kumar Singh; orientadora Célia Regina da Silva Garcia. -- São Paulo, 2018.

149 p.

Tese (Doutorado) -- Universidade de São Paulo, Instituto de Ciências Biomédicas.

1. Malaria. 2. Calcium. 3. Plasmodium. 4. Melatonin. 5. GPCR. I. da Silva Garcia, Célia Regina, orientador. II. Título.

UNIVERSIDADE DE SÃO PAULO
INSTITUTO DE CIÊNCIAS BIOMÉDICAS

Candidato: **Maneesh Kumar Singh**

Titulo da Dissertação/Tese: **Dissecting intracellular calcium signaling mechanism and characterization of Pf1468 gene in human malaria parasite *P. falciparum***

Orientadora: **Profa. Dra. Célia Regina da Silva Garcia**

A Comissão Julgadora dos trabalhos de Defesa da Dissertação de Mestrado/Tese de Doutorado, em sessão publica realizada a **26/11/2018**, considerou o(a) candidato(a):

(X) Aprovado(a) ( ) Reprovado(a)

Examinador(a): Assinatura: .....
Nome: Prof. Gerhard Wunderlich
Instituição: Instituto de Ciências Biomédicas, USP.

Examinador(a): Assinatura: .....
Nome: Prof. Marcus Fernandes de Oliveira
Instituição: Instituto de Bioquímica Médica, UFRJ.

Examinador(a): Assinatura: .....
Nome: Prof. Fábio Trindade Maranhão Costa
Instituição: Instituto de Biologia, UNICAMP.

Presidente: Assinatura: .....
Nome: Profª. Drª. Célia Regina da Silva Garcia
Instituição: Faculdade de Ciências Farmacêuticas, USP.

ICB USP

Cidade Universitária "Armando de Salles Oliveira", Butantã, São Paulo, SP · Av. Professor Lineu Prestes, 2415 - ICB III - 05508 000
Comissão de Ética em Pesquisa - Telefone (11) 3091-7733 - e-mail: cep@icb.usp.br

CERTIFICADO DE ISENÇÃO

Certificamos que o Protocolo CEP-ICB nº **772/2015** referente ao projeto intitulado: *"Sinalização de cálcio em parasitas da malária humana Plasmodium falciparum"* sob a responsabilidade de Maneesh Kumar Singh e orientação do(a) Prof.(a) Dr.(a) **Célia Regina da Silva Garcia,** do Departamento de Parasitologia, foi analisado pela **CEUA** - Comissão de Ética no Uso de Animais e pela **CEPSH** - Comissão de Ética em Pesquisa com Seres Humanos, tendo sido deliberado que o referido projeto não utilizará animais que estejam sob a égide da Lei nº 11.794, de 8 de outubro de 2008, nem envolverá procedimentos regulados pela Resolução CONEP nº 466 de 2012.

São Paulo, 06 de outubro de 2015

Prof. Dr. **Anderson de Sá Nunes**
Coordenador CEUA ICB/USP

Prof. Dr. **Paolo M. A. Zanotto**
Coordenador CEPSH ICB/USP

I dedicate this thesis to my loving wife Youvika and my parents.

ACKNOWLEDGEMENTS

One of the joys of completion is to look over the journey past and remember everyone who have helped and supported me along this long but fulfilling road.

Foremost, I would like to express my sincere gratitude to my thesis advisor ***Prof. Celia Regina da Silva Garcia*** *for her confidence and giving me the opportunity to work in her lab. Your excellent mentoring, optimistic in extracting positive outcome from experiments, continuous support and valuable suggestions were always a driving force to made this journey easier. Your ideas and knowledge in calcium signaling has been always an inspiration and this thesis would not have got this present shape without your intellectual ideas and support. Sometimes, we did not agree on same ideas even after long conversation but I believe it is good to have a different opinion to make a great team.*

My heartfelt thanks to ***Dr. Myna Nakabashi*** *for her endless support in both academics and administration. Her patience and support always kept my mind in peace to keep me focused in various lab projects.*

My sincere thanks to ***Prof. David Fidock****, Columbia University, USA) and* ***Dr. Rafael Guido****, USP, Sao Carlos for including me in their exciting projects. I am profoundly grateful to* ***Prof. Jude M. Przyborsky****, Marburg University, Germany with whom we have developed very exciting projects.*

I would like to express my sincere gratitude to the members of my PhD qualification ***Dr. Gerhard Wunderlich, Dr. Carsten Wrenger*** *and* ***Dr. Andréa Cristina Fogaça*** *for their wonderful suggestions that I greatly appreciate.*

I would also like to thank my former lab members ***Dr. Miriam Moraes*** *and* ***Dr. Giulliana Tessarin-Almeida*** *for their support, knowledge and cheering attitude to move the project forward. The same goes with* ***Dr. Alexandre Budu, Dr. Julio Levano-Garcia, Dr. Laura Cruz and Dr. Kenia Lopes*** *for sharing their invaluable knowledge and expertise.*

My special thanks to my lab colleagues ***Dr. Lucas Borges-Pereira, Mateus Pecenin, Pedro Pereira*** *and* ***Barbara Dias*** *for their tireless*

patience, kind support, laughs, cakes, football discussions, drinks and many more.

I would also like to thanks other former and current members ***Camila, Ricardo, Gabriella, Bruno, Fahyme, Amanda*** *and* ***Yayra*** *for their love and encouragement.*

I am also grateful to ***Dr. Andrew P. Thomas*** *and* ***Dr. Paula Bartlett*** *from NJMS-RHBS, Rutgers, USA, who gave me the opportunity to work in their lab and shared their expertise.*

Above all, I am grateful to my parents and my brother who always showed faith in me, kept me away from family responsibilities, and encouraged me to concentrate on my work. It would not have been possible to achieve this without their blessings and unflinching support.

I extend my gratitude to my wife ***Dr. Youvika Singh*** *for always encouraging me and having patience with me. Being in the research field she always understood my feeling, helped me to concentrate on completing this dissertation, and provided emotional support during the course of this work. My special gratitude to my in-laws for their loving support.*

I would also like to acknowledge Department of Parasitology administrative staff members ***Silvia, Dalva*** *and* ***Sabrina*** *for their help to ease the administrative formalities. At last, no research work of enduring value can be accomplished without the support of the funding agency. I acknowledge my gratitude to the* ***CAPES*** *for financially sustaining me during the whole period of research.*

Finally, I thank the GOD, whose blessings have enabled me to accomplish my work successfully.

Place: Sao Paulo, Brazil ***Maneesh Kumar Singh***

The good thing about science is that it's true whether or not you believe in it.

—Neil deGrasse Tyson

RESUMO

SINGH, M.K. Dissecting intracellular calcium signaling mechanism and characterization of Pf1468 gene in human malaria parasite *P. falciparum*. 2018. 149 f. Tese (Doutorado em: Departamento de Parasitologia) - Instituto de Ciências Biomédicas, Universidade de São Paulo, São Paul, 2018.

A sinalização intracelular do cálcio é fundamental para o crescimento do parasita da malária humana *P. falciparum* e para a transmissão da doença. A presença de distintas organelas para armazenamento de cálcio indica a coordenação mútua para a homeostase do íon durante o crescimento do parasita. O aumento do cálcio citosólico durante o ciclo assexuado regula muitos eventos *downstream*, especialmente a saída e a invasão do parasita. No entanto, nosso entendimento atual é limitado aos eventos upstream relacionados a flutuações de cálcio e aos eventos que iniciam as cascatas de sinalização durante a saída ou invasão do parasita. Já foram descobertas proteínas semelhantes a GPCRs no genoma do *P. falciparum*, mas a caracterização funcional ainda estava faltando. No presente estudo, demonstramos que o *P. falciparum* percebe a mudança extracelular de K^+ no microambiente por uma das proteínas semelhantes a GPCR, PfSR25, e desencadeia o aumento do cálcio citosólico. Parasitas *knockout* PfSR25 foram incapazes de responder a mudança na concentração de K^+, sugerindo fortemente que PfSR25 seja um sensor de potássio. Em estudo paralelo, descobrimos que o efluxo de cálcio citosólico no parasita também é atribuído ao vacúolo alimentar. O PfCRT, um transportador presente na membrana do vacúolo alimentar, é fundamental no efluxo de cálcio e a mutação nesta proteína que levam à resistência a cloroquina em parasitas também afeta o efluxo de cálcio citosólico. Por outro lado, investigamos e caracterizamos uma nova proteína em *P. falciparum*, PfMel, que é modulada por melatonina. A marcação de PfMel com sonda de proteína fluorescente indicou a sua localização nuclear no ciclo parasitário intraeritrocítico. Nós descobrimos que o *knocking down* condicional de PfMel levou a incapacidade dos parasitas de sicronizar em cultura na presença da melatonina. Simultaneamente, os parasitas que expressam menos PfMel têm redução significativa no efluxo intracelular de Ca^{2+} induzido pela melatonina.

Palavras-chave: *Plasmodium*, Malária, GPCR, Calcio, Melatonina

ABSTRACT

SINGH, M.K. Dissecting intracellular calcium signaling mechanism and characterization of Pf1468 gene in human malaria parasite *P. falciparum* 2018. 149 p. Ph.D. thesis (Dapartment of Parasitology) - Instituto de Ciências Biomédicas, Universidade de São Paulo, São Paulo, 2018.

Intracellular calcium signaling is fundamental for human malaria parasite *P. falciparum* growth and disease transmission. Presence of distinct calcium storage organelle indicates the mutual coordination for calcium homeostasis during parasite growth. Cytosolic calcium increase in asexual cycle regulates many downstream events specially the parasite egress and invasion. However, our current understanding is limited to the upstream of cytosolic calcium fluctuation and the events initiating the signaling cascades during parasite egress or invasion. Finding of GPCR-like proteins in *P. falciparum* genome was already revealed but the functional characterization was still lacking. In this study, we have demonstrated that *P. falciparum* perceives the extracellular change in K^+-microenvironment by one of the GPCR-like protein, PfSR25, and trigger the cytosolic calcium increase. The PfSR25 knockout parasites were unable to respond with change in K^+ concentration, strongly suggesting PfSR25 as potential potassium sensing candidate. In a parallel study, we found that cytosolic calcium efflux in the parasite is also attributed by the food vacuole. The PfCRT, a transporter present on the food vacuole membrane is fundamental in calcium efflux and mutations that lead to chloroquine resistance in parasites also affect the cytosolic calcium efflux. On the other hand, we have investigated and characterized a novel protein PfMel in *P. falciparum* that is modulated by melatonin. Tagging the PfMel with fluorescent protein probe indicated a nuclear localization in parasite intraerythrocytic cycle. We found that conditionally knocking down the PfMel, parasites were unable to synchronize with melatonin in the culture. Simultaneously, parasites expressing less PfMel have significant reduction in the intracellular Ca^{2+} efflux induced by melatonin.

Keywords: *Plasmodium,* Malaria, GPCR, Calcium, Signaling, Melatonin

LIST OF FIGURES

LIST OF TABLES

TABLE OF CONTENTS

1 INTRODUCTION

1.1 History and origin of malaria

Malaria is one of the most lethal forms of infectious disease to humans, caused by apicomplexan protozoa of genus *Plasmodium*. The five *Plasmodium* species - *P. falciparum, P. vivax, P. ovale*, *P. malariae* and the monkey malaria parasite *P. knowlesi* are known to transmit from human to human (Nadjm and Behrens 2012). Despite the increasing concern of *P. vivax* infection (Galinski and Barnwell 2008), *P. falciparum* remains the most lethal form in the malaria endemic areas especially in sub-Saharan Africa and Asia. The related pathogen *Toxoplasma gondii* causes opportunistic infection in immunocompromised individuals (Sibley, Khan et al. 2009). Although the origin of *P. falciparum* was controversial until recently a single-genome amplification study suggested a gorilla origin of the parasite. This study was different from the previously reported chimpanzee, pygmy chimpanzee (bonobo) or ancient human origin (Liu, Li et al. 2010). *P. vivax* was most likely originated from African gorillas and chimpanzees (Liu, Li et al. 2014). Dormant hypnozoites of both *P. vivax* and *P. ovale* present inside liver cells and symptomatic relapse occurs months later after the initial infection. *P. malariae* exhibits mild symptoms compared to other species and less prevalent. However, *P. malariae* infection induces immune complexes in the kidney and nephrotic syndrome has also been reported (Collins and Jeffery 2007).

The presence of malaria parasites dates back millions year ago when scientists discovered completely preserved mosquito fossils (Poinar 2005). Many ancient civilizations like Assyrian, Chinese, Egyptian, Greek, Indian and Roman documented the malaria-like symptoms in sick

people from the period of 3000 to 200 BC (Cox 2002). Hippocrates of Greece in the 5th century BC described the disease in details and claimed its origin from marshes and swamps. Later, Chinese scholars in mid-300 BC reported the epidemic disease with fever relapse associated with enlarged spleens. At the end of 18th century, the French surgeon Alphonse Laveran discovered that malaria disease was of parasite origin. Later, Patrick Manson and Ronald Ross independently found that mosquito was a transmission vector for malaria (Cox 2002). For their discovery, both Ronald Ross and Alphonse Laveran were awarded the Nobel Prize in 1902 and 1907 respectively.

1.2 Geographical distribution and global health

Malaria is widespread in the tropical and sub-tropical regions. Combined epidemiological, geographic, and demographic data from the World Health Organization in 2016 reported that more than 91 countries are endemic for malaria and approximately 3 billion people were at risk **(Figure 1).** However, this number is down from the WHO-2000 report due to global malaria intervention efforts. Despite these efforts, there were more than 200 million new cases of malaria and more than 400 thousand deaths were reported in 2015 (WHO Malaria Report 2016). More than 90% of the fatalities were reported in sub-Saharan Africa especially in pregnant women and children below 5 years of age.

In South America, most cases of malaria are reported in vicinity to the Amazon rain forest, accounting for more than 80% cases in the continent (**Figure 2)** (Recht, Siqueira et al. 2017). However, in some countries like Colombia, Ecuador and Venezuela, the percentage of *Plasmodium falciparum* related cases are growing where initially *Plasmodium vivax* related cases were high. A similar pattern was seen in Honduras and Peru where the ratio of *P.*

falciparum versus *P. vivax* infections were enlarged significantly over the years (PAHO/WHO, 2017).

In Brazil, the prevalence of *P. falciparum* and *P. vivax* cases were similar until the late 1980s. Since 1980, *P. falciparum* related malaria progressively declined while *P. vivax* increased and became predominant in the country accounting for over 90% of malaria episodes in 2011 (Siqueira, Mesones-Lapouble et al. 2016).

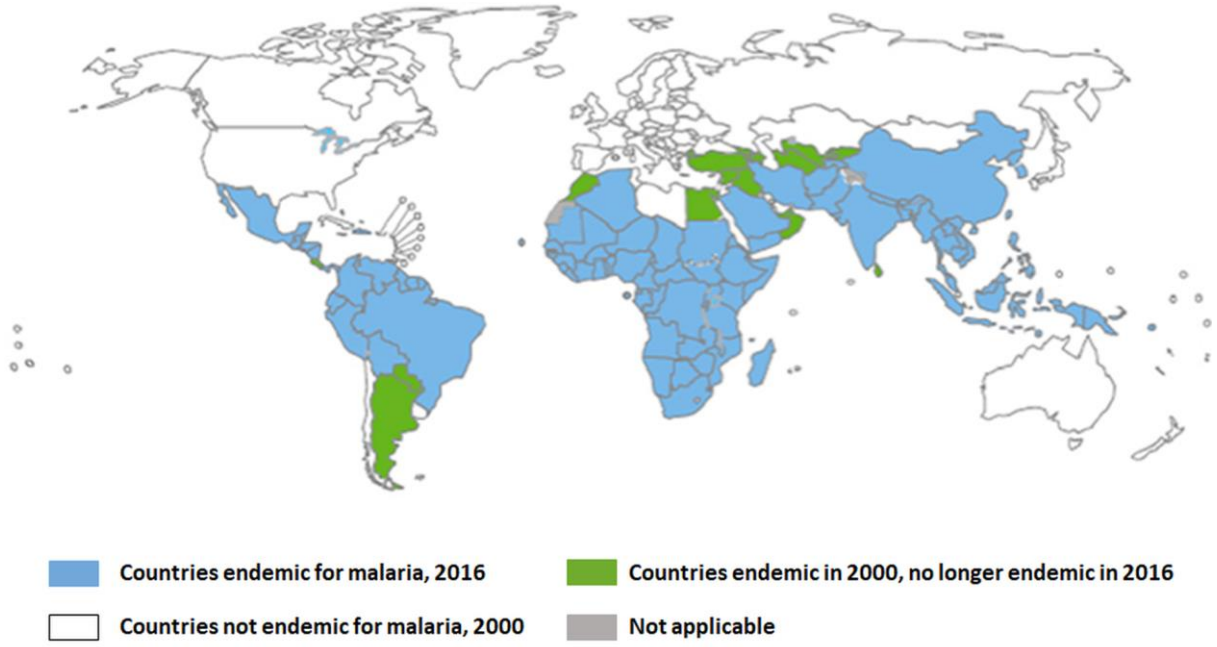

Figure 1: Worldwide malaria dispersal in 2000 and 2016.

Blue color areas representing the countries still endemic to malaria while green areas showing that the countries that had malaria in year 2000 are no longer endemic since 2016. While white color representing the countries are no longer endemic to malaria since 2000. (WHO - World Malaria Report, 2016.)

Figure 2: Malaria distribution in South American countries.

Malaria is widespread in South American countries near the Amazon River basin. Most affected countries are Brazil followed by Colombia, Peru and Venezuela (affected areas are shown in green). Modified from Recht, Siqueira et al. 2017.

1.3 Malaria pathophysiology and prevention

Clinical manifestations and pathology of malaria is associated with blood stage parasites, while the liver and gametocyte stages are rarely exhibit any disease symptoms (Mackintosh, Beeson et al. 2004). The periodicity of malarial paroxysm follows the multiple of 24 hours *i.e.* 24 h for *P. knowlesi,* 48 h for *P. vivax* and *P. falciparum* while 72 h for *P. malariae* (Mideo, Reece et al. 2013). However, life-threatening malaria is associated mostly with *P. falciparum* infection but other non-falciparum infections like *P. vivax* may cause complications as well. The periodic

rupture of red blood cells (RBCs) releases erythrocyte debris and parasite's metabolic products, which induces the host response causing malaria disease symptoms. Infected patients experience chills, fever, often accompanied with nausea, headache and fatigue (White, Pukrittayakamee et al. 2014).

The growing parasite modulated the erythrocyte surface by exporting and recruiting antigenic proteins. Therefore, the infected erythrocytes have increased adhesiveness to the microvasculature of many organs (cytoadherence) (Udeinya, Schmidt et al. 1981) such as with endothelial cells (sequestration) or to uninfected RBCs (rosetting) and with other infected RBC (autoagglutination) (Udomsangpetch, Wahlin et al. 1989). Current evidence suggested that the cytoadherence is attributed by an antigenically diverse protein family - erythrocyte membrane protein-1 (PfEMP1) (Smith, Chitnis et al. 1995). It is now evident that infected parasites can bind to various endothelial receptors including thrombospondin, CD36, CD31, ICAM-1, vascular cell adhesion molecule 1 (VCAM1), chondroitin sulfate A (CSA), P-selectins, the endothelial protein C receptor (EPCR), and neural cell adhesion molecule (Craig, Khairul et al. 2012). Unhindered growth results in higher parasite load and ultimately reducing the blood flow, lower oxygen supply (hypoxia) and stimulating cytokines production; together these factors may favor revolution to severe malaria (Taylor, Fu et al 2004, Dondrop, Ince et al. 2008).

A pro-inflammatory cytokine, tumor necrosis factor (TNF) levels have been reported to be changed in viral and bacterial infection (Grau, Taylor et al. 1989). Higher concentration of TNF in plasma is also associated with malarial pathology (Karunaweera, Grau et al. 1992). A recent study on comparative plasma cytokine levels showed higher concentration of cytokines (IL-2, IL-6, IL-6, IL-10, TNF and IFN-γ) in primary and recurrent *P. vivax* infected patients when equated to healthy endemic controls (Chaves, da Costa et al. 2016). Higher plasma TNF

levels in hypoglycemic patients caused the obstruction in blood circulation due to cytoadherence inside the blood vessels. The cells aggregation in blood vessel promotes anaerobic glycolysis that produces large amount of lactic acid causing acidosis in infected patients (Dondorp, Chau et al. 2004). TNF was also reported to modulate the adhesive properties of leucocytes and of endothelial cells (Grau, Piguet et al. 1989) and inhibiting the TNF production significantly reduced the cytoadherence of infected erythrocytes (Wassmer, Cianciolo et al. 2006, Chakravorty, Hughes et al. 2008). Interestingly, the molecular mechanism of TNF signaling and its components are yet to be discovered in *P. falciparum*. However, a fluctuation in the cytokine level in host plasma is associated with TNF during malaria pathology (Mendonca, Souza et al. 2014). In *P. vivax* infection, it was indicated that ligand-receptor (TNF-TNFR1) interaction induced apoptosis in CD4 T cells (Hojo-Souza, Pereira et al. 2015). Recently, it was also reported that TNF reduced the *P. falciparum* proliferation in culture by a downstream Ca^{2+}-cAMP signaling pathway (Cruz, Wu et al. 2016).

There are only a limited number of drugs available to treat malaria and the emerging drug resistant *P. falciparum* strains in the South-East Asia is rapidly compromising the malaria prevention strategy (Bloland 2001). Most widely used antimalarial drugs are divided into six classes based on their site of actions i.e. 4-aminoquinolines, 8-aminoquinolines, artemisinins, antifolates, arylamino alcohols and respiratory chain inhibitors (Cui, Mharakurwa et al. 2015). Chloroquine (4-aminoquinolines) is gold standard drug to treat malaria but prolonged use of chloroquine (CQ) resulted in emergence of resistant parasites making it less effective in many countries (Wellems, Panton et al. 1990, Fidock, Nomura et al. 2000, Ridley 2002). In most cases, CQ resistance is caused by a mutation in the chloroquine resistance transporter (PfCRT) and multidrug resistant protein (PfMDR1), both of which localize to the digestive vacuole membrane

of *P. falciparum* (Fidock, Nomura et al. 2000, Veiga, Dhingra et al. 2016). The digestive vacuole (DV) is a bilayer membrane compartment in *P. falciparum* where host hemoglobin is metabolized and free heme is sequestered as an inert crystal called hemozoin (Hz) (Kapishnikov, Weiner et al. 2013). The world health organization has recommended the artemisinin-based combination therapy (ACT) for severe and complicated malaria in the endemic countries. The emergence of resistant parasite population for artemisinin (ART) based drugs further limits the malaria prevention strategy (Ashley, Dhorda et al. 2014). Several efforts are in progress to find the new compounds to counteract the parasite growth in erythrocytes (Schuck, Ferreira et al. 2013, Sharma, Santos et al. 2013).

1.4 Life cycle of Plasmodium

The *P. falciparum* has a complex life cycle and is divided into well-defined developmental stages and are specialized to alternate between insect vector and vertebrate host. The life cycle of *P. falciparum* is divided into sexual and asexual phase. The sexual phase completes inside the female *Anopheles* mosquito vector and the asexual phase takes place inside the vertebrate host body (Cowman, Healer et al. 2016).

1.4.1 Parasite life cycle in vertebrate host

P. falciparum transmission to the vertebrate host begins when sporozoites are inoculated by an infected female Anopheles mosquito into the subcutaneous tissue. These sporozoites traverse through the tissue system and enter into host blood circulation (Amino, Giovannini et al. 2008). Inside the vertebrate host, the parasite life cycle is divided into the exoerythrocytic (hepatocytes) and the intraerythrocytic (erythrocyte) phase. During the exoerythrocytic phase, sporozoites invade the liver hepatocytes where, they surround itself by a parasitophorous vacuole

membrane (PVM) and grow within. Inside liver cells, parasites differentiate into schizont that took approximately 6-7 days and the infected person did not develop any symptoms (Sturm, Amino et al. 2006). The circumsporozoite protein (CSP) and sporozoite surface molecule thrombospondin-related adhesive proteins (TRAP) mediates liver cell invasion (Rodrigues, Hannus et al. 2008). The receptor for these domains is recognized as heparin sulfate proteoglycans (HSPG) on the basolateral domain of the plasma membrane of hepatocytes (Frevert, Sinnis et al. 1993). After a week, thousands of invasive merozoites are released from the hepatocytes into circulation and infect the red blood cells (RBCs) to initiate the asexual or intraerythrocytic phase of development. Asexual parasites undergoes through different growth phases that can be differentiated as ring, trophozoite and schizont (Bannister, Hopkins et al. 2000). A single schizont can divided into 16-32 new merozoites and after rupturing the RBCs (egress), parasites invade new RBCs (Invasion) **(Figure 3)**. Clinical manifestations appear during the intraerythrocytic phase and febrile waves after every 48 hours caused by merozoite release and red blood cell lysis (Bannister and Mitchell 2003).

Interestingly, few blood-stage parasites differentiate into transmissible male and female gametocytes (gametocytogenesis) (Carter and Miller 1979). The molecular events lead to gametocytogenesis was poorly understood and it was thought that various factors such as stress due to increase parasitemia, drug pressure and rising immunity triggered the gametocytogenesis (Sinden 1983). Recently, it was found that the activation of the transcription factor AP2-G is necessary for gametocyte formation and recognized as first step of sexual differentiation. Expression of AP2-G acted as a transcriptional control that triggers the commitment towards gametocytogenesis (Kafsack, Rovira-Graells et al. 2014). Two epigenetic factors - histone deacetylase 2 (HDA2) and heterochromatin protein 1 (HP1) suppress the *ap2-g* expression to

hinder gametocyte differentiation (Brancucci, Bertschi et al. 2014, Coleman, Skillman et al. 2014). It was shown that host derived serum factor acts upstream to AP2-G and controls the sexual commitment. Human serum contains lysophosphatidylcholine (LysoPC) that actively repress *P. falciparum* sexual commitment. During asexual cycle, parasites metabolize the LysoPC to synthesize choline and fatty acids results in reduction of LysoPC level that activate sexual differentiation (Brancucci, Gerdt et al. 2017).

1.4.2 Parasite life cycle in mosquito vector

Plasmodium undergoes obligatory sexual phase inside the mosquito vector, which is divided into (i) gametocytogenesis (described earlier), (ii) gametogenesis and (iii) zygote formation. Female *Anopheles* mosquito ingests both male and female gametocytes from the infected person during blood meal. Inside the midgut, parasites sense changes in pH from 7.4 to 8.0-8.2 and sudden temperature drop from 39°C (vertebrate host) to 20°C.

These changes activate the gametocytes to round up and shed the erythrocyte membrane (Nijhout and Carter 1978, Sinden 1983). Later, it was found that exposure to xanthurenic acid stimulate exflagellation in *P. berghei* (Billker, Shaw et al. 1997, Billker, Lindo et al. 1998). Together these factors trigger the gametogenesis where ingested gametocytes mature into macrogametes and flagellated microgametes. The flagellated microgametes fertilize the macrogametes and form diploid zygotes that develop into ookinetes. The ookinetes penetrate and traverse the mid-gut wall and form the encysted oocyst structure at the outer surface of the mid-gut. Ookinetes multiply into thousands of haploid sporozoites and after 10-15 days oocyst rupture to release the sporozoites into body cavity of mosquito. These sporozoites then travel to the salivary glands where, only few hundreds of sprozoites manage to invade the salivary glands.

Various proteins are thought to be involved during the process that occurs when parasite penetrates the salivary gland, to name few of them: circumsporozoite (CS) proteins (Kojin, Costa-da-Silva et al. 2016), thrombospondin related adhesive protein (TRAP) (Robson, Frevert et al. 1995) and merozoite adhesive erythrocyte binding ligand (MAEBL) (Kariu, Yuda et al. 2002). Interestingly, an oocyst released sporozoites have poor hepatocyte invasion ability than sporozites present in the salivary gland, thus suggesting that sporozoites undergo maturation process.

1.5 Erythrocyte invasion and asexual development

Blood stage parasites multiply and expand in numbers by passing through various developmental phases and ultimately releasing more invasive parasites i.e. merozoites (Dvorak, Miller et al. 1975). These free parasite forms must invade the new RBC to sustain the infection. The parasite egress and invasion is highly coordinated and sophisticated process and carried out by an arsenal of proteins secreted by parasite's apical organelles. These apical organelles are known as rhoptries, microneme, exoneme (Bannister, Hopkins et al. 2000, Yeoh, O'Donnell et al. 2007) and dense granules along with conventional eukaryotic organelles.

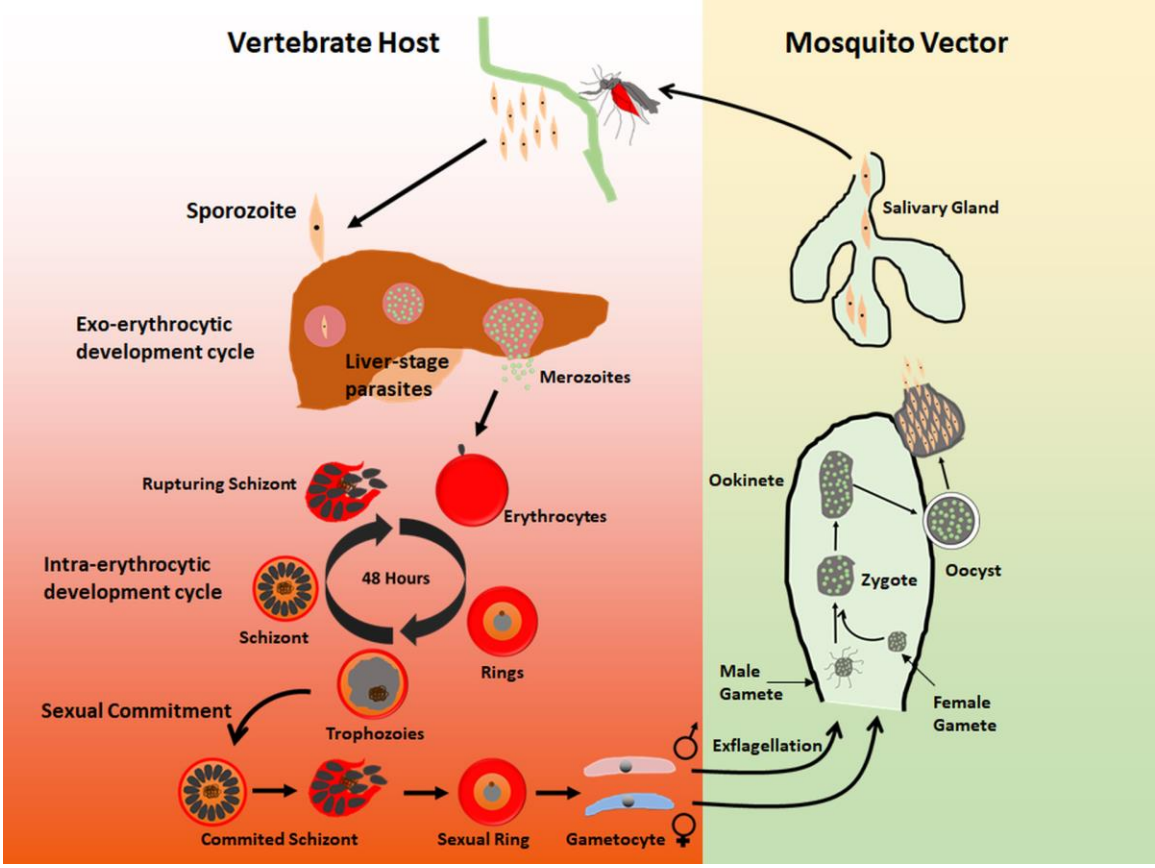

Figure 3: Life cycle of *P. falciparum* in host and vector.

Sporozoites are injected into host dermis and enter the vasculature from where they reach the liver by passing through the Kupffer cells followed by hepatocytes infection. Parasitophorous vacuole membrane is formed immediately after invasion and parasites undergo schizogony to form thousands of merozoites that rupture via merosomes and are released in the circulation to start the intraerythrocytic phase. Some parasites sexually differentiate into gametocytes and are taken up by mosquitos to start the sexual phase inside the insect midgut. Modified from (Josling and Llinas 2015).

Invasion includes the host erythrocyte recognition by the parasite following the resealing of the RBC membrane. This whole process is completed in less than a minute to avoid host immune response against parasites variant surface antigens (VSAs). The invasion process comprises (i) adhesion, where a primary contact between merozoite and the erythrocyte surface

occurs; (ii) reorientation, where the merozoite's apical end reorients towards the RBC surface so that apical end of the merozoite juxtapose to the RBC membrane; (iii) tight junction formation, where high affinity interaction between the parasite surface proteins with the erythrocyte surface occurs; and (iv) invasion and resealing of the erythrocyte membrane as shown in **Figure 4** (Cowman, Berry et al. 2012).

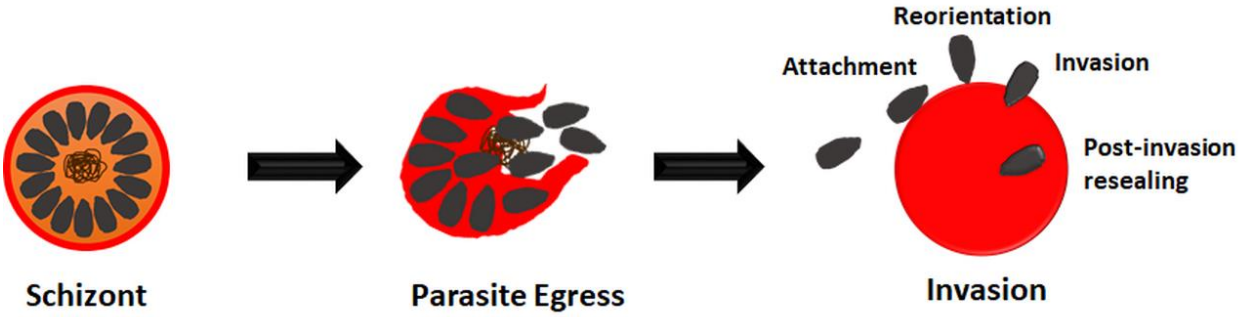

Figure 4: Parasite egress and steps involved in merozoite invasion.

Stepwise demonstration from egress to invasion and critical steps that takes place by free merozoites from initial attachment to its final entry in red blood cells (Image adapted from Cowman and Crabb, 2006).

1.6 Signaling in the malaria parasite

Cells have adapted the unique ways to communicate with each other to maintain the cellular homeostasis and development. Distinct external and internal signaling molecules trigger the signaling cascade, which is eventually converted into a cellular response. Malaria parasites development switches from vector to host and faces adverse environmental paradox. Transition from vector to host and from one to another developmental stage is a highly complex process and

is most likely regulated by extensive signaling pathways. Our knowledge of signaling cascades that leads to parasite morphogenesis is very limited although various components such as protein kinases, nucleotide cyclases and Ca^{2+} signaling have identified. Genome availability of *P. falciparum* has allowed exploring extensively to search for new molecules to get more access to the biological function of specific genes (Gardner, Hall et al. 2002). Several different key proteases are involved in parasite egress from red blood cells and expose the merozoites in host circulation system. Temporal processing of the papain-like cysteine peptidases SERA proteins by a subtilisin-like serine protease SUB1 in parasitophorous vacuole (PV) is necessary for asexual merozoites egress (Yeoh, O'Donnell et al. 2007, Agarwal, Singh et al. 2013) and sporozoites egress in mosquito (Aly and Matuschewski 2005). Surprisingly, many parasite's proteins and kinases are absent in other organisms causing a daunting task to map the signaling cascades and their regulation. Meanwhile, it will also give an advantage for new drugs screening. Though earlier attempts to eradicate this deadliest disease have been failed due to emergence of drug resistance by the parasites, it will be very interesting to study the signaling mechanisms which control the parasite life cycle may lead to find novel drugs to prevent the new infection.

1.6.1 Calcium signaling: General perspective

Binding of Ca^{2+} to effector proteins provides the driving force for the conformational changes and permits them to regulate multiple cellular events. The importance of Ca^{2+} has been shown in cell excitability, exocytosis, motility, apoptosis, fertilization, muscle contraction and transcription (Berridge, Lipp et al. 2000).

The Ca^{2+} signaling starts with the activation of phospholipase C (PLC) by G protein-coupled receptor (GPCR) or receptor tyrosine kinase which further hydrolyses the membrane bound phospholipid phosphatidylinositol-4,5-bisphosphate (PIP_2) to inositol-1,4,5-triphosphate

(IP_3) and diacylglycerol (DAG). IP_3 diffuse to the cytoplasm and bind to IP_3 receptor (IP_3R), which is Ca^{2+} channel on the ER membrane to release Ca^{2+}. Sudden influx of $[Ca^{2+}]_{cyt}$ triggers various kinases and proteins to initiate signaling cascade. The majority of cellular proteins including several protein kinases adapted to bind Ca^{2+} in order to perform specific cell functions; probably this is why Ca^{2+} is important for cell survival. The most important factor governing the Ca^{2+} signaling is relied on the speed, amplitude and spatio-temporal pattern emerged from the wide components of Ca^{2+} signaling molecules (Berridge, Lipp et al. 2000).

1.6.1.1 Calcium homeostasis in *P. falciparum*

In eukaryotes, intra- and extra-cellular cellular Ca^{2+} concentration has been reported to nanomolar and millimolar respectively and uses large amount of energy to maintain homeostasis between these boundaries (Clapham 2007). Homeostasis is achieved by various Ca^{2+} pumps *i.e.* the sarcoendoplasmic reticular Ca^{2+} ATPase (SERCA) and the plasma membrane Ca^{2+} ATPases (PMCA). Other mechanisms employ Na^+/Ca^{2+} and Na^+/Ca^{2+}-K^+ exchanger present on the host plasma membrane signifying the importance of Ca^{2+} in cell development.

Parasites have tight control over intracellular calcium $[Ca^{2+}]_{cyt}$ homeostasis but precise mechanism is still poorly understood because the canonical Ca^{2+} channels, transporters and regulators are not identified. Biological function of specific genes and their regulation were relatively well characterized in another Apicomplexan parasite *T. gondii* and similar approaches have been applied subsequently to *Plasmodium*. Intracellular growth of *T. gondii* in the host cell is separated by formation of the PVM, which is permeable to small diffusible ions and Ca^{2+} to maintain the cellular homeostasis (Pingret, Millot et al. 1996). This group have monitor the Ca^{2+} concentration inside the PV and shown that rise of Ca^{2+} in PV leads to egress of *Toxoplasma gondii*. Likewise, *P. falciparum* maintains nanomolar cytosolic Ca^{2+} at resting state and holds

micromolar Ca^{2+} in the PV (Garcia 1999). The concentration of Ca^{2+} in PV was measured by allowing the parasites to invade the RBC in the presence of a Ca^{2+} indicator dye Fluo-3AM. It was found that parasites accumulate micromolar range of Ca^{2+} in PV which was sufficient to support the growth. Even a transient drop in Ca^{2+} concentration for very short period of time was enough to affect the parasite growth as well as the invasion (Gazarini, Thomas et al. 2003). Hotta *et al* have also reported that *P. falciparum* exhibits a thapsigargin (THG) sensitive Ca^{2+} pool and releases Ca^{2+} from ER by inhibiting Ca^{2+}-ATPase (SERCA) **(Figure 5)**. Later, it was confirmed that THG only affects the ER but not the acidic organelle DV and depleting acidic pool by either monensin or nigericin did not prevented THG to release Ca^{2+} (Varotti, Beraldo et al. 2003). Apart from ER and acidic pools, it was shown that mitochondria of malaria parasite are able to reversibly accumulate part of THG-induced cytosolic Ca^{2+} thus indicating the participation of mitochondria in Ca^{2+} homeostasis (Gazarini and Garcia 2004).

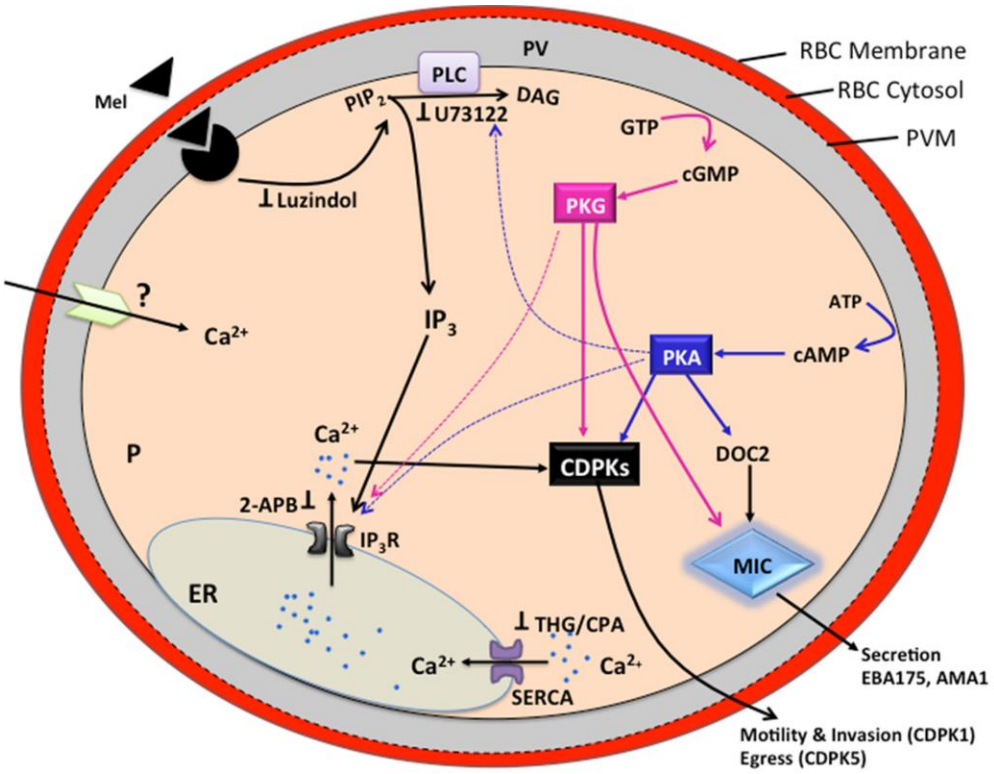

Figure 5: Signaling pathways in *P. falciparum*.

Activation of PLC leads to breakdown of PIP2 into DAG and IP_3. IP_3 stimulates IP_3R present on ER and efflux Ca^{2+} in parasite cytosol. Distinctly, activation of PKA and PKG also activate cytosolic Ca^{2+} release. Temporal rise in intracellular Ca^{2+} activates parasites proteins that facilitate erythrocyte rupture and release of merozoites. 2-APB: 2-Aminoethoxydiphenyl borate; Ca^{2+}: Calcium; CDPK: Ca^{2+}-dependent protein kinase; CPA: Cyclopiazonic acid; ER: Endoplasmic reticulum; DOC2: Double C2 domain; MIC: Microneme P: Parasite; PLC: Phospholipase C; PV: Parasitophorous vacuole; PVM: Parasitophorous vacuole membrane; THG: Thapsigargin.

Despite all these evidences, the putative Ca^{2+} pumps and channels are not identified. Until now, only one sarcoendoplasmic reticulum Ca^{2+}-ATPase PfATP6 was identified in *P. falciparum*, which is sensitive to artemisinin and thapsigargin (Krishna, Woodrow et al. 2001, Eckstein-Ludwig, Webb et al. 2003). A canonical non-SERCA sub-class of Golgi-like Ca^{2+}-ATPase (PfATP4) and a single Ca^{2+}/H^{+} exchanger (PfCHA) were found in *Plasmodium* (Nagamune and Sibley 2006, Prole and Taylor 2011). However, Na^{+}/Ca^{2+} exchangers,

homologues of PMCA Ca^{2+}-ATPases and voltage-dependent Ca^{2+} channels could not be identified in apicomplexans. Pharmacological evidence suggests that *Plasmodium* does exhibit the IP_3 and ryanodine receptor (RyR) mediated $[Ca^{2+}]_{cyt}$ signaling although no canonical IP_3R or RyR have been identified in *Plasmodium* genome (Jones, Cottingham et al. 2009, Alves, Bartlett et al. 2011). It suggests that IP_3R is expressed in *Plasmodium* but probably with a highly divergent gene sequence compared with their higher eukaryotic counterpart. Unlike the eukaryotic system, where calmodulin (CaM) is the most ubiquitous Ca^{2+} sensor containing four EF-hand motifs, only one CaM gene is identified in *Plasmodium.* Instead, a large repertoire of other Ca^{2+}-dependent or –binding proteins with EF hands such as CDPKs (Nagamune, Moreno et al. 2008), protein phosphatases including calcineurin (Dobson, May et al. 1999, Kumar, Musiyenko et al. 2004) are present.

1.6.1.2 Calcium signaling in *P. falciparum* development

Malaria parasites are genetically closer to dinoflagellates and ciliates rather than yeast and higher eukaryotes *i.e.* plants and animals which make them unique in terms of their Ca^{2+} signaling pattern when compared to other eukaryotes although they often contain some plant-like unique features (Baldauf 2003). The parasite senses the environmental changes and responds accordingly, which relies on intracellular signaling. Secondary messengers are important component within the cell during integration and transmission of signal. In *Plasmodium*, apart from Ca^{2+} ions, other secondary messengers such as cyclic nucleotides and phospholipid-derived molecules were also identified. Their stimulation leads to activation of many cellular functions. Studies in apicomplexans have shown the importance of Ca^{2+} in parasite growth and survival and its activation from a vast signaling network to control the malaria pathogenesis and disease transmission.

In *T. gondii*, rise in Ca^{2+} concentration is related to substantial morphological changes, rapid egress and secretion of invasive proteins (Arrizabalaga and Boothroyd 2004). In *Plasmodium*, Ca^{2+} controls various critical events such as secretion of adhesins, egress, invasion and gliding motility (Garcia, de Azevedo et al. 2008). A rapid and transient rise in $[Ca^{2+}]_{cyt}$ was seen in *P. falciparum* mature schizont prior to egress and the released free merozoites maintained the elevated Ca^{2+} until they bind to the host membrane (Singh, Alam et al. 2010, Agarwal, Singh et al. 2013, Glushakova, Lizunov et al. 2013). cGMP-dependent Ca^{2+} signaling was studied in *P. falciparum* and it was found that inhibition of protein kinase G (PKG) prevent merozoite egress; however, blocking cGMP phosphodiesterase with zaprinast triggers PKG-mediated premature egress of parasites (Taylor, McRobert et al. 2008, Collins, Hackett et al. 2013). Downstream to PKG, $[Ca^{2+}]_{cyt}$ chelation with BAPTA-AM or inhibition of PLC by U73122 severely disrupts the merozoite egress by inhibition of PfSERA5 processing by PfSUB1 in PV due to its impaired discharge from exonemes (Agarwal, Singh et al. 2013). A recent study has been shown the Ca^{2+}-dependent permeabilization and membranolytic activity of perforin like protein-1 (PLP1) plays a significant role in host cell egress (Garg, Agarwal et al. 2013). Unlike higher eukaryotic organisms, apicomplexans possess plant-like Ca^{2+}-dependent protein kinases (CDPKs) having Ca^{2+}-binding EF-hand motif, identified as indispensable in parasite egress and invasion. In a conditional knockdown study, FKPBP destabilizing domain (DD) was fused to PfCDPK5 and expressed as stable fusion protein PfCDPK5-DD in the presence of a rescue ligand shield-1. In the absence of shield-1, PfCDPK5-DD protein rapidly degrades and parasites were arrested as segmented schizont, while PfSUB1 discharge was unaffected (Dvorin, Martyn et al. 2010). Apart from egress, $[Ca^{2+}]_{cyt}$ has been also implicated in invasion and Ca^{2+} influx was seen in live cell imaging of invading merozoites just before the internalization (Weiss, Gilson et al. 2015). It also

revealed that low K^+ acts as natural extracellular signal and triggers rise in cytosolic Ca^{2+} in the PLC mediated pathway. The rise in cytosolic Ca^{2+} trigger the microneme discharge of EBA175 and initiates invasion (Singh, Alam et al. 2010). Later, it was shown that Ca^{2+}-dependent EBA175 secretion requires PfDOC2 and knocking it down impairs the merozoite invasion and block micronemal secretion (Farrell, Thirugnanam et al. 2012). Another protein, calcineurin (CnA: catalytic domain and CnB: regulatory domain) has been shown to affect invasion. Depleting either CnA or CnB has no effect on asexual development but exhibit very strong effect in invasion especially merozoite attachment to erythrocyte membrane (Paul, Saha et al. 2015). Role of other Ca^{2+}-dependent kinases such as PKB and CDPK1 is also studied and it has been thought that they can differentially phosphorylate the parasite's actomyosin motor to regulate the merozoite penetration in host erythrocyte (Green, Rees-Channer et al. 2008, Vaid, Thomas et al. 2008). Apart from that, Ca^{2+} ions also play role in cyclic nucleotide cAMP and cGMP mediated signaling events in diverse biological processes including merozoite invasion, discharge of secretory organelles, motility and invasion of ookinetes and sporozoits and sexual differentiation (**Figure 5)** (Gantt, Persson et al. 2000, Billker, Dechamps et al. 2004, Ono, Cabrita-Santos et al. 2008, Vaid, Thomas et al. 2008).

The evolutionary distance of parasites with higher eukaryotes made it difficult to identify the signaling events experimentally. The major restraint to establish the Ca^{2+} signaling network is halted by the fact that more than half of the *Plasmodium* genome is yet to be characterized. Another obstruction is the limitation of computational analysis to find the canonical Ca^{2+} signaling components in *Plasmodia.* Finding these Ca^{2+} transporters and Ca^{2+}/calmodulin dependent kinases might provide new insight to understand the pathogen biology and to identify the druggable targets for novel antimalarials.

1.6.2 Ionic fluctuation in *P. falciparum* development

Depending on their developmental stages, malaria parasites encounter extremely diverse environmental changes in the host (hepatocytes, blood plasma, erythrocyte cytosol etc.) and arthropod vector (in midgut and salivary glands etc.). Molecular mechanisms facilitating the parasites to sense the intra- and extra-cellular environments and respond accordingly are the key features for proliferation and transmission (Doerig, Baker et al. 2009).

Normally, blood plasma has high Na^+ and low K^+ ionic concentration while cytosol of red blood cell has high K^+ but low Na^+ concentration (Krishna and Ng 1989) **(Figure 6A)**. Infected parasite maturation leads to an alteration of the erythrocyte membrane permeability by inducing broad selective channels for uncharged or negatively charged solutes while actively maintained the transport of positive charged cation solutes. This phenomenon was described as the new permeability pathway (NPP) and is believed to participate in the uptake of several important nutrients, waste clearance, volume regulation and host cation remodeling **(Figure 6B)** (Ginsburg, Krugliak et al. 1983, Kirk, Horner et al. 1994, Staines, Powell et al. 2004). Role of ionic fluctuation in parasites was emphasized in *T. gondii*. When *T. gondii* tachyzoites experiences low K^+, a sharp rise in cytosolic Ca^{2+} was seen that activated the parasite motility and eventually egress (Moudy, Manning et al. 2001). It was also reported that exposing *P. berghei* and *P. yoelii* sporozoites to intracellular K^+ concentration enhances the parasite infectivity many folds in time and concentration dependent manner while the infectivity was decreased in presence of K^+ channel inhibitors (Kumar, Garcia et al. 2007). Similarly in *P. falciparum*, when merozoites were transferred from intracellular high K^+ to extracellular low K^+ environment, this shift causes a rise in cytosolic Ca^{2+} that triggered the sequential release of the

microneme and rhoptries to the merozoites surface enabling host receptor arrangement during invasion process **(Figure 6C)** (Singh, Alam et al. 2010).

A recent study has shown that a lower K^+ is not a necessary trigger for apical discharge as well as invasion (Pillai, Addo et al. 2013). More importantly, parasites exhibit a broad range of flexibility and probably sensing K^+ is one of them that could explain why they grew normally in high K^+ environment. For instance, *T. gondii* produces abscisic acid that controls the merozoite egress by triggering cytosolic Ca^{2+} (Nagamune, Hicks et al. 2008) and a similar rise in cytosolic Ca^{2+} was observed in *P. falciparum* prior to egress (Agarwal, Singh et al. 2013, Glushakova, Lizunov et al. 2013). Alternatively, *P. falciparum* also respond to extracellular ATP that causes rise in cytosolic Ca^{2+}. Nucleotide signaling is poorly known in *Plasmodium* although use of the purinergic receptor antagonists severely reduced the parasite invasion (Levano-Garcia, Dluzewski et al. 2010) indicating an alternative mode of signaling rather than the sole dependence of ionic fluctuation for invasion process.

However, how the malaria parasite senses the extracellular K^+ during asexual progression remains elusive until recently, when we reported that parasite G-protein coupled receptor (GPCR) *PfSR25* senses the switch from high to low K^+ and induce intracellular Ca^{2+} while *PfSR25* knockout (*PfSR25*$^-$) parasites were unable to respond for such switching (Moraes, Budu et al. 2017). Interestingly this is the only reported GPCR in any eukaryotic organism that is known to respond to changes in the environmental K^+ concentration **(Figure 6C)**.

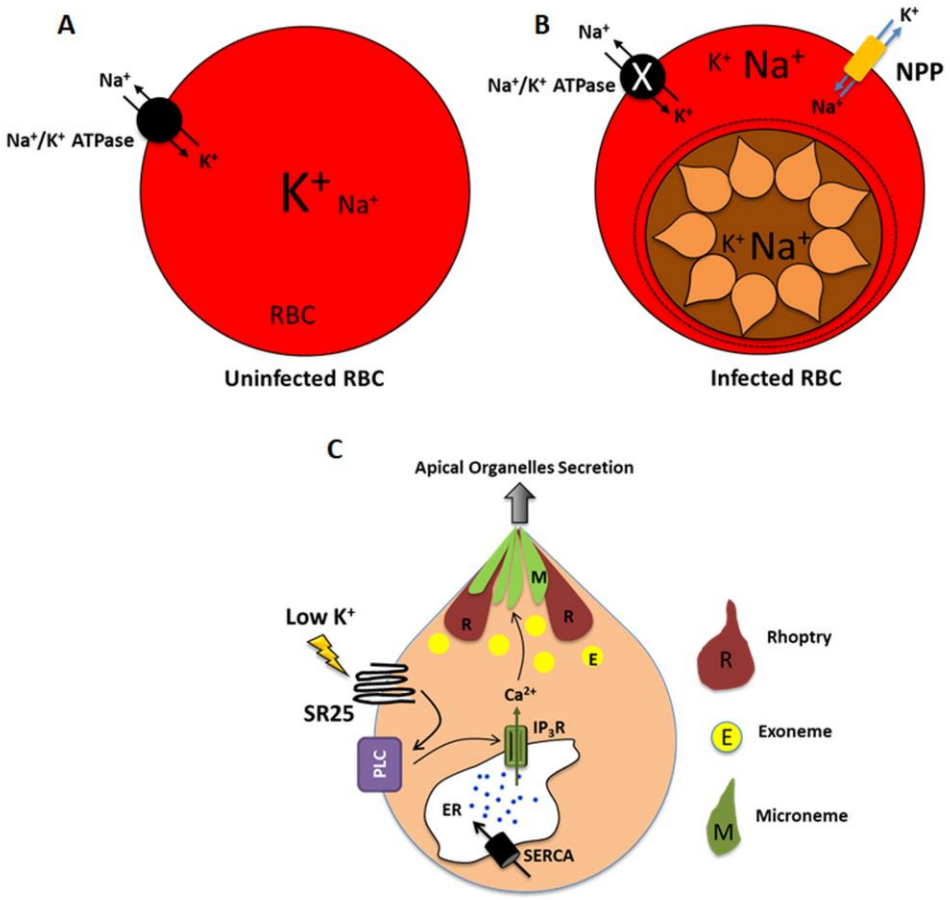

Figure 6: Erythrocyte ionic remodeling and sensing low K^+ by *P. falciparum*.

(A) Uninfected erythrocyte cytosol has high K^+ and low Na^+ and the ionic difference across RBC cytosol is maintained by erythrocyte membrane Na^+/K^+ ATPase (black sphere). **(B)** Erythrocyte cytosol with mature parasite maintains high Na^+ and low K^+ due to activation of new permeation pathway (NPP- yellow graphics) and inactivation of Na^+/K^+ ATPase. Modified from (Chitnis and Staines 2013) **(C)** Exposure of parasite to low K^+ environment is sensed by PfSR25, which further activates IP_3R to induce cytosolic Ca^{2+} release. Temporal Ca^{2+} rise activated apical organelle secretion necessary for parasite invasion.

1.6.3 Role of melatonin and its derivatives in the *Plasmodium* life cycle

Melatonin (N-acetyl-5-methoxytryptamine), an indolamine, was first isolated from beef pineal gland and also reported in peripheral nerve of man, cow and monkey (Lerner, Case et al. 1959). Presence and synthesis of melatonin in plants, bacteria, unicellular organisms and

invertebrates has also been reported (Paredes, Korkmaz et al. 2009, Rodriguez-Naranjo, Torija et al. 2012, Roopin and Levy 2012). Melatonin biosynthesis begins after tryptophan entry into the pineal gland from the blood circulation. In the pineal gland, tryptophan is converted into 5-hydroxytryptophan, serotonin and N-acetylserotonin. O-methylation of N-acetylserotonin by the enzyme hydroxyindole-o-methyl transferase (HIOMT) produces melatonin and the whole melatonin synthesis is affected by light (Wurtman, Axelrod et al. 1963). Melatonin is known to regulate the rhythm with respect to the measurement of day/night interval (Reiter 1993). Its metabolites are known to be involved in controlling various physiological processes such as sleep, vasomotor regulator, anti-excitatory activities, immunomodulatory and antioxidant properties (Silvestri and Rossi 2013). A circadian rhythm has been widely recognized in a vast range of organisms from bacteria, fungi, plants and animals (Cassone and Natesan 1997, McClung 2006, Edgar, Green et al. 2012). In higher vertebrates such as mammals, it has been estimated that approximately 10% of the genome is under circadian control (Storch, Lipan et al. 2002).

Like higher animals, circadian rhythm plays phenomenal role in parasites especially in disease transmission to a new host so the new wave of parasites can spread. The time window from erythrocyte rupture to invasion is very short and the only phase when parasite become exposed to host defense system. To avoid the prolong exposer to host immune system, parasite egress is very synchronous and cell cycle follows the multiple of 24 hours cycle, for example 24 hours in *P. knowlesi*; 48 Hrs in *P. falciparum*, *P. vivax* and 72 hours in *P. malariae* (Hawking et al. 1972). Nevertheless, the role of the circadian rhythm was unnoticed until Hotta *et al.* for the first time studied the role of melatonin in the modulation of parasite growth (Hotta, Gazarini et al. 2000). It is already known that *P. falciparum* loses the synchrony in *in vitro* growth

conditions. When Hotta *et al.* treated the *in vitro* parasites with melatonin, the number of mature stage parasites (schizont) increased. Interestingly, the synchrony is lost in *P. berghei* infected pinealectomized mice but injecting melatonin expedites the parasites towards mature form, supporting the influence of host circadian rhythm and melatonin involvement. It was also found that melatonin triggered the release of Ca^{2+} from intracellular stores of the *Plasmodium* by binding to a yet identified receptor and activating the IP_3 signaling pathway. Blocking PLC by U73122 abolishes the effect of melatonin, supporting this view (Hotta, Gazarini et al. 2000). In another study, blocking PLC by U73122 inhibited Ca^{2+} release and prevented PKB mediated upstream signaling events in *P. falciparum* (Vaid and Sharma 2006) and transcriptional analysis of PLC in blood stage of *P. falciparum* showed transient increase in PLC expression in late schizonts (Raabe, Berry et al. 2011). Alves *et al.* reported that melatonin acts upstream and stimulates PLC to produce IP_3 and opens ER-localized IP_3-sensitive Ca^{2+} channels in *P. falciparum* inside erythrocyte host cell (Alves, Bartlett et al. 2011). *P. falciparum* and *P. chabaudi* sustain intracellular Ca^{2+} stores and IP_3-dependent Ca^{2+} discharge has already been demonstrated in isolated, permeabilized *P. chabaudi* (Passos and Garcia 1998), however, a IP_3R transcript has yet to be identified in *P. falciparum.* Recently, an IP_3R has been characterized in *T. cruzi* (Hashimoto, Enomoto et al. 2013) and food vacuole of *T. brucei* (Huang, Bartlett et al. 2013). These groups have shown that disrupting or inhibiting IP_3R leads to impaired growth and reduced infection rate. Additionally, melatonin precursors N-acetylserotonin (NAS), tryptamine and serotonin can also trigger $[Ca^{2+}]_{cyt}$ in both *P. falciparum* and *P. chabaudi* (Hotta, Markus et al. 2003, Beraldo and Garcia 2005). Nonetheless, N^1-acetyl-N^2-formyl-5-methoxykynuramine (AFMK), produced as a result of melatonin degradation has a positive effect on synchronization of *P. chabaudi* and *P. falciparum* and using melatonin receptor antagonist, luzindole, severely

abrogated the synchronization (Budu, Peres et al. 2007). Another crosstalk was established between melatonin induced cAMP rises, which was impaired when PLC inhibitor U73122 was introduced in the buffer suggesting the possibility of melatonin-induced activation of $[Ca^{2+}]_{cyt}$ that further triggers the cAMP activation. cAMP activates PKA (**Figure 5)** and further it was shown that 3',5'-cyclic monophosphate N^6-benzoyl/protein kinase A activator (6BZ-cAMP), a membrane permeable cAMP analog also increase $[Ca^{2+}]_{cyt}$ levels and blocking PKA with peptide inhibitor of PKA (PKI) prevents rises in $[Ca^{2+}]_{cyt}$ induced by 6BZ-cAMPindicates that PKA is require for Ca^{2+} induction (Beraldo, Almeida et al. 2005). In higher vertebrates, melatonin receptors have been identified that belong to a G-protein coupled receptor (Dubocovich and Markowska 2005) but no such melatonin receptor has been identified in *P. falciparum* genome. Considering all the factors, it would be interesting to investigate the physiological and molecular aspects of Ca^{2+} signaling in the parasites.

It is evident that Ca^{2+} homeostasis is linked to various signaling pathways in the parasite and parasite expresses many channels to regulate the Ca^{2+} fluctuation. Targeting these components that can disrupt the Ca^{2+} signaling are critical steps for successful parasite propagation in the human population, and major targets of the ongoing malaria eradication program. How the parasites are sensing and activating the signaling cascades by rise in cytosolic Ca^{2+} from internal stores are never reported. Continuing the same agenda, it would be fascinating to study the molecular aspects and significance of the genetic alteration in parasite proteins that affects the *P. falciparum* growth.

2 OBJECTIVES

As a part of broader objective, these studies contribute to our understanding of the role of Ca^{2+} signaling in human malaria parasite *P. falciparum* in the following aspects:

In the first part of the study, we explored the effect of ionic interchange in intracellular Ca^{2+} efflux. For this purpose, we studied how changing the ionic microenvironment triggers $[Ca^{2+}]_{cyt}$ increase in parasite that is important for parasite invasion to red blood cell. Moreover, we have also investigated the effect of extracellular ATP in isolated merozoites.

The second part of the study covers the Ca^{2+} efflux from the digestive food vacuole (DV) of parasite mediated by various ionophores. We have investigated whether mutation in chloroquine resistance transporter (PfCRT) has any effect on Ca^{2+} efflux from DV. This study was designed in collaboration of Dr. David Fidock, Columbia University, USA.

Moreover, in another approach, we have characterized the function of Pf1468 (PlasmoDB ID – PF3D7_1468100) that was previously identified in melatonin-agarose beads by our lab. In this part, we have studied the gene function of Pf1468 using reverse genetics approach in collaboration with Prof. Jude M. Przyborsky, Marburg University, Germany. We also studied the effect of melatonin in the successfully engineered clone of the parasite.

3 MATERIAL & METHODS

3.1 Plasmodium falciparum in vitro culture maintenance

Plasmodium falciparum (3D7 strain) was used for all experiments and generation of transgenic parasite lines.

3.1.1 Red Blood Cells to culture *P. falciparum*

Red blood cells (Type A+) procured from the blood bank were washed once with incomplete RPMI 1640 (iRPMI) medium (supplemented with 5.95 g HEPES, 2 g $NaHCO_3$ and 40 mg Gentamycin) and resuspended to a final concentration of 50 % hematocrit in iRPMI. The RBC suspension was aliquoted and stored at 4°C for a maximum period of 21 days from the date of drawing.

3.1.2 Thawing of *P. falciparum* culture from frozen parasite stocks

Frozen stocks stored in liquid N_2 were thawed at 37°C and resuspended in 0.1 volume of solution 1 (12 % NaCl) and wait for 5 min. Then 10 volume of solution 2 (1.6 % NaCl) followed by 10 volume of solution 3 (0.9 % NaCl & 0.2 % Dextrose) was added drop wise. The mixture was centrifuged immediately at 2000 rpm for 5 min at room temperature. The RBC pellet obtained was washed once with iRPMI medium. The pellet was resuspended in complete 1640 (cRPMI) medium (supplemented with 5.95 g HEPES, 2 g $NaHCO_3$, 50 mg Hypoxanthine, 40 mg Gentamycin and 5 g Albumax or 10 % heat inactivated human serum), plated at 4 % hematocrit, gassed with 5 % CO_2, 3 % O_2 and 92 % N_2 and maintained at 37°C.

3.1.3 **Maintenance of *P. falciparum* cultures**

Parasite cultures were maintained in accordance with the previously published protocol (Trager and Jensen 1976). Parasites were grown in RBCs of preferably A^+ blood group at 2-3 % hematocrit. Cultures were maintained at 37°C in cRPMI medium (supplemented with 10% human serum or 0.5 % albumax). Cultures were gassed with 5 % CO_2, 3 % O_2 and 92 % N_2 for 15 seconds and maintained at 37°C.

3.1.4 **Preparation of smears to visualize infected- RBCs**

Approximately 10-20 µl of parasite culture was collected from the flask and centrifuged. The RBC pellet was resuspended in minimum amount of culture supernatant and thin smear was made on a clean glass slide. The slide was air dried and stained with Panotico Rapido (Laborclin). The slides were washed with distilled water, dried and visualized at 100x magnification under a light microscope.

3.1.5 **Synchronization of *P. falciparum* cultures**

Predominantly the ring infected RBCs cultures were collected by centrifugation and mixed in 5-10 volume of 5 % sorbitol and incubated at 37°C for 10 minutes. The RBC suspension was washed once with iRPMI medium at 2000 rpm for 5 min and plated with fresh cRPMI media (Lambros and Vanderberg 1979).

3.1.6 **Freezing the parasite stocks**

Cultures predominantly at ring stage were pelleted and resuspended dropwise in 1.5 volume freezing solution (45% Glycerol, 4 mM KCl, 143 mM Sodium lactate, 8.75 mM Na_2HPO_4 and 3.75 mM NaH_2PO_4). 1 ml aliquots were transferred to cryovials and stored in liquid N_2.

3.2 Measurement of intracellular Ca^{2+} levels in P. falciparum

Infected RBC at the trophozoite stage were centrifuged (2,000 rpm, 5 min), and the ~1 ml pellet was washed and isolated with 0.05% saponin (PBS) and incubated with Ca^{2+} indicator Fluo-4 AM (5 μM) in Buffer M (116 mM NaCl, 5.4 mM KCl, 0.8 mM $MgSO_4$, 5.5 mM D-Glucose, 50 mM MOPS and 2 mM $CaCl_2$; pH 7.2) supplemented with 2.8 mM probenecid and incubated for 60 min at 37°C. After incubation, cells were washed and resuspended in the same buffer. Measurement of Ca^{2+} was done in cell suspension using a Shimadzu spectrofluorophotometer (RF5301PC, Japan) and fluorescence was measured continuously (acquisition rate: every 1 seconds) for 600 seconds. Excitation/emission wavelengths were adjusted to 505/530 nm for Fluo-4 AM.

Similarly, to monitor Ca^{2+} by flow cytometry, infected RBC at the trophozoite stage were centrifuged (2,000 rpm, 5 min), and the ~1 ml pellet was washed and isolated with 0.05 % saponin in respective high K (140 mM) or low K (5.4 mM) buffer so that the parasites will remained in a high or low potassium environment followed by loading with 10 μM Fluo4-AM for 30 min at 37°C in high K^+ (140 mM KCl, 5.4 mM NaCl, 0.8 mM $MgSO_4$, 5.5 mM D-glucose, 50 mM MOPS, 2 mM $CaCl_2$; pH 7.2); low K^+ (5.4 mM KCl, 140 mM NaCl, 0.8 mM $MgSO_4$, 5.5 mM D-glucose, 50 mM MOPS, 2 mM $CaCl_2$; pH 7.2); K-gluconate (140 mM K-gluconate, 5.4 mM Na-gluconate, 0.8 mM $MgSO_4$, 5.5 mM D-glucose, 50 mM MOPS, 2 mM $CaCl_2$; pH 7.2) and Na-gluconate (5.4 mM K-gluconate, 140 mM Na-gluconate, 0.8 mM $MgSO_4$, 5.5 mM D-glucose, 50 mM MOPS, 2 mM $CaCl_2$; pH 7.2) respectively. Parasites were then washed three times in respective buffer and ~$5x10^7$ parasites were transferred to high or low K^+ buffer containing vial prior to the experiment. For U73122 and U73343, parasites were pretreated with 2μM concentration for 1 min after Fluo4-AM loading. The Fluo4-AM signal was

measured for 2 min for each experiment by flow cytometry (FACSCalibur, Becton Dickinson, USA) excited with a 488 nm Argon laser and fluorescence emission was collected at 520–530 nm. All data were analyzed by FlowJo software with Histogram at y-axis and FL-1 at x-axis.

3.3 Polymerase chain reaction (PCR)

PCR allows amplification of specific DNA- fragments from a template DNA with a DNA polymerase using 5´and 3´ DNA oligonucleotide primers. The PCR reaction leads to an exponential increase in DNA fragment numbers, which can be used for investigation or cloning (Mullis, Faloona et al. 1986). PCR products designated for cloning where purified either with the PCR cleanup kit (QIAGEN) or with the Gel extraction kit (QIAGEN) following gel electrophoresis. The amplification of fragments for cloning was performed with KOD Polymerase (Merck Millipore). A typical reaction contained 5 µl 10x KOD Buffer, 5 µl 8mM dNTP- Mix, 3 µl 25 mM $MgSO_4$, 25 pmol forward primer, 25 pmol reverse primer, 0.25- 0.35 µg template DNA and 1 U KOD polymerase followed by final adjustment of the volume up to 50 µl with ddH2O.

PCR reactions were conducted with the following program:

Step	Temperature (°C)	Time	Remarks
1	95	10 min	Initial denaturation of template DNA
2	95	1 min	Denaturation of template DNA
3	45- 50	1 min	Annealing of Primers
4	68	30s/ kb	Polymerization step
5	68	10 min	Final polymerization step
6	4	∞	Pause

The steps 2- 4 where repeated for 25 cycles.

Table 1: List of oligonucleotides used for clone confirmation by PCR

S. N.	Description	Sequence 5´→ 3´
1	Pf1468 Fw	AAATGAAAATGAAGAGAAACCAAATGATGG
2	Pf1468 Rev	GATGCCGAGGAGGAAGATACCATA
3	Not_70 F	GGCGGATAACAATTTCACACAGG
4	PARL_Rev	CAGTTATAAATACAATCAATTGG

The serial numbers are depicted in construct model to predict the expected length of positive clones.

3.4 Agarose gel electrophoresis of plasmid or P. falciparum genomic DNA

Agarose gels were prepared by dissolving agarose (Invitrogen) in 1x TAE by boiling it. Afterwards ethidium bromide was added (f.c. 50 ng/ ml) and the agarose solution was poured into a gel form for solidification at room temperature. After that, the gel was transferred into a gel chamber and covered with 1x TAE buffer. The agarose concentration of the gels was selected based on the lengths of the DNA fragments, since lower concentration allow a better resolution of longer fragments. Therefore, the agarose concentration of the gels varied between 0.8 % and 2 %. The DNA was then loaded into the gel on the side of the cathode. Therefore, the DNA was mixed with a loading dye and placed into a well of the agarose gel. Afterwards the DNA was exposed to an electric field (110- 140V, 500mA, 150W) for 20-50 min. The length of the DNA fragments was then assessed by comparison with a DNA size standard (Thermo Fisher).

3.5 Glucosamine treatment for PfMel-HA and PfMel-HA-glmS parasites

P. falciparum 3D7 constructs PfMel-HA-glmS and PfMel-HA parasites were synchronized with 5% sorbitol at least two times to achieve higher synchrony. Halfway of the parasite cycle, which is 24 hpi, various concentration (0.5-2.5 mM) of glucosamine hydrochloride (Sigma) was

added in the culture along with no glucosamine as control. Infected erythrocytes were incubated until trophozoite stage of the next cycle.

3.6 Western Blot for identification of PfMel protein with anti-HA and anti-GFP probes

P. falciparum infected erythrocytes with or without treatment where ever mentioned were lysed with 0.05 % saponin prepared in PBS. The parasite pellet was recovered by centrifugation at 8000 g for 10 min at 4°C, washed and resuspended in lysis buffer (in mM): 50 Tris, pH 8.0, 150 NaCl, 5 EDTA, and 0.5% Nonidet P40 supplemented with the following mixture of protease inhibitors: 1 mM PMSF, 0.01 mM benzamidine, 10 µg ml^{-1} aprotinin, 10 µg ml^{-1}, leupeptin, 10 µg ml^{-1} pepstatin, 10 µg ml^{-1} chymostatin. Equal amount of protein sample (25 µg) was loaded in each well and protein fractions were separated on 6% SDS-PAGE gels, transferred to nitrocellulose membrane, blocked with 5% powdered milk, and probed with rabbit anti-HA (1:1500), mouse anti-tubulin (1:5000) and rabbit anti-GFP (1:2000) for overnight at 4°C. After washing, membrane was probed with horseradish peroxide-conjugated secondary anti-rabbit (1:30000), anti-mouse (1:5000) antibody at room temperature for 2 hours. The membrane was developed using ECL solution (GE Healthcare) in 1:1 ratio and 1 µl 30% H_2O_2. X-ray films were exposed to the membrane and developed.

3.7 Immunofluorescence confocal microscopy in P. falciparum-infected RBCs

IFA was performed essentially as described previously (Tonkin, van Dooren et al. 2004). Infected parasites were fixed for 30 min with 4% paraformaldehyde, 0.0075% glutaraldehyde in PBS. Cells were washed and permeabilized for 15 min with 0.1% Triton X-100 in PBS followed by washing. Fixed cells were then blocked with 3% BSA (in PBS) for 1 hour at room temperature. Primary antibody labeling was done overnight at 4°C with rabbit anti-HA (1:500)

in PBS containing 3% BSA and 0.01% Triton X-100. Cells were washed and secondary antibody anti-IgG Rabbit Alexa 488 (Invitrogen) labeling was done at 1:300 dilutions in PBS containing 3% BSA for 1h at room temperature. Cells were incubated for 5 min with DAPI 1:1000 and washed three more times in PBS. Cells were mounted using Vectashield (Vector). Images were acquired with a Zeiss confocal microscope (LSM 780-NLO) using UV and Argon 488 lasers. The main dichroic HFT UV (375) and 435-485 band-pass filters were used to collect DAPI fluorescence. The main dichroic HFT 488-514 band-pass filters were used to collect Alexa 488 fluorescence. The objective used was a plan-Neofluar 100x/1.3 with immersion oil.

3.8 Parasitemia and merozoite assessment in PfMel parasites after glucosamine induction

For parasitemia assessment, young trophozoites were incubated at 0.1% parasitemia in 1 mL RPMI 1640 containing 0.5% albumax for 6 days in the presence of different concentration of glucosamine. To estimate the growth progression, at least one thousand cells were counted on Giemsa stained slides prepared every day.

To assess the number of merozoites in each schizont, a synchronized culture was maintained in RPMI containing 0.5% albumax and glucosamine until the next developmental stage when majority of the parasites were segmented schizonts. From Giemsa stained slides, at least 50 schizonts were assessed in each slide. All these experiments were repeated 3 independent times in triplicate.

3.9 Flow Cytometry for analysis of parasitemia and maturation forms distribution

Asynchronous PfMel-HA and PfMel-HA-glmS parasites were first treated with and without glucosamine for 48 h. After 48 hours approximately 5% infected erythrocytes in 2% hematocrit were incubated with 100 nM of melatonin for 24 h. Parasites then were fixed in 2%

formaldehyde in phosphate buffered saline (PBS) for 24 h at room temperature and permeabilized with 0.1% Triton X-100 (Sigma-Aldrich) and 20 μg mL^{-1} RNAse (Invitrogen Life Technologies), incubated for 15 minutes at 37°C and stained with 5 nM YOYO-1 (Molecular Probes) as performed by Schuck et al. (Schuck et al. 2011). Parasitemia and proportions of parasites at each stage were determined from dot plots [side scatter (SSC) versus fluorescence] of 10^5 cells acquired on a FACS Calibur flow cytometer using CELLQUEST software (Becton & Dickinson). YOYO-1 was excited with a 488 nm Argon laser and fluorescence emission was collected at 520–530 nm. Initial gating was carried out with unstained, uninfected erythrocytes to account for erythrocyte auto-fluorescence. Stages of parasites were standardized with synchronized cultures.

3.10 Co-Immunoprecipitation of PfMel-GFP

Infected erythrocytes were washed 3 times in phosphate buffered saline (PBS). The pellet was suspended in PBS containing 0.05 % (w/v) saponin in order to lyse the erythrocytes. It was then incubated centrifuged at 8000 g for 10 min. The resulting pellet was washed 3 times in PBS and resuspended in lysed in 5 volumes of modified RIPA buffer (50 mM Tris, pH 7.5, 150 mM NaCl, 0.5 % sodium deoxycholate, 1 % Nonidet P-40, 10 μg/ml aprotinin, 10 μg/ml leupeptin, 10 μg/ml, 1mM phenylmethylsulfonyl fluoride, benzamidine) The lysate was solubilized by incubation at 4°C for 30 min, pre-cleared with 50 μl of protein A/G-Agarose beads at 4°C for 1 h, and clarified by centrifugation at 10000 g for 10 min. The pre-cleared lysate was incubated with an anti-GFP-Trap-A beads (ChromoTek, gta-20) antibody overnight. The magnetic beads were then pelleted using a magnet (Invitrogen) and the beads were washed extensively. To elute the immunoprecipitated proteins, the magnetic beads were resuspended in 2X SDS loading buffer and resolved by SDS-PAGE. Following SDS-PAGE, selected gel sections were excised

and further analyzed by mass-spectrometry. We used a service provider (CEFAP core-facility de Espectometria de Massa) to analyze GFP-co-immunoprecipitated proteins.

3.11 Mass spectrometry

The gel slices were washed sequentially for 15 min and three times each step with: 1) Acetonitrile (ACN) 50 %, 2) 25 mM ammonium bicarbonate (NH_4HCO_3) and then dehydrated with ACN 100% for 5 min followed by vacuum centrifugation. Disulfide bridges were reduced using 10 mM DTT in 100 mM NH_4HCO_3 for 1 h at 56°C. The reduced cysteines were alkylated with 55 mM Iodoacetamide in 100 mM NH_4HCO_3 for 45 min in the dark and then washed twice for 15 min each with 100 mM NH_4HCO_3. Gel slices were dehydrated with ACN 100 % for 5 min followed by vacuum centrifugation and the digestion buffer containing Sequencing Grade Trypsin (Promega, Madison, WI, USA) in 20 mM ammonium bicarbonate, incubated for 1 h at room temperature and then overnight at 37°C. The supernatant was transferred to a low protein binding tube and tryptic peptides were extracted from the gel slices using sequentially ACN 50 %, Trifluoroacetic acid (TFA) 5 % for 30 min. The peptides were desalted using Stage Tips with C18 disks (Sigma Aldrich).

Peptide samples were resuspended in 0.1 % formic acid (FA) before analysis using a nano-flow EASY-nLC™ 1200 system (Thermo Scientific) coupled to Orbitrap Fusion Lumos mass spectrometer (Thermo Scientific). The peptides were loaded on an Acclaim PepMap C18 (Thermo Germany) trap column (2 cm x 75 µm inner diameter; 3 µm, 100 Å) and separated onto an Acclaim PepMap C18 (15 cm x 50 µm inner diameter; 2 µm, 100 Å) column with a gradient from 100 % mobile phase A (0.1 % FA) to 34 % phase B (0.1 % FA, 95 % ACN) during 30 min, 34-95 % in 10 min and 5 min at 95 % at a constant flow rate of 300 nL/min. The mass spectrometer was operated in positive ion mode with data-dependent acquisition. The full scan

was acquired in the Orbitrap at a resolution of 120,000 full width at half maximum (FWHM) in the 400-1600 m/z mass range with max injection time of 50ms and AGC target of 5e5. Peptide ions were selected using the quadrupole with an isolation window of 1.2 and fragmented with HCD MS/MS using normalized collision energy of 30. Data dependent acquisition with a cycle time of 3 seconds was used to select the precursor ions for fragmentation. All raw data were accessed in Xcalibur software (Thermo Scientific).

Raw data were processed using MaxQuant software version 1.5.2.8 and the embedded database search engine Andromeda. The MS/MS spectra were searched against the Uniprot *Plasmodium* (isolate 3D7) (Strain: Isolate 3D7) Protein Database (downloaded September, 2017; 5369 entries), with the addition of common contaminants, with an MS accuracy of 4.5 ppm and 0.5 Da for MS/MS. Cysteine carbamidomethylation (57.021 Da) was set as the fixed modification, and two missed cleavages for trypsin. Methionine oxidation (15.994 Da), protein N-terminal acetylation (42.010 Da) and asparagine and glutamine deamidation (+0.984 Da) were set as variable modifications. Proteins and peptides were accepted at false discovery rate (FDR) less than 1%. Proteins with at least two peptides and two ratio counts were accepted for further validation. Label-free quantification was performed using the MaxQuant software with the "match between run" and Intensity Based Absolute Quantification (iBAQ) features activated. Protein Label-free quantification (LFQ) and iBAQ ratio was calculated for the two conditions and the protein IDs divided accordingly.

3.12 Total RNA isolation and Quantitative Real-Time Polymerase Chain Reaction (qRT-PCR)

Total RNA was extracted from various parasites cultures using TRIZOL (Invitrogen, USA). Synchronized parasites, with or without *in vitro* stimulation, were lysed directly in a culture flask by adding TRIZOL. The homogenates were incubated for five minutes at room temperature to permit complete dissociation of nucleoprotein complexes. Next, 0.2 ml chloroform was added per milliliter of extraction reagent; the mixture was shaken vigorously for 15 seconds and incubated for two to three minutes at 4°C. Centrifugation separated the homogenates into two phases: a lower brown phenol/chloroform phase and a colorless upper aqueous phase containing RNA. The aqueous upper phase was transferred to a fresh tube, and 0.5 ml isopropanol was added per 1 mL of TRIZOL. This mixture was incubated at room temperature for 10 minutes and then centrifuged for 10 minutes at 12,000×*g*. Supernatants were removed, and the RNA pellet was washed once with 75 % ethanol by vortexing and subsequent centrifugation at 7500 × g for five minutes at 4°C. The extracted RNA in the pellet was air dried and dissolved in DEPC-H_2O for use in qRT-PCR analysis and measured using a NanoDrop 2000c spectrophotometer (Thermo Scientific). Equal amounts of total RNA were synthesized into cDNA using a First-Strand cDNA Synthesis kit (Invitrogen). ABgene Absolute qPCR SYBR Green Master Mix (ABgene, Surrey, UK) with ROX dye was used for all PCR protocols.

qRT-PCR reactions were run in triplicate, in 96-well plates on an ABI Prism® 7900HT real-time PCR machine. Thermal cycling conditions were as follows: one cycle at 50°C for 2 min for enzyme activation; one cycle at 95°C for 15 min for enzyme activation; forty cycles at 95°C for 15 sec for Denaturation and 60°C for 1 min for the Anneal/Extension step. Threshold

cycle number (Ct) of gene was calculated, and the serine tRNA-ligase was used as reference gene. Delta–delta Ct values of genes were presented as relative fold induction.

Table 2: List of oligonucleotides used for real-time PCR.

Primer	Sequence
Mel1_Fwd	AGCACAACACAAATGCCACT
Mel1_Rev	AGCGAAAGCTCCAAAGAGCC
Seryl-tRNA Synthetase_Fwd	TGGAACAATGGTAGCTGCAC
Seryl-tRNA Synthetase_Rev	TCATGTATGGGCGCAATTT

4 RESULTS

4.1 P. falciparum senses the environment: Calcium signaling upon shift in K^+ concentration

The malaria parasite *P. falciparum* has highly polarized organelles and its regulated secretion directs the parasite entry into host cells. The secretion of the apical organelle is controlled by intracellular Ca^{2+} and plays crucial role in parasite gliding, invasion into and egress from erythrocytes (Garcia, de Azevedo et al. 2008). Resting Ca^{2+} is maintained at lower concentration (100 nM) in resting cells but the various environmental cues such as hormones or stress can dramatically increase the cytosolic Ca^{2+} (Berridge, Lipp et al. 2000, Gazarini, Thomas et al. 2003). The Ca^{2+} influx in the cytosol is derived from either internal stores or from extracellular space (Clapham 2007). However, in *P. falciparum,* several putative Ca^{2+} storage organelles such as the endoplasmic reticulum (ER), mitochondria and digestive vacuole (DV) have been reported (Garcia, Ann et al. 1998, Gazarini and Garcia 2004, Alves, Bartlett et al. 2011). The dynamic process of Ca^{2+} signaling is extensively studied and well defined in animal models, however, Ca^{2+} mediated regulatory events are still lacking in *Plasmodium spp.* Thus, decoding the Ca^{2+} signaling and its origin may provide a structural map to understand the regulatory roles of various molecular players in parasite.

In this study, we have investigated the intracellular Ca^{2+} mobilization in live *P. falciparum* parasites using intracellular Ca^{2+} indicator Fluo-4AM. More specifically, we have studied three different aspects of $[Ca^{2+}]_{cyt}$ signaling (i)- interchanging ionic environment to identify how parasite sense the fluctuation of K^+ ion; (ii)- effect of extracellular ATP; and (iii)- Ca^{2+} homeostasis mediated by the digestive vacuole in CQ sensitive and CQ resistant strains.

The idea was to investigate the molecular mechanism of Ca^{2+} signaling during asexual growth of *P. falciparum*. Moreover, we have also searched for alternative signaling routes that may equally be important for parasite invasion. Further, we have investigated the role of the DV of *P. falciparum* in Ca^{2+} homeostasis using various ionophores.

4.1.1 Spectrofluorometric measurement of $[Ca^{2+}]_{cyt}$ in *P. falciparum*

Human malaria parasite *P. falciparum* senses a broad range of environmental fluctuation in both vector and host, which could be detrimental for parasite without the maintenance of a proper homeostasis (Chitnis and Staines 2013). Asexual multiplication is necessary for parasite propagation and mature parasites sense the plasma ionic fluctuation to initiate cell escape and invasion. Lower potassium ion (K^+) concentration in plasma induces the intracellular Ca^{2+}, which in turn trigger the apical proteins discharge (Singh, Alam et al. 2010). The apical proteins facilitate the parasite release from erythrocyte and provide the anchor for invasion. However, the mechanism that mediates the sensing of ionic fluctuation is remains elusive.

In this part of the study, we have examined the role of extracellular K^+ ion in intracellular Ca^{2+} mobilization in human malaria parasites *P. falciparum* late trophozoites. We used doubly synchronized 34-38 h *P. falciparum* cultures to keep the growth window as much as close (4-6 h) for at least 80 % parasite population to avoid any experimental deviation. The harvested parasites were washed with high K^+ buffer and loaded with the intracellular Ca^{2+} indicator dye Fluo-4AM in the same buffer. After 1 h, cells were subjected to detect the intracellular Ca^{2+} trace using a spectrofluorometer after stimulating with the either K^+ or Na^+.

In these experiments, we have investigated the effect of higher concentration of K^+ on Ca^{2+} increase along with the most abundant plasma monovalent cation Na^+. The goal of the

experiment was to investigate the specific role of K^+ in Ca^{2+} efflux. *P. falciparum* late trophozoites were isolated as previously and Fluo-4AM probing was done in low K^+ buffer. Parasites were maintained in the low K^+ buffer stimulated with 50 mM KCl. We found that parasites were able to efflux $[Ca^{2+}]_{cyt}$ upon 50 mM KCl stimulus as shown in **Figure 7A**. Moreover, when parasites were given 50 mM NaCl stimulus, it was unable to trigger $[Ca^{2+}]_{cyt}$ **(Figure 7B)**. These results suggest that parasites are only able to trigger Ca^{2+} efflux with K^+ fluctuation while plasma abundant monovalent ion Na^+ was unable to influence intracellular Ca^{2+} fluctuation.

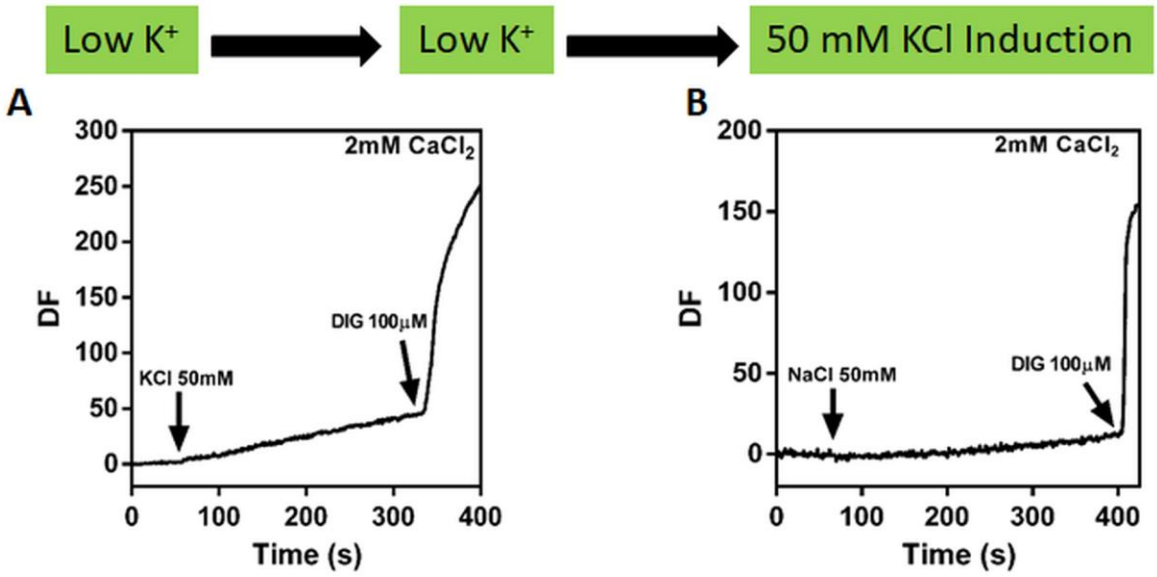

Figure 7: Ionic effect on $[Ca^{2+}]_{cyt}$ efflux in *P. falciparum* trophozoites.

Kinetics of $[Ca^{2+}]_{cyt}$ signals induced by **(A)** Fluo-4AM loaded trophozoites in low K (5 mM) and then stimulated with 50 mM KCl that elicit intracellular Ca^{2+}. **(B)** Similar concentration of NaCl was unable to trigger Ca^{2+} increase. These experiments were performed in presence of extracellular Ca^{2+} and above are the graphical representation of a single repeat from three independent experiments. Membrane permeabilizing detergent digitonin was used as a control to achieve maximum Ca^{2+} fluorescence. The above kinetics represent a single trace of at least three different experiments that were performed in triplicates.

4.1.2 **Effect of ionic interchange in $[Ca^{2+}]_{cyt}$ levels of *P. falciparum***

As we discussed previously, in intraerythrocytic cycle, varying extra- and intra-cellular concentration of K^+ and Na^+ ions are important for apical organelles discharge. When parasites come in contact with extracellular environment, low K^+ triggers cytosolic Ca^{2+} that in turn activate the micronemal protein followed by rhoptry discharge (Singh, Alam et al. 2010). However, there is a conundrum between the parasite K^+ sensing and the apical discharge that leads to parasite invasion in the red blood cells. We have studied the effect of external K^+ in *P. falciparum* late trophozoite stage parasites and monitor the intracellular Ca^{2+} fluctuation. Similar experiments on merozoites were previously performed by Singh *et al.*, which reported that shifting parasites from high to low K^+ triggers cytosolic Ca^{2+}. However, the research work did not discuss how parasites sense the changing environment that triggers intracellular Ca^{2+}.

In this part of the study, we have examined the effect of external K^+ in *P. falciparum* to investigate the upstream molecular sensor that detects the environmental change to trigger intracellular Ca^{2+} efflux. For this purpose, we used two different buffers named as low K^+ (5 mM KCl, 140 mM NaCl, 0.8 mM $MgSO_4$, 5.5 mM D-Glucose, 50 mM MOPS and 2 mM $CaCl_2$; pH 7.2) and high K^+ (140 mM KCl, 5 mM NaCl, 0.8 mM $MgSO_4$, 5.5 mM D-Glucose, 50 mM MOPS and 2 mM $CaCl_2$; pH 7.2) buffer. Initially we performed the experiment with highly synchronous *P. falciparum* late trophozoite parasites loaded with Fluo-4AM in low K^+ buffer. Afterwards, parasites were detected through flow cytometry in low K^+ buffer. Then parasites were switched to high K^+ from low K^+ buffer and detected in the flow cytometer. Both histograms were then overlaid where x-axis represent Fluo-4AM shift indicating increase cytosolic Ca^{2+} rise. Our result in **Figure 8A** shows that parasites did not show internal Ca^{2+} rise in either low K^+ or changing from low to high K^+. Additionally, parasites were loaded with Fluo-

4AM in high K^+ buffer and Ca^{2+} was monitored first high K^+ and then high to low K^+ buffer. In this condition the overlaid histogram showed a shift at x-axis that indicate that changing K^+ concentration to low K^+, mimicing extracellular conditions, does elicit $[Ca^{2+}]_{cyt}$ (**Figure 8B**). Rise in intracellular Ca^{2+} could be the result of either internal stores or due to presence of extracellular Ca^{2+}. To test this possibility, we performed the experiment in Ca^{2+}-free buffer. Removing extracellular Ca^{2+} did not have any effect in intracellular Ca^{2+} release when KCl composition was switched (**Figure 8C**). This indicates that the intracellular Ca^{2+} is released from parasite's internal stores. In **Figure 8D**, we have calculated the average geometric mean of Fluo-4AM to calculate the statistical differences for three independent repeats of each experiments.

Moreover, to test if the Ca^{2+} response was not due to Cl^- ion present in KCl, we have also tested the parasites in buffer containing either Na- or K-glutamate. In this case the KCl and NaCl was replaced with equimolar concentration of either Na- or K-glutamate and named it low K-glu (5 mM K-glutamate, 140 mM Na-glutamate, 0.8 mM $MgSO_4$, 5.5 mM D-Glucose, 50 mM MOPS and 2 mM $CaCl_2$; pH 7.2) and high K-glu (140 mM K-glutamate, 5 mM Na-glutamate, 0.8 mM $MgSO_4$, 5.5 mM D-Glucose, 50 mM MOPS and 2 mM $CaCl_2$; pH 7.2). The data obtained from these assays showed exactly the same effect as in normal KCl or NaCl containing buffer **(Figure 9A & 9B).** We have calculated the average geometric mean of Fluo-4AM to calculate the statistical differences for three independent repeats of each experiments shown in **Figure 9C**.

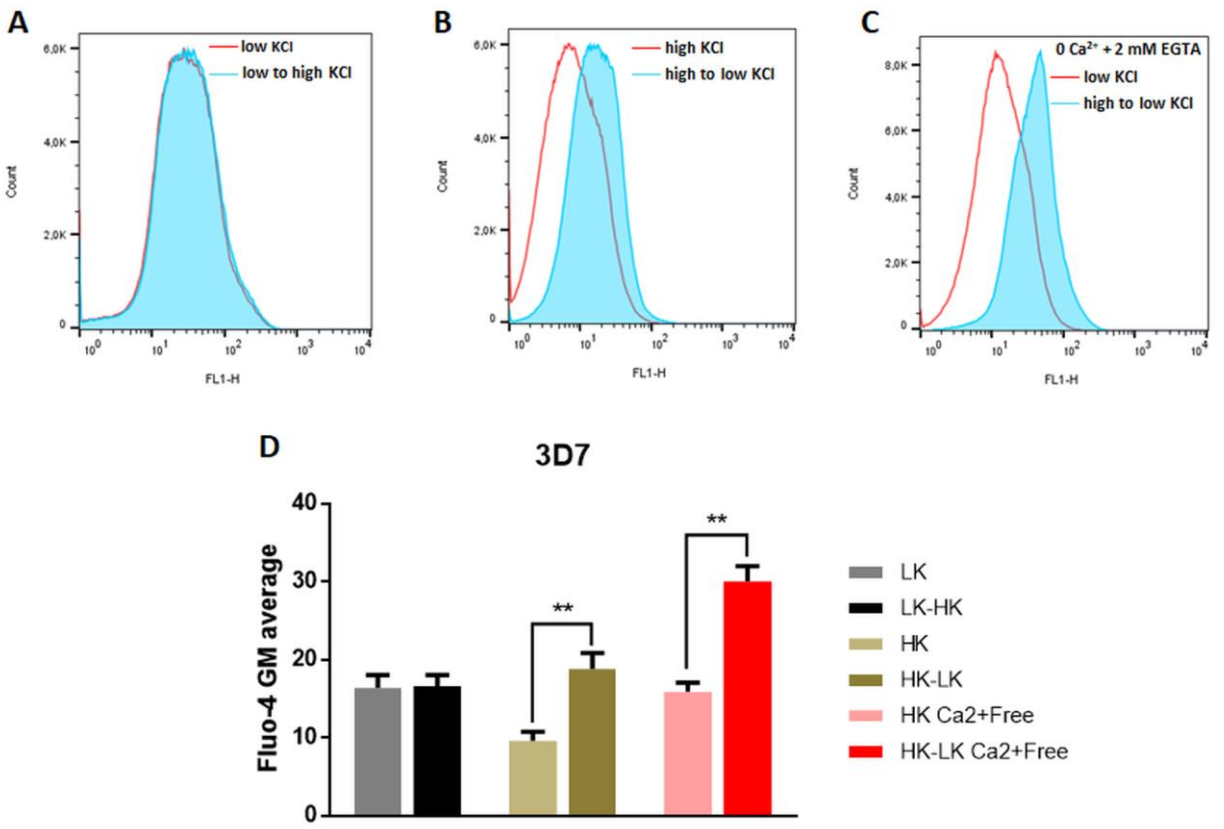

Figure 8: Effect of KCl change in Ca^{2+} response in *P. falciparum* trophozoites.

(A) No change in $[Ca^{2+}]_{cyt}$ level was detected when parasites were first tested in low K^+ buffer and switched from low K^+ to high K^+ buffer; but **(B)** in opposite condition where parasites were tested first in high K^+ buffer had no effect on Ca^{2+} efflux. However, switching the parasites from high K^+ to low K^+ elicits Ca^{2+} efflux and overlay image showed the shift at x-axis. **(C)** Absence of extracellular Ca^{2+} showed similar effect as shown in presence of external Ca^{2+}. Cytosolic Ca^{2+} elevation was seen in overlay images of high K^+ and high K^+ to low K^+ buffer. **(D)** All experiments were performed in at least three times in triplicate and shift at x-axis was calculated by geometric mean of Fluo-4AM. Statistical difference was evaluated by student's t-test against controls. ** $p<0.01$

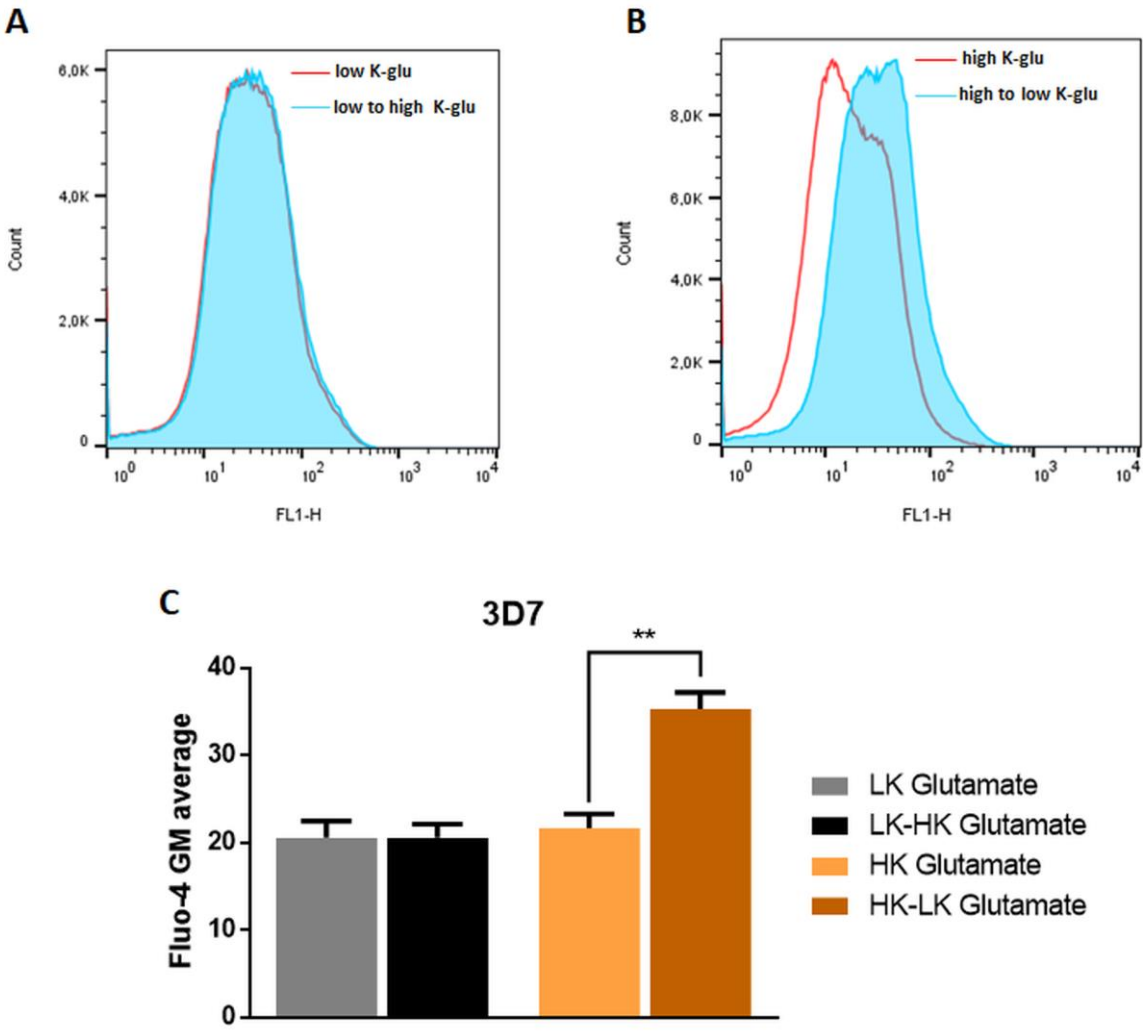

Figure 9: Effect of K-glutamate change in Ca^{2+} flux in *P. falciparum* trophozoites.

(A) *P. falciparum* Fluo-4AM loaded parasites were first tested in low K-glu buffer and then switching from low K-glu to high K-glu buffer did not evoked $[Ca^{2+}]_{cyt}$. **(B)** Similarly when parasites were first tested in high K-glu and then switched from high K-glu to low K-glu, a rise in $[Ca^{2+}]_{cyt}$ was noted. **(C)** All experiments were performed in at least three times in triplicate and shift at x-axis was calculated by geometric mean of Fluo-4AM. Statistical difference was evaluated by student's t-test against control. ** $p<0.01$

4.1.3 **Treatment of *P. falciparum* trophozoites with PLC and SERCA inhibitors**

In our previous result, we saw that the intracellular Ca^{2+} $[Ca^{2+}]_{cyt}$ influx in Ca^{2+}-free buffer when the parasites were moved from high K^+ to low K^+ buffer. The intracellular Ca^{2+} increase in the Ca^{2+}-free buffer leads us to investigate the source of Ca^{2+}. In majority of the cases, $[Ca^{2+}]_{cyt}$ when stimulated with agonist released from ER by PLC-IP_3 pathway. To test this hypothesis, we used the Phospholipase-C (PLC) inhibitor U73122. PLC hydrolyses phosphatidylinositol 4,5-bisphosphate (PIP2) and releases soluble inositol 1,4,5-trisphosphate (IP3) and diacylglycerol (DAG) that triggers the release of $[Ca^{2+}]_{cyt}$ to initiate the Ca^{2+}-mediated signaling pathway (Garcia, Alves et al. 2017). Several studies have shown that PLC activation is involved in multiple processes during parasite growth ranging from sporozoite motility to egress, gametocytogenesis and invasion of merozoites via regulated Ca^{2+} release (Raabe, Wengelnik et al. 2011, Agarwal, Singh et al. 2013, Carey, Singer et al. 2014).

Based on these evidences, we performed experiments where parasites were first loaded with Fluo-4AM in high K^+ buffer and pre-treated with 1 μM U73122. First, parasites were passed through a flow cytometer in the presence of high K^+ and were then transferred from high K^+ to low K^+ buffer. Our overlay data shown in **Figure 10A** showing that U73122 treatment blocks the intracellular Ca^{2+} release thus no shift at x-axis was seen. On the other hand, when we pretreated the Fluo-4AM loaded parasites with the U73343, an inactive analogue of U73122, a rise in $[Ca^{2+}]_{cyt}$ was observed **(Figure 10B)**. The statistical differences of the average geometric mean of Fluo-4AM for each experiment is represented in **Figure 10C**. These results clearly suggest that blocking PLC significantly impairs the $[Ca^{2+}]_{cyt}$ rise and also indicates that the Ca^{2+} flux is via IP_3 activation. However, IP_3 releases intracellular Ca^{2+} by activating IP_3 receptor

(IP_3R) on the endoplasmic reticulum (Berridge, Lipp et al. 2000) but there is no genomic evidence for the presence of IP_3R in *P. falciparum*. In the next test, we ran the control experiment to confirm the source of intracellular Ca^{2+} release using the sarcoendoplasmic reticulum Ca^{2+}-ATPases (SERCA) inhibitor cyclopiazonic acid (CPA). The Ca^{2+} ion from ER store leaks to the cytosol and is taken back to ER by SERCA pump. The SERCA inhibitor CPA prevent the cytosolic Ca^{2+} uptake to the ER resulting high concentration of Ca^{2+} in the cytosol. We tested the parasites loaded with Fluo-4AM in high K^+ buffer and observed the Ca^{2+} level in presence of 10 μM CPA in both high K^+ buffer and then high K^+ to low K^+ buffer. The result in **Figure 10C** shows that the ER store of the parasites were filled with Ca^{2+} and addition of CPA overwhelmed the cytosolic Ca^{2+}. A similar effect was also seen when the parasites were switched from the high K^+ to low K^+ buffer. The results obtained in presence of CPA suggests that blocking SERCA affect the inversion of cytosolic Ca^{2+} to the ER store and once the ER store became empty, there was no Ca^{2+} influx when parasites were transferred to the low K^+ buffer from high K^+ buffer. In **Figure 10D**, we calculated the average geometric mean of Fluo-4AM to calculate the statistical differences for three independent repeats of each experiments

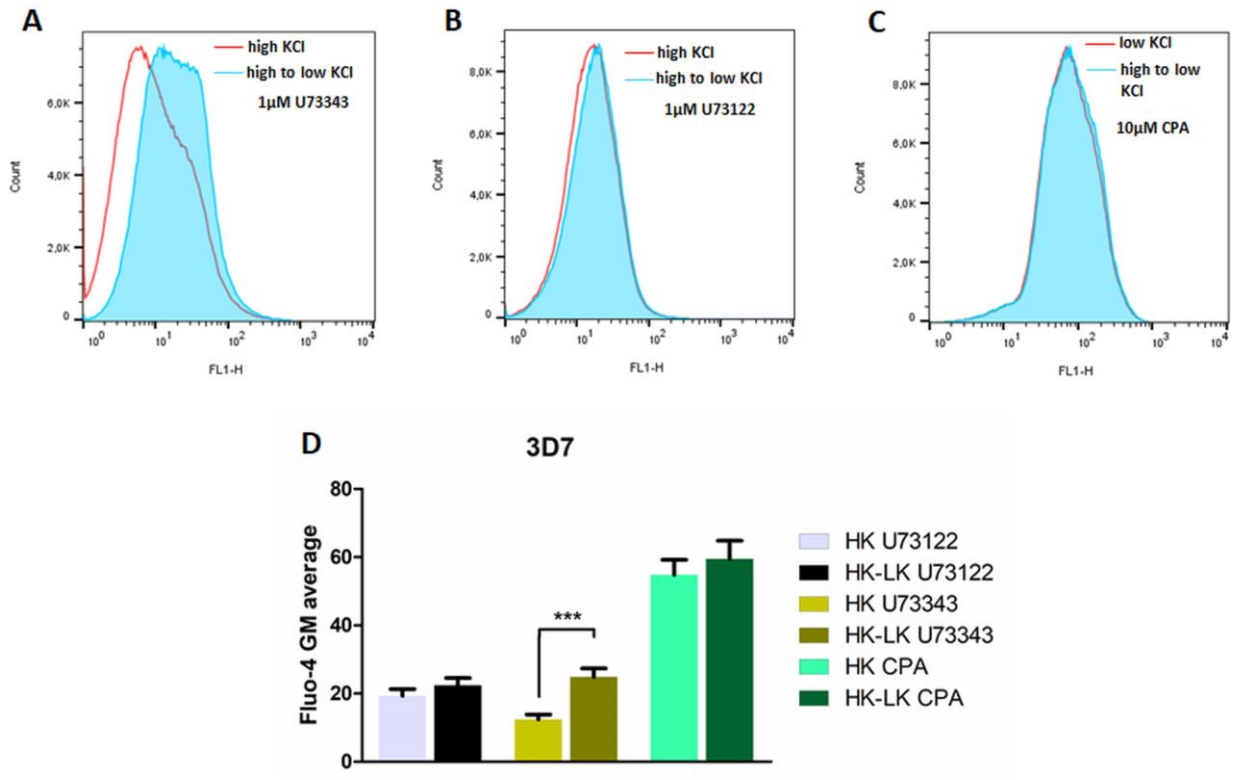

Figure 10: Effect of PLC and SERCA inhibitor on $[Ca^{2+}]_{cyt}$ level in trophozoites.

Change in $[Ca^{2+}]_{cyt}$ and shift at x-axis was observed when Fluo-4AM loaded parasites were pre-treated with inactive PLC inhibitor U73343 **(A)** but active PLC inhibitor compound U73122 abolish the shift and no $[Ca^{2+}]_{cyt}$ increase was detected **(B)** when parasites were switched from high to low K buffer. **(C)** Similarly blocking Ca^{2+} ATPases SERCA with CPA increases the $[Ca^{2+}]_{cyt}$ level in both high K and switching from high to low K. **(D)** Geometric mean average of Fluo-4AM of three independent experiments was calculated and statistical analysis was done by student's t-test using Graphpad prism V5. *** $p<0.001$

4.1.4 Effect of low K^+ concentration in internal Ca^{2+} in PfSR25 knockout parasites

The goal of this study is to identify the upstream molecule that senses the change in ionic microenvironment. In above studies, we have seen that changing the ionic composition leads to $[Ca^{2+}]_{cyt}$ rise in PLC-dependent manner. However, there are no previous reports available that describe the upstream sensing mechanism by *P. falciparum.* To gain further insight, our group

has identified a GPCR protein SR25 in *P. falciparum* (Madeira, Galante et al. 2008). We have generated the gene knockout for *P. falciparum* SR25 (*PfSR25*$^{-}$) and in order to understand the *in vivo* properties of the SR25, we attempted to construct the *P. berghei* SR25 (PbSR25) gene knockout but these parasites were not able to grow after injecting in mice (Moraes, Budu et al. 2017). Successful gene knockout for *PfSR25*$^{-}$ gave us the opportunity to study both physiological and morphological characters in the *P. falciparum* life cycle. We found that *PfSR25* expression was on the parasite surface and became higher in later stage of the asexual cycle (Moraes, Budu et al. 2017). The expression profile certainly indicates a role for *PfSR25* in a signaling mechanism. Keeping this hypothesis in mind, we tried to find if *PfSR25* play any role in Ca^{2+} homeostasis. Thus late *PfSR25*$^{-}$ trophozoites were loaded with Fluo-4AM in low K^{+} buffer and Ca^{2+} flux was detected as change in fluorescence by flow cytometry. Similarly, parasites were submitted to changes in the buffer content from low K^{+} to high K^{+} buffer and the internal Ca^{2+} fluctuation was observed. The result in **Figure 11A** depicts that *PfSR25*$^{-}$ fail to show internal Ca^{2+} mobilization as seen in wild type 3D7 parasites. We also performed the experiment in opposite condition, when *PfSR25*$^{-}$ parasites were loaded with Fluo-4AM in high K^{+} and then switched from high K^{+} to low K^{+} buffer. Surprisingly, our result in **Figure 11B** showed that contrary to wild type 3D7 parasites, *PfSR25*$^{-}$ parasites were unable to show internal Ca^{2+} efflux in low K^{+} change. The average geometric mean of Fluo-4AM calculation in **Figure 11D** did not exhibit any statistical difference in both interchangeable buffer.

The inability of knockout parasites to respond in low K^{+} could be due to unavailability of Ca^{2+} in *PfSR25*$^{-}$ internal pools. To discard this possibility, we performed another control experiment to validate that these parasites do maintain basal levels of Ca^{2+}. Unable to respond to low K^{+} is the result of change in genetics but not the fitness or lower Ca^{2+} in internal pools. We

treated the *PfSR25*$^{-}$ parasites with another Ca^{2+} ATPase SERCA inhibitor thapsigargin (THG). We found that when *PfSR25*$^{-}$ parasites were moved from high K^{+} to low K^{+} in presence of 5 μM THG, Ca^{2+} efflux from internal stores occurred. The results in **Figure 11C & D** indicate that in *PfSR25*$^{-}$ parasites, internal Ca^{2+} stores are normally filled and *PfSR25* senses the change in lower potassium.

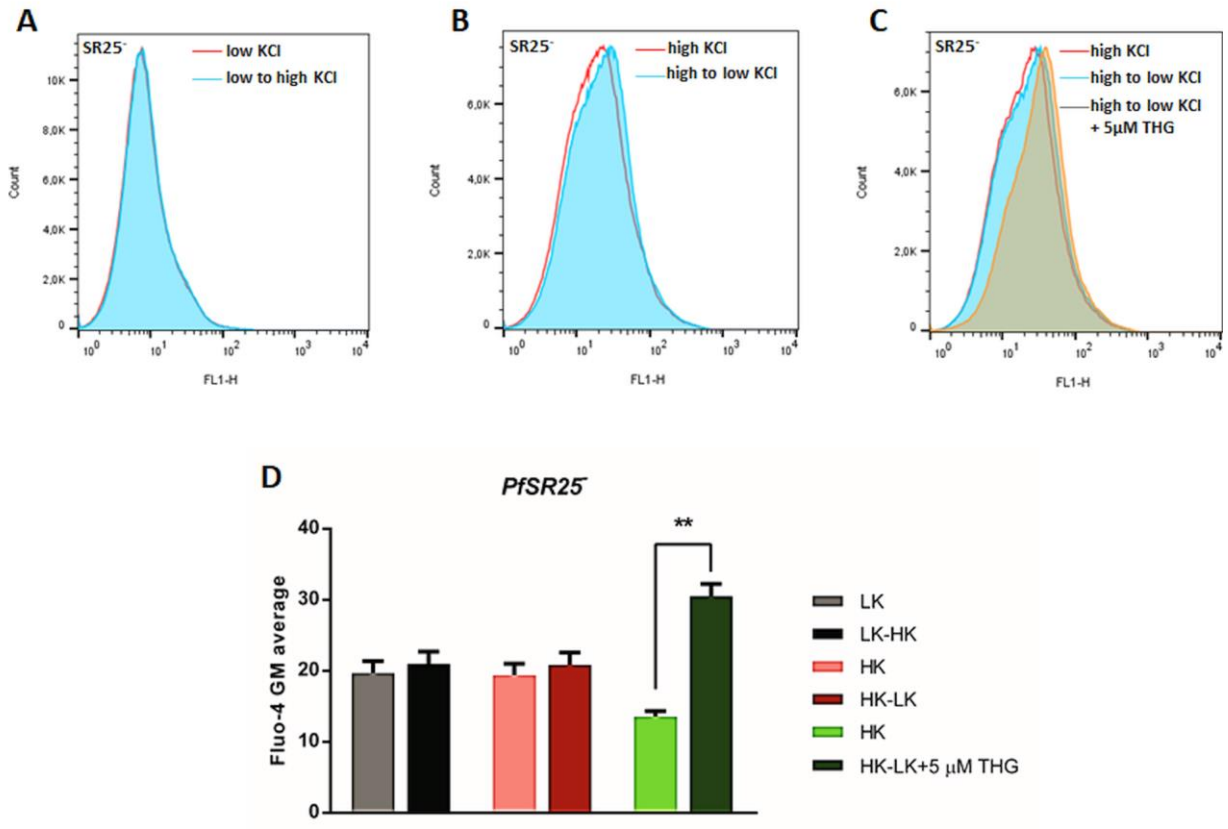

Figure 11: Effect of $[Ca^{2+}]_{cyt}$ level in PfSR25 knockout parasites.

(A) Isolated trophozoite stage *PfSR25* knockout parasites were first loaded with Fluo-4AM dye in high K buffer for an hour and switching to low K did not elicit any $[Ca^{2+}]_{cyt}$ rise. Similarly, opposite treatment was unable to show any response **(B).** When parasites were switched from high to low K buffer and SERCA inhibitor thapsigargin was added a shift at x-axis was observed **(C). (D)** Geometric mean average of Fluo-4AM of three independent experiments was calculated and statistical analysis was calculated by student's t-test using Graphpad prism V5. ** $p<0.01$

4.1.5 ATP triggers increase in $[Ca^{2+}]_{cyt}$ in *P. falciparum* merozoites

We have also investigated another aspect of signaling mechanism such as ATP and that if it played any role in molecular signaling in *P. falciparum* merozoites. Malaria parasites exhibit a broad range of tolerance to the ionic environment and in an *in vitro* study demonstrated that high potassium has no effect in growth or invasion (Pillai, Addo et al. 2013). The redundancy in host cell entry indicates that parasites use multiple signaling pathways for erythrocyte invasion. Our group has shown that isolated trophozoites and schizont stage parasites loaded with Ca^{2+} indicator dye Fluo-4AM exhibit Ca^{2+} release upon ATP addition. The concentration of ATP was titrated down and it was found that 50 μM ATP has maximal release in cytosolic Ca^{2+}. Blocking purinergic receptor by KN62 or degrading ATP by apyrase enzyme reduces the erythrocyte invasion of rupturing schizont (Levano-Garcia, Dluzewski et al. 2010). It was also reported that malaria parasite infected erythrocytes releases higher amount of ATP than uninfected (Akkaya, Shumilina et al. 2009). These results open the new avenue of parasites using multiple pathways inside the host's circulation for cell entry. Interestingly, in the work of Levano-Garcia et al., ATP activity for intracellular Ca^{2+} response in the parasite has been performed with either trophozoite or schizont stage of parasites. It would be more interesting to see how merozoites respond to ATP because merozoites are the only form of the RBC cycle of the parasite that directly comes in contact with the host immune response. Dissecting the signaling mechanism mediated by ATP would add our understanding of parasite invasion redundancy and may also provide the evidence that the parasites have putative purinergic signaling mechanism.

Based on the information from Levano-Garcia et al., we investigated the role of extracellular ATP in *P. falciparum* merozoites. We followed the previously reported protocol of merozoite isolation using a highly synchronous *P. falciparum* culture (Singh, Alam et al. 2010).

When majority of parasites become segmented schizonts, we allow them to rupture naturally in incomplete media and free merozoites in the media were collected by differential centrifugation (details in methods).

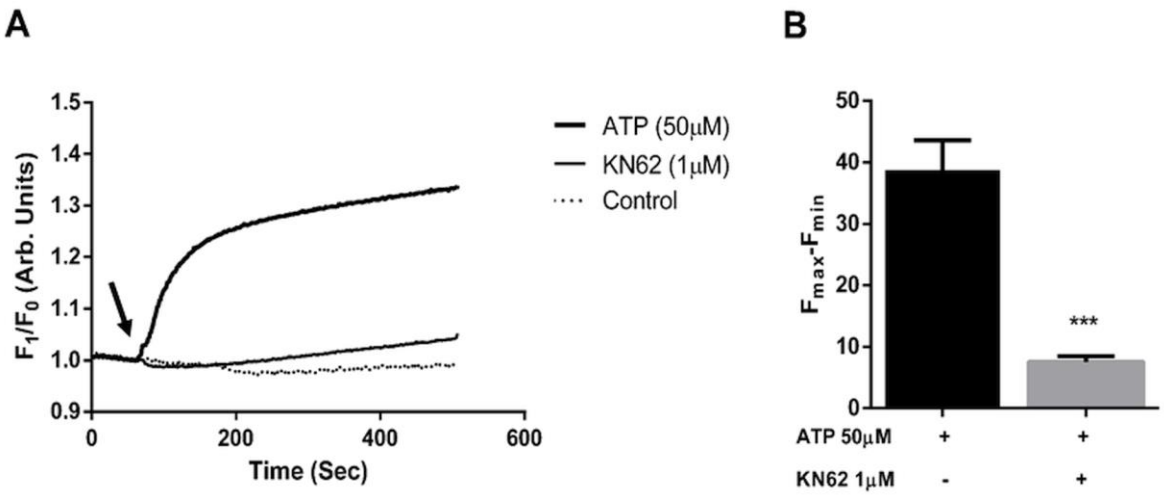

Figure 12: ATP mediated Ca^{2+} response with and without antagonist pretreatment in isolated merozoites loaded with Fluo-4AM.

(A) Fluorescence increase was depicted at y-axis (in arbitrary units, A.U.) versus time (in seconds) at x-axis. **(B)** Histogram shows the significant difference in $[Ca^{2+}]_{cyt}$ when ATP was added in untreated and KN62 pretreated merozites. Arrow indicates the time point when solvent control and ATP (50 μM) were added. $p<0.01$, two tailed unpaired t-test. Graph display mean ± SEM. n=3 in triplicate for all samples.

The Fluo-4AM loaded isolated merozoites were subjected to intracellular Ca^{2+} measurement upon 50 μM ATP stimulation. Our data in **Figure 12A** showed the typical trace of intracellular Ca^{2+} efflux after ATP addition. We found that addition of ATP triggers Ca^{2+} efflux from parasite internal stores while in the control experiment, solvent addition had no effect on the parasite Ca^{2+} rise **(Figure 12A)**. When we incubated the merozoites with the purinergic receptor P2X blocker KN62 for brief period of time, it significantly abolished the ATP-mediated $[Ca^{2+}]_{cyt}$ release **(Figure 12A & B)**. Our results of ATP-induced Ca^{2+} release opens the possibility that merozoite may also have alternate machinery for host cell invasion that depend on ATP via $[Ca^{2+}]_{cyt}$ release. In *P. falciparum,* the identification of a purinergic receptor has not been reported yet but using KN62 prevents the Ca^{2+} efflux. It suggests that ATP binding to the hypothetical purinergic receptor may stimulate downstream signaling to facilitate invasion. The phenomenon of Ca^{2+} rise is essential for invasion, which was already observed by many groups.

On the other hand, not just ATP but other purines (ADP, CTP, GTP, and UTP) have been shown to couple with cAMP and Ca^{2+}-mediated signaling pathway in other eukaryotic systems. Our group has shown that infected parasites do exhibited Ca^{2+} response to ADP but the response was rather lower than ATP. We also investigated that unlike trophozoites or schizonts, whether ADP can modulate the Ca^{2+} rise in free merozoites. We have performed the experiment with merozoites loaded with Fluo-4AM and measured the Ca^{2+} release upon 50 μM ADP stimulus. Surprisingly, our result in **Figure 13 A & B** showed that merozoite stage parasites were able to efflux significant Ca^{2+} upon ADP addition when compared to the control experiment. Ca^{2+} efflux was comparatively similar to ATP response.

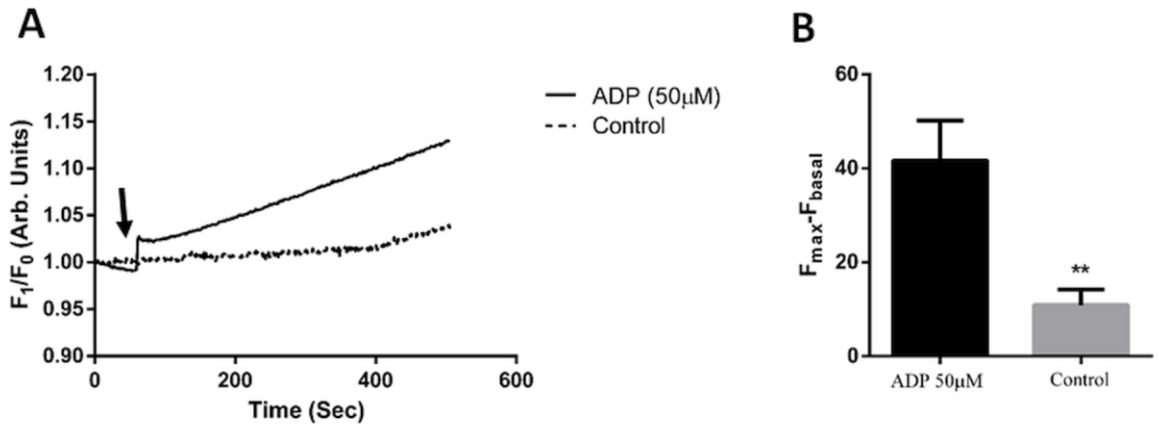

Figure 13: ADP mediated Ca^{2+} response in isolated merozoites loaded with Fluo-4AM.

(A) Fluorescence increase was depicted at y-axis (in arbitrary units, A.U.) versus time (in seconds) at x-axis. **(B)** Histogram shows the significant difference in $[Ca^{2+}]_{cyt}$ when ADP and solvent control was added. Arrow indicates the time point when solvent control and ADP (50 μM) were added. $p<0.01$, two tailed paired t-test. Graph display mean ± SEM. n=3 in triplicate for all samples.

4.1.6 Calcium efflux by digestive vacuole conferred to PfCRT mutation

The third subproject on signaling in malaria is related to investigating the Ca^{2+} homeostasis by digestive vacuole (DV) in collaboration with Dr. David Fidock (Columbia University, USA). In *P. falciparum,* three major Ca^{2+} storage pools, namely, the endoplasmic reticulum (ER), mitochondria and acidic digestive vacuole (DV) have been widely regarded (Garcia, Ann et al. 1998, Varotti, Beraldo et al. 2003, Gazarini and Garcia 2004, Alves, Bartlett et al. 2011). Capability to mobilize Ca^{2+} from not only the ER but also from an acidic compartment by IP_3 in *P. chabaudi* provides the evidence of an acidic organelle involvement in Ca^{2+} signaling (Passos and Garcia 1998). A recent study demonstrated the Ca^{2+} flux from an acidic compartment by disrupting the proton gradient using ionophores such as monensin or nigericin (Varotti, Beraldo et al. 2003). *P. falciparum* converts free heme into inert the hemozoin crystal that accumulates and grows inside the DV as the parasite matures. The digestive vacuole membrane (DVM) contains the protein chloroquine resistant transporter (PfCRT) (Fidock, Nomura et al. 2000). The DV is also the target of the antimalarial compound chloroquine (CQ) that acts on the PfCRT. It was proposed that CQ is accumulated inside the DV and impairs the hemozoin conversion, while PfCRT plays a role in the CQ efflux from the DV **(Figure 14A)**. Inability of the parasite to convert heme into hemozoin is detrimental for the parasite's survival, however; mutation in PfCRT renders the parasite resistant to CQ. The PfCRT is a transmembrane protein and mutation at K76T (Lysine is replaced by Threonine) attributes to the parasite resistance to CQ **(Figure 14B).**

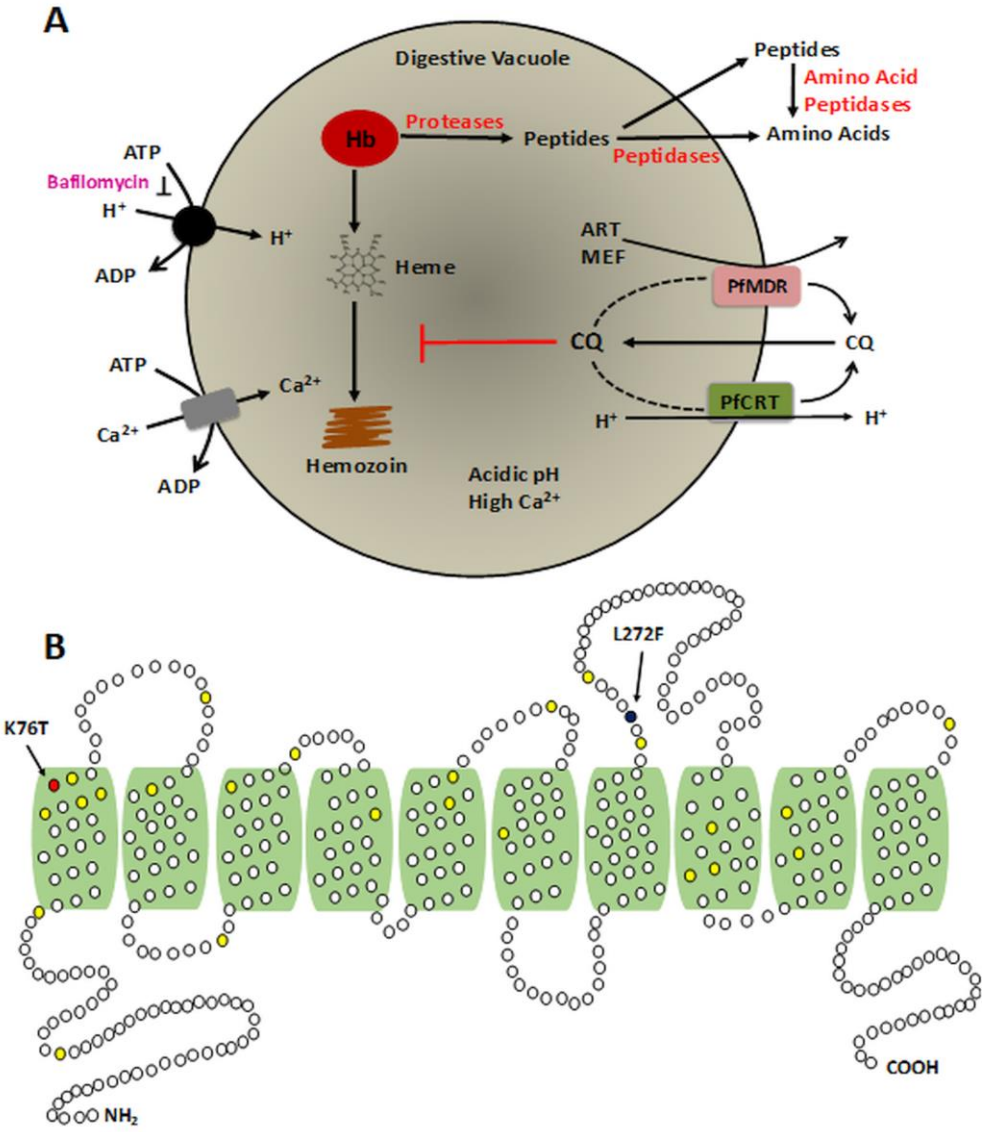

Figure 14: Schematic diagram of *P. falciparum* digestive vacuole and organization of chloroquine resistance transporter.

(A) Schematic representation of a typical digestive food vacuole, which has low pH and high Ca^{2+}. Hemoglobin is transported inside DV and digested into heme and peptides, where peptides get converted into smaller amino acids. The remaining heme fragments get converted into inert hemozoin molecule and the antimalarial CQ blocks the hemozoin conversion. **(B)** Typical representation of *P. falciparum* chloroquine resistance transporter (PfCRT) where various reported mutations are shown in yellow color. The red dot represents the K76T mutation that is reported in virtually all drug resistant *P. falciparum.* Figure 14B is modified from (Ecker, Lehane et al. 2012).

Based on this, we have investigated the role of PfCRT in Ca^{2+} efflux from the digestive vacuole. We used genetically modified *PfCRT* locus to explore the intracellular Ca^{2+} homeostasis in *P. falciparum*. For the Ca^{2+} measurement studies, we used six *P. falciparum* strains that were categorized into chloroquine sensitive (CQS) - GC03, 3D7, $Dd2^{GC03}$ & $Dd2^{Dd2\ L272}$ and chloroquine resistant (CQR) - Dd2, $Dd2^{Dd2}$ **(Table 3)**. This study was done in collaboration with Dr. David Fidock, Columbia University, USA. He has provided all PfCRT haplotype strains and we used 3D7 parasite for additional control.

Table 3: Detail list of parasite strains used for Ca^{2+} measurement

Strains	Characteristics	Drug Sensitivity
3D7	Wild type *P. falciparum* strain having original pfcrt gene.	CQS*
GC-03	Wild type *P. falciparum* strain having original pfcrt gene.	CQS
Dd2	Parental *P. falciparum* strain having mutated pfcrt gene.	CQR*
$Dd2^{Dd2}$	Dd2 background strain, endogenous Dd2 pfcrt locus replaced with cDNA pfcrt	CQR
$Dd2^{GC-03}$	Dd2 background strain, endogenous Dd2 pfcrt locus replaced with GC-03 cDNA pfcrt	CQS
$Dd2^{Dd2\ L272F}$	Dd2 background strain, endogenous Dd2 pfcrt locus replaced with cDNA pfcrt L272F cDNA	CQS

*CQS – Chloroquine sensitive; COR – Chloroquine resistant

We used mid stage trophozoites (approximately 30-34 hpi) to conduct the Ca^{2+} experiment because at this phase, trophozoites are metabolically very active and the rate of hemoglobin digestion is high. Parasites were challenged with Na^+/H^+ ionophore monensin at 25 µM, **(Figure 15A)**, K^+/H^+ ionophore nigericin at 10 µM **(Figure 16A)** and the antimalarial compound CQ at 80 µM **(Figure 17A)**. Monensin and nigericin is known to disrupt the Na^+/H^+

and K^+/H^+ electrochemical gradients respectively study by (Gazarini, Sigolo et al. 2017) showed that CQ also attribute to alkalization by mobilizing H^+ and subsequently Ca^{2+} release.

Monensin, nigericin or CQ stimulus disrupted the ionic balance and changed the electrochemical gradient across the DV in CQS strains 3D7 and GC03, as a result, higher Ca^{2+} was released in the cytosol from the DV. Meanwhile, $[Ca^{2+}]_{cyt}$ influx in the CQR strains (Dd2 and $Dd2^{Dd2}$) was significantly reduced to 1.5 fold when compared to the CQS strains (3D7 or GC03). Moreover, when the $[Ca^{2+}]_{cyt}$ efflux in Dd2 was compared with CQS isogenic background GC03 expressed in Dd2 ($Dd2^{GC03}$), the restoration in Ca^{2+} mobilization was observed with almost 1.4-fold change in $[Ca^{2+}]_{cyt}$. A similar observation was seen in $Dd2^{Dd2}$ strain when Dd2 background strain, endogenous Dd2 pfcrt locus was replaced with cDNA pfcrt. It is important to note that the Dd2 and isogenic strain $Dd2^{Dd2}$ is CQR and contain K76T mutation conferred to drug resistance. Introduction of another mutation by changing the amino acid at 272 (L272F) drastically changes the $[Ca^{2+}]_{cyt}$ efflux from the DV irrespective of monensin, nigericin or CQ treatment for $Dd2^{Dd2\ L272F}$ parasites. The reduction observed in $Dd2^{Dd2\ L272F}$ parasites was approximately 2-2.5 fold with CQS strains 3D7, GC03 and in $Dd2^{GC03}$ for monensin, nigericin and CQ. Relative to Dd2 or $Dd2^{Dd2}$, the L272F mutant further reduced free Ca^{2+} release by 1.6-fold (p<0.0001), 1.2-fold (p<0.0001), and 1.3-fold (p<0.01), for treatments with monensin, nigericin and chloroquine, respectively. The typical Ca^{2+} response is depicted for monensin **(Figure 15C),** for nigericin **(Figure 16C)** and for antimalarial drug CQ **(Figure 17C)**. Similarly, solvent control DMF for monensin **(Figure 15D)**, DMSO for nigericin **(Figure 16D)** and buffer M for chloroquine **(Figure 17D)** did not confer a $[Ca^{2+}]_{cyt}$ rise.

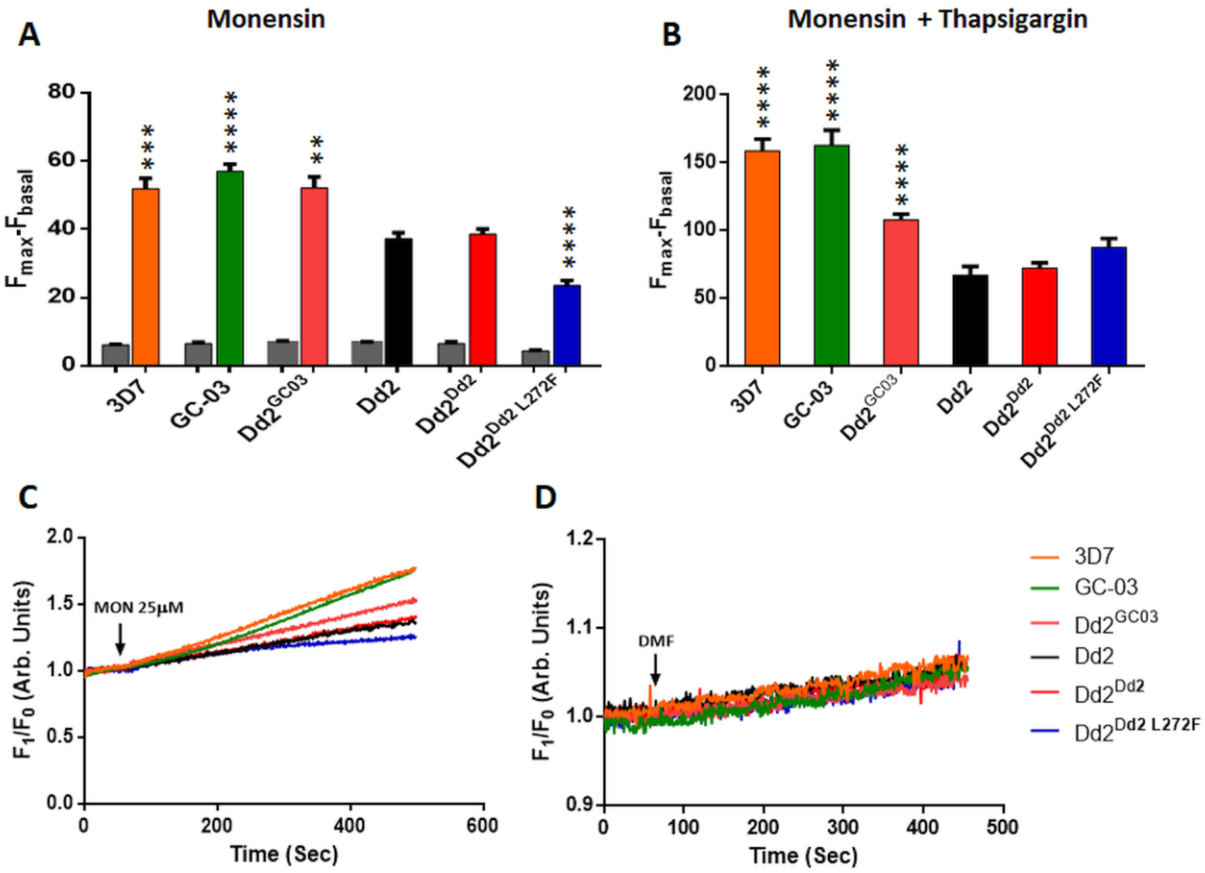

Figure 15: Monensin triggers intracellular Ca^{2+} from the *P. falciparum* digestive vacuole.

(A) The efflux of free Ca^{2+} from the DV into the cytoplasm was measured using the fluorescent dye Fluo-4 AM for 3D7 (orange), GC03 (green), $Dd2^{GC03}$ (pink), Dd2 (black), $Dd2^{Dd2}$ (red), $Dd2^{Dd2\ L272F}$ (blue) after monensin treatment. All three CQS strains expressing wild-type *pfcrt*, namely 3D7, GC03 and the $Dd2^{GC03}$, efflux significantly more free Ca^{2+} than the CQR line $Dd2^{Dd2}$, whose Ca^{2+} efflux is very similar to non-recombinant Dd2. The Dd2+L272F variant, which is nearly fully sensitive to CQ, shows the lowest rate of Ca^{2+} efflux. **(B)** Each strain was independently treated with monensin (25 µM) plus thapsigargin (5 µM) as ER Ca^{2+} efflux control. Ca^{2+} efflux from ER was more pronounced than CQS strains. Representative fluorescence intensity (F_1/F_0) over a time course for single experiment was presented for each strain for **(C)** monensin and **(D)** control addition. F_1 is the Fluo-4 AM signal intensity of monensin-treated parasites; and F_0 is the signal intensity for control treatments. Data are presented as means ± SEM, calculated from nine independent experiments. **p< 0.01, ***p< 0.001, ****p< 0.0001; two-tailed Mann-Whitney *U* test relative to $Dd2^{Dd2}$.

In all these experiments, drugs were added anywhere between 50-60 sec and then Ca^{2+} was monitored for 400-500 sec and then the SERCA inhibitor compound thapsigargin (THG) as positive control was added. Interestingly the pattern of the ER Ca^{2+} flux after THG addition was undistinguishable among CQS haplotype 3D7 and GC03 **(Figure 15B, 16B & 17B)**. Similar pattern was observed among CQR haplotype Dd2 or $Dd2^{Dd2}$. However, replacing the CQR endogenous PfCRT with CQS cDNA in Dd2 background restore the ER Ca^{2+} mobilization as observed in wild CQS strains, not fully but significantly different from $Dd2^{Dd2}$ haplotype. The pattern of the ER Ca^{2+} efflux was rather higher in $Dd2^{Dd2\ L272F}$ than Dd2 haplotypes but significant difference was observed only in K^+/H^+ ionophore nigericin treatment. These data together reflect the important role for PfCRT mutations in regulating DV membrane permeability to Ca^{2+} and also pointed out that along with the parasite ER and mitochondria, DV also plays a relevant role in Ca^{2+} homeostasis.

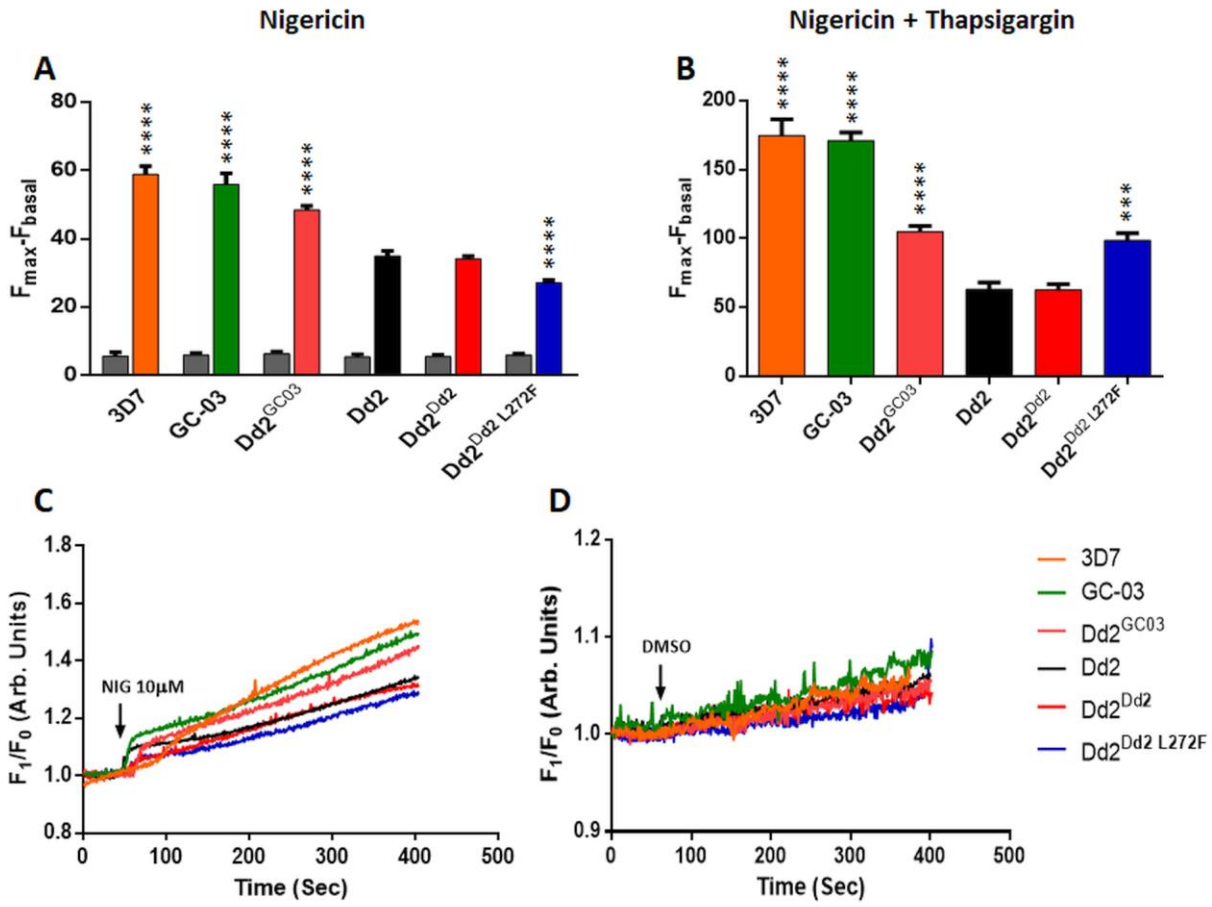

Figure 16: Nigericin triggers intracellular Ca^{2+} from the *P. falciparum* digestive vacuole.

(A) The efflux of free Ca^{2+} from the DV into the cytoplasm was measured using the fluorescent dye Fluo-4 AM for 3D7 (orange), GC03 (green), $Dd2^{GC03}$ (pink), Dd2 (black), $Dd2^{Dd2}$ (red), $Dd2^{Dd2\ L272F}$ (blue) after nigericin treatment. All three CQS strains expressing wild-type *pfcrt*, namely 3D7, GC03 and the $Dd2^{GC03}$, efflux significantly more free Ca^{2+} than the CQR line $Dd2^{Dd2}$, whose Ca^{2+} efflux is very similar to non-recombinant Dd2. The Dd2+L272F variant, which is nearly fully sensitive to CQ, shows the lowest rate of Ca^{2+} efflux. **(B)** Each strain was independently treated with nigericin (10 µM) plus thapsigargin (5 µM) as ER Ca^{2+} efflux control. Ca^{2+} efflux from ER was more pronounced than CQS strains. Representative fluorescence intensity (F_1/F_0) over a time course for single experiment was presented for each strain for **(C)** nigericin and **(D)** control addition. F_1 is the Fluo-4 AM signal intensity of monensin-treated parasites; and F_0 is the signal intensity for control treatments. Data are presented as means ± SEM, calculated from nine independent experiments. $^{**}p< 0.01$, $^{***}p< 0.001$, $^{****}p< 0.0001$; two-tailed Mann-Whitney *U* test relative to $Dd2^{Dd2}$.

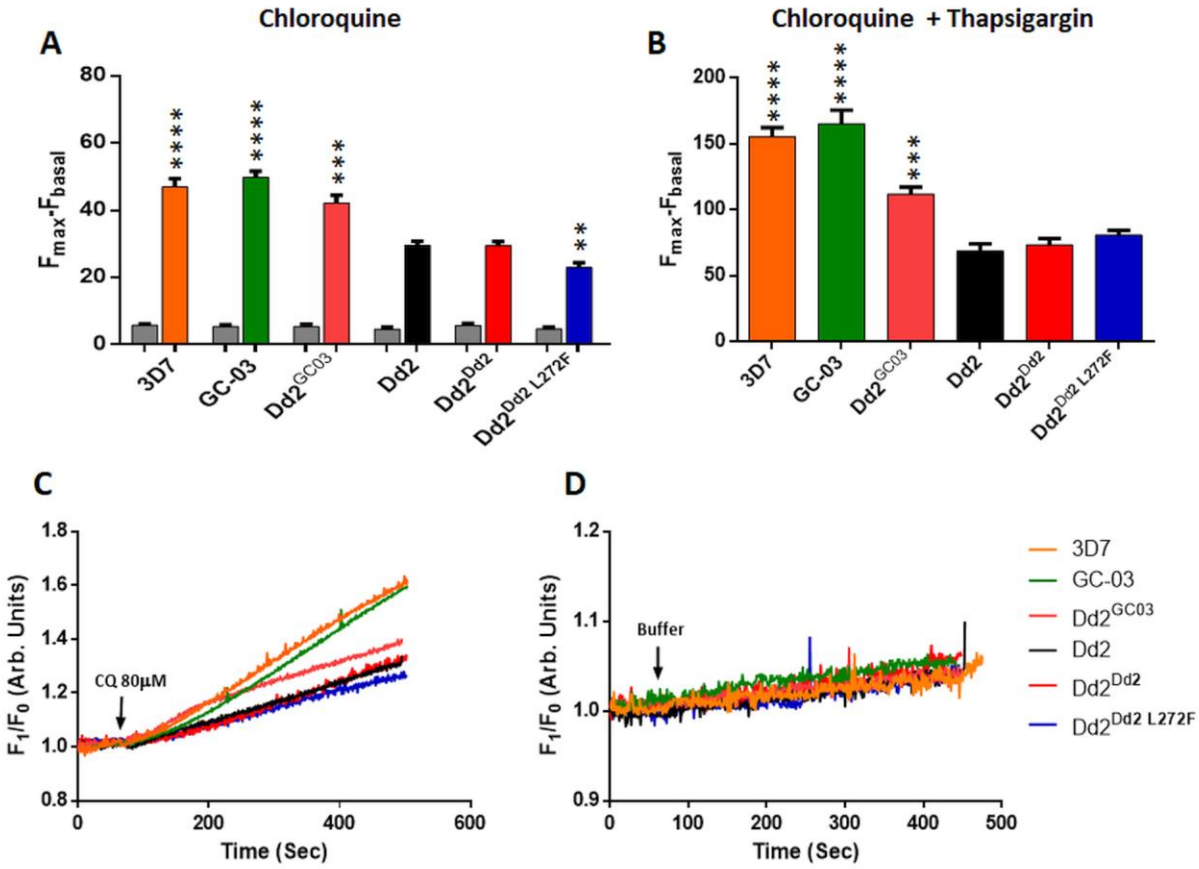

Figure 17: Chloroquine triggers intracellular Ca^{2+} from the *P. falciparum* digestive vacuole.

(A) The efflux of free Ca^{2+} from the DV into the cytoplasm was measured using the fluorescent dye Fluo-4 AM for 3D7 (orange), GC03 (green), $Dd2^{GC03}$ (pink), Dd2 (black), $Dd2^{Dd2}$ (red), $Dd2^{Dd2\ L272F}$ (blue) after monensin treatment. All three CQS strains expressing wild-type *pfcrt*, namely 3D7, GC03 and the $Dd2^{GC03}$, efflux significantly more free Ca^{2+} than the CQR line $Dd2^{Dd2}$, whose Ca^{2+} efflux is very similar to non-recombinant Dd2. The Dd2+L272F variant, which is nearly fully sensitive to CQ, shows the lowest rate of Ca^{2+} efflux. **(B)** Each strain was independently treated with chloroquine (80 µM) plus thapsigargin (5 µM) as ER Ca^{2+} efflux control. Ca^{2+} efflux from ER was more pronounced than CQS strains. Representative fluorescence intensity (F_1/F_0) over a time course for single experiment was presented for each strain for **(C)** chloroquine and **(D)** control addition. F_1 is the Fluo-4 AM signal intensity of monensin-treated parasites; and F_0 is the signal intensity for control treatments. Data are presented as means ± SEM, calculated from nine independent experiments. $^{**}p< 0.01$, $^{***}p< 0.001$, $^{****}p< 0.0001$; two-tailed Mann-Whitney *U* test relative to $Dd2^{Dd2}$.

4.2 Melatonin signaling in the P. falciparum

Another aspect of this thesis is related to investigate the molecular mechanism by which melatonin plays a role in *P. falciparum* asexual development. Melatonin does modulate the expression pattern of various genes, especially genes involved in ubiquitin/proteasome system (UPS) in both mammalian cells and human malaria parasite *P. falciparum* (Cho, Kim et al. 2007, Sung, Cho et al. 2009, Koyama, Ribeiro et al. 2012). In *P. falciparum,* melatonin and its derivatives modulate the asexual cycle in a Ca^{2+}-dependent manner (Hotta, Gazarini et al. 2000, Beraldo and Garcia 2005). How melatonin governs the signaling event affecting cell cycle is still poorly understood. Although receptors for melatonin have been identified in mammalian systems, they are yet to be identified in *Plasmodium* genome. In this study, we have investigated the regulating factor modulated by melatonin and identified the gene that plays a melatonin-induced regulatory role in the *P. falciparum* intraerythocytic cycle.

4.2.1 Identification of a protein sensitive to melatonin

Dr. Luciana Madeira da Silva, a former PhD student in our lab, has searched the melatonin receptor in *P. falciparum.* Dr. Luciana (thesis title: Identificação molecular de proteínas envolvidas na transdução de sinal em *Plasmodium falciparum*) has performed a detailed work in our laboratory following a protocol in which authors have isolated the melatonin receptor from lizard brain (Rivkees, Conron et al. 1990). Melatonin-agarose (Mel-Aga) resins, was prepared by coupling 6-hydroxymelatonin to 6-epoxy activated sepharose and was used for unbiased binding and isolation of hypothetical melatonin receptor. Mass spectrometry (LC-MS/MS) was performed to identify the unknown binding proteins from genomic DNA data bank of *P. falciparum* PlasmoDB server. Unfortunately, no success was achieved to isolate such

receptor, although two important proteins that bound with melatonin were identified. One of the identified proteins was Pf1468 (PlasmoDB ID: PF3D7_1468100) that does not have any functional topology resemble to putative melatonin receptor. It is located on chromosome 14 of *P. falciparum* spanning from 2786308-2794323 bp having 2 exons. The transcript length is 7677 bp with 2558 amino acids and its approximate molecular weight is 295 kDa.

We performed a bioinformatics analysis using the SMART server (http://smart.embl-heidelberg.de/), which suggested that Pf1468 protein contains a Kelch motif and a Histidine kinase ATPase (HATPase) domain which reside from 802-1040 aa and 1280-1356 aa, respectively (**Figure 18A).** We also validated the domain organization of Pf1468 using the BLAST server (https://blast.ncbi.nlm.nih.gov/Blast.cgi?PAGE=Proteins). From the full-length protein, we took the 750-1500 amino acid region where the SMART server predicted the Kelch motif and HATPase and ran PSI-BLAST. In the first specific hit, Kelch motif was observed from 118-163 aa and a second specific hit confirmed the HATPase from 538-592 aa from the selected protein sequence **(Figure 18B)**. The result indeed illustrated the homology with both Kelch motif and HATPase in PSI-BLAST. Transcriptomic analysis showed the continuous expression of Pf1468 mRNA throughout the *P. falciparum* life cycle. The expression level of Pf1468 becomes higher in the asexual cycle especially in early- and late trophozoites. Expression of mRNA became relatively lower in gametocytes and mosquito stage parasites suggesting the possible role of Pf1468 in modulation of parasite growth at late stage (**Figure 19).**

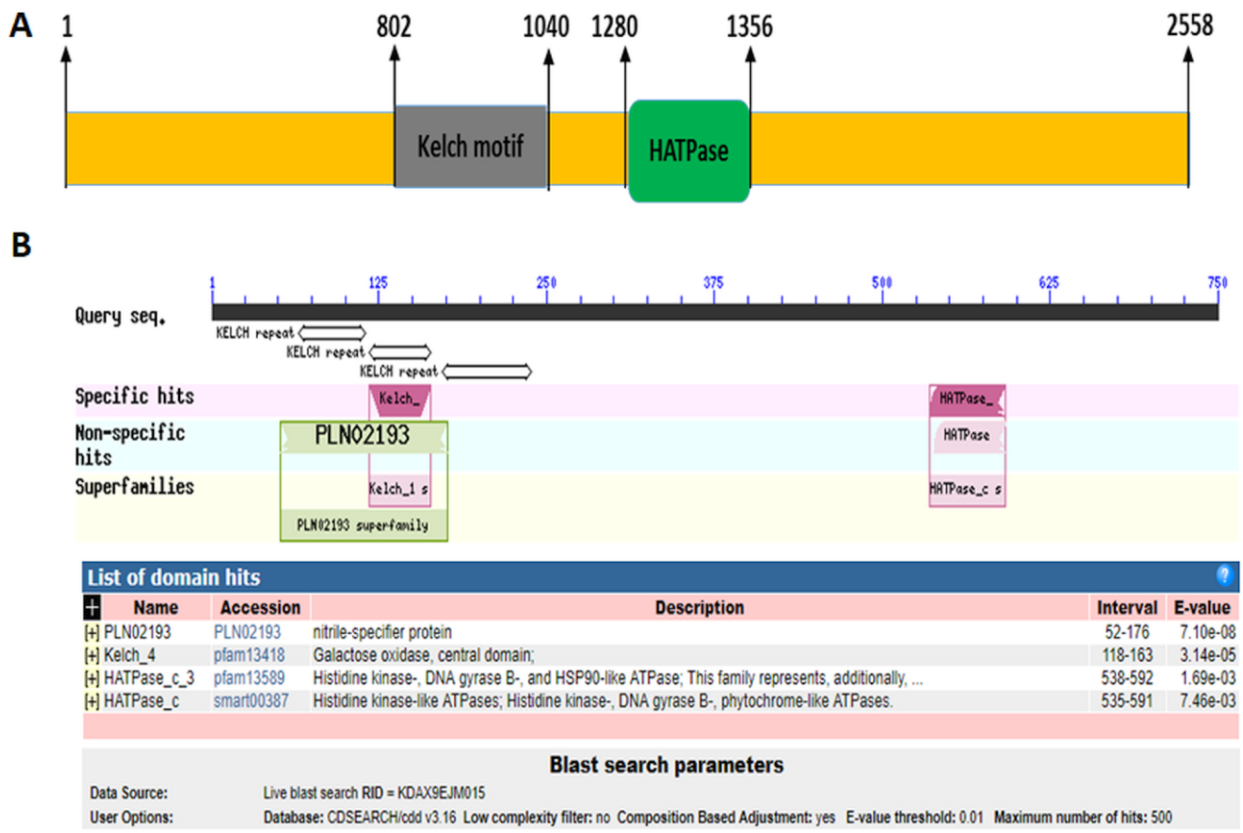

Figure 18: Domain architecture of Pf1468 protein.

(A) Schematic representation of full-length protein architecture of Pf1468. Black arrow indicating the amino acid sequence and predicted domains are shown in colored box. **(B)** Analysis of the Pf1468 protein from 750-1500 amino acids from full length was performed by PSI-BLAST search to validate the domain organization of Pf1468 protein. BLAST search gave the specific hits for Kelch motif as well as HATPase.

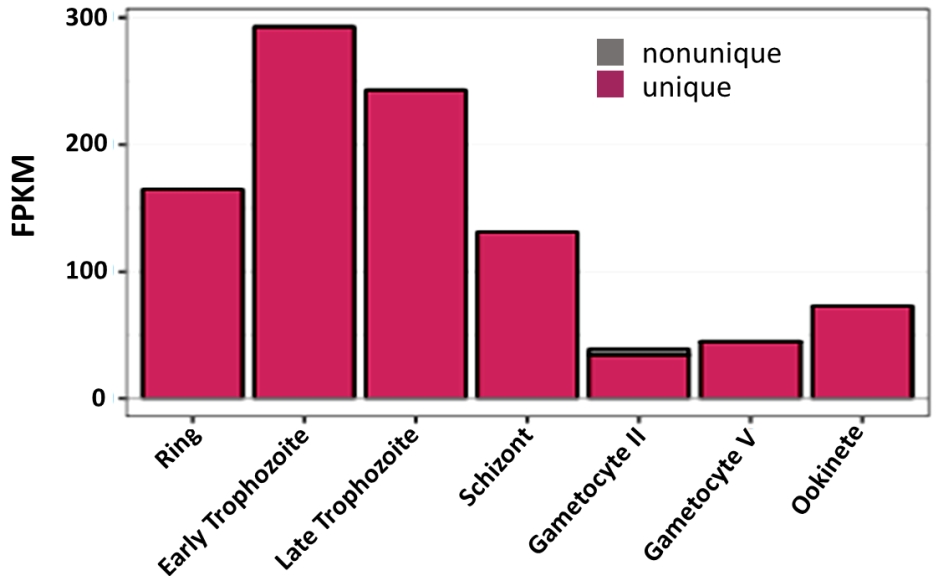

Figure 19: Expression of Pf1468 in *P. falciparum.*

Both asexual and sexual cycle transcriptome of Pf1468 at each stage is shown as transcript levels of fragments per kilobase of exon model per million mapped reads (FPKM). Figure is taken from PlasmoDB.

4.2.2 Real time PCR for Pf1468 within asexual cycle

The PlasmoDB data on expression of Pf1468 at the various development stages are given but this profiles varies with the strains. We investigated the expression of Pf1468 in wild type 3D7 parasites and Dr. Giulliana Tessarin from our lab has examined the Pf1468 mRNA transcript expression in each morphological stage of intraerythrocytic cycle. *P. falciparum* culture at ring, trophozoite and schizont stage was harvested. Total mRNA was isolated and cDNA was prepared with random primers. Primers specific for Pf1468 was used to perform the real time PCR and data was analyzed in fold change expression with ring stage parasites. The data in **Figure 20A** shows similar Pf1468 expression pattern as PlasmoDB transcriptome data

depicted in Figure 19. We found that Pf1468 expression in trophozoites and schizont was approximately 3 and 2.7 fold respectively. The result suggested that higher expression of Pf1468 transcript in late stage of asexual development (trophozoite and schizont) implicating the importance of the gene during late stage.

In vitro study reported that melatonin treatment modulate the expression of various genes, however, an orphan kinase PK7 knockout (PfPK7^{-}) was unable to exert a similar response as wild type parasites to melatonin treatment (Koyama, Ribeiro et al. 2012, Lima, Tessarin-Almeida et al. 2016). PK7 displays homology to MAPKKs C-terminal kinase domain and to N-terminal is similar to fungal protein kinase A (PKA). However, no orthologues of PfPK7 were found in the mammalian system (Dorin, Semblat et al. 2005). Interestingly, lower merozoites per schizont were observed which also implicates the role of PfPK7 in parasite proliferation and development (Dorin-Semblat, Sicard et al. 2008). To find a correlation between Pf1468 mRNA expression to melatonin treatment in wild type verses PfPK7^{-} parasites, we have performed real time PCR. Early stage trophozoites of 3D7, PfPK7^{-} and PfPK7 complement parasite strains were treated with 100 nM melatonin for 5 h and 17 h, respectively, after which total RNA was extracted. We then carried out real-time PCR with Pf1468 primers. In 3D7 parasites **(Figure 20B)**, no difference was observed in 5 h melatonin treatment but 17 h treatment showed almost 2-fold increase expression. On the other hand, PfPK7^{-} parasites exhibit partial but significant increase in 5 h melatonin treatment but contrarily 17 h treatment showed reduced expression of Pf1468 transcript **(Figure 20C)**. However, complementing PfPK7 gene in *P. falciparum* parasites significantly increase the Pf1468 transcript in 5 h melatonin treatment but 17 h treatment partially but not significantly restored the Pf1468 expression **(Figure 20D)**. These results illustrate that melatonin treatment somehow modulate the expression of Pf1468. More

importantly, down regulation in PfPK7^{-} suggests that other factors whose expression is higher at trophozoite stage may also regulate Pf1468 expression. PfPK7 somehow suppresses these unknown factors, but in PfPK7^{-}, non-suppression of PfPK7 leads to partially increased Pf1468 expression. Based on these results, henceforth we named Pf1468 as PfMel due to its sensitivity in expression against melatonin treatment.

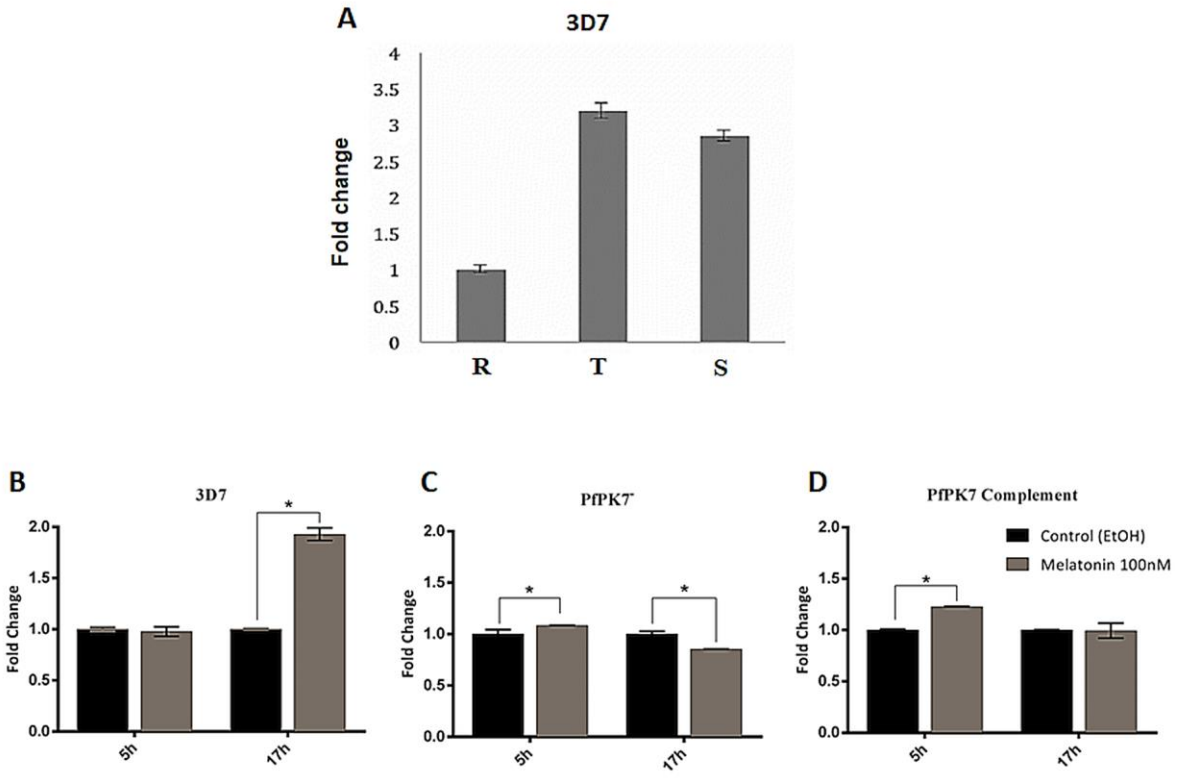

Figure 20: Real-time PCR of Pf1468 in 3D7, PfPK7 and PfPK7 complement parasites.

(A) Validation of Pf1468 transcript expression in various stages of *P. falciparum* (3D7) intraerythrocytic cycle. Stages – R: (Ring, ~10h), T: (Trophozoite, ~30h) and S: (Schizont, ~42h). Ring stage parasites are used to compare the fold change. Young trophozoite stage parasite strains 3D7 **(B)**, PfPK7^{-} **(C)**, and PfPK7 complement **(D)** were treated with 100 nM melatonin for 5 h and 17 h respectively. All experiments were performed three times in triplicate. Solvent control ethanol (EtOH) was used for statistical comparison and student t-test was carried to determine the significant difference. Representative graphics is the result of three independent experiments in triplicate. *$p<0.05$. The data in this figure was gathered by Dr. Giulliana Tessarin.

4.2.3 Construction of PfMel-GFP and protein localization in *P. falciparum* parasites

To address the localization of PfMel, we have generated parasites with the endogenous gene PfMel tagged with green fluorescent protein (GFP). PfMel-GFP construct allow us to track the localization of the protein during parasite growth in side red blood cells. The GFP containing plasmid vector were transfected into *P. falciparum* 3D7 **(Figure 21A)** and dihydrofolate reductase (DHFR) inhibitor WR99210 was used for positive selection. The positive transfected clones were verified via DNA extraction from saponin isolated parasites using PCR and restriction digestion **(Figure 21B)**. We also performed the western blots for the positive clone of *P. falciparum* transfected with PfMel-GFP, which shows clear band of approximately ~300 kDa protein while no signal was detected for control 3D7 parasites **(Figure 21C)**. To investigate the expression of PfMel in the intraerythrocytic stages of *P. falciparum* and the localization in the parasite, we performed immunofluorescent assay with PfMel-GFP construct. The parasite fractions were collected at ring, early trophozoites, late trophozoites and segmented schizonts. Fixation followed by staining with nuclear stain DAPI was done and images were captured. Our imaging data in **Figure 22** showed that PfMel colocalized with nuclear stain DAPI in all asexual stages. Thus immunofluorescent assay confirmed the nuclear localization of PfMel in ring, trophozoite and schizont.

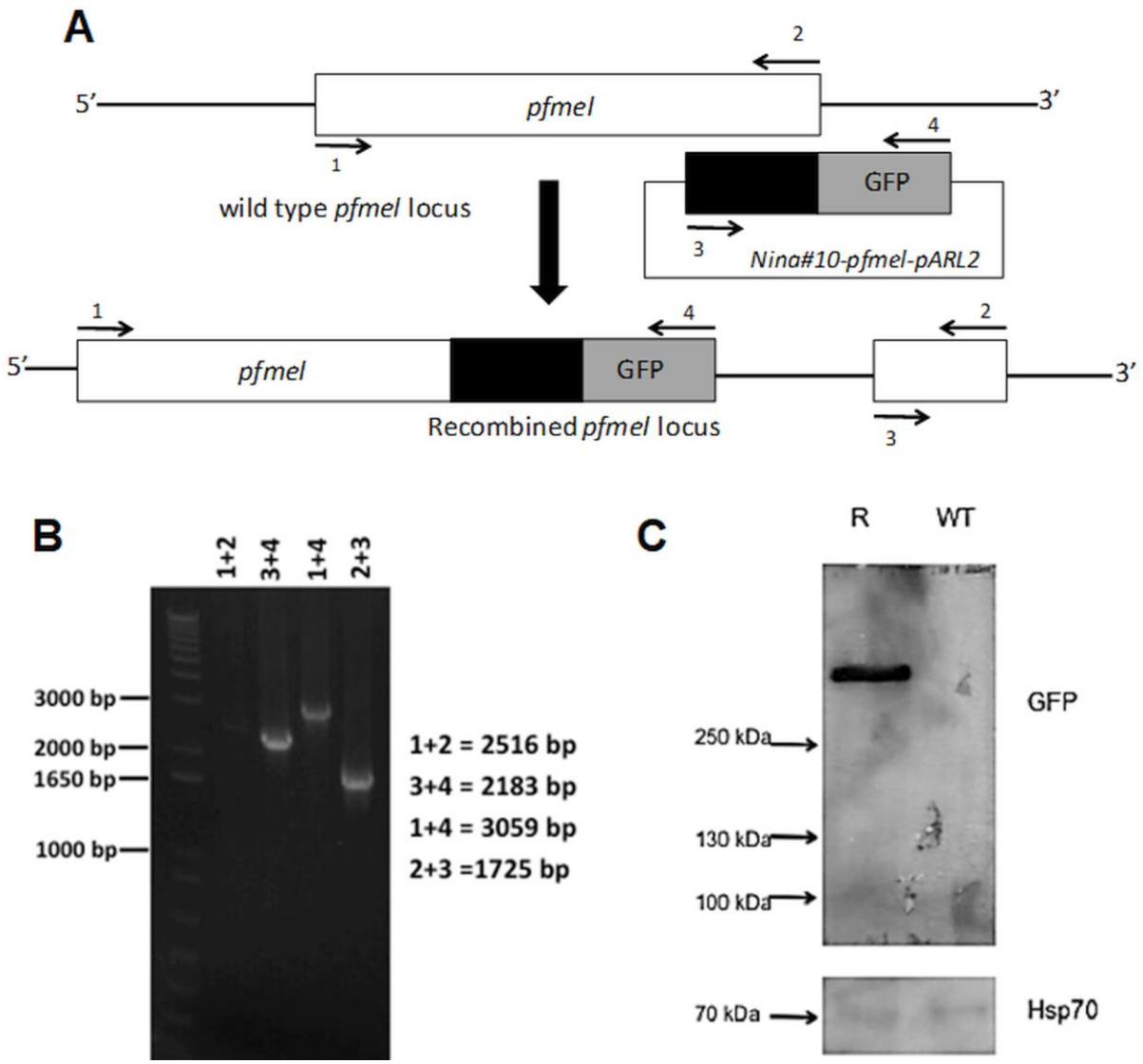

Figure 21: Schematic representation of the PfMel-GFP integration strategy.

(A) Represented cartoon of pARL2-GFP plasmid recombination with wild type *pfmel* locus to generate PfMel-GFP construct. **(B)** PCR and restriction digestion based confirmation of GFP integration in PfMel 3'-locus in isolated genomic DNA from recombinant strain. **(C)** Western blot using anti-GFP antibody to confirm the PfMel-GFP construct in recombinant (R) and wild type negative control 3D7. The PfMel-construct was prepared in Prof. Jude M. Przyborsky laboratory and Dr. Giulliana Tessarin collected the data.

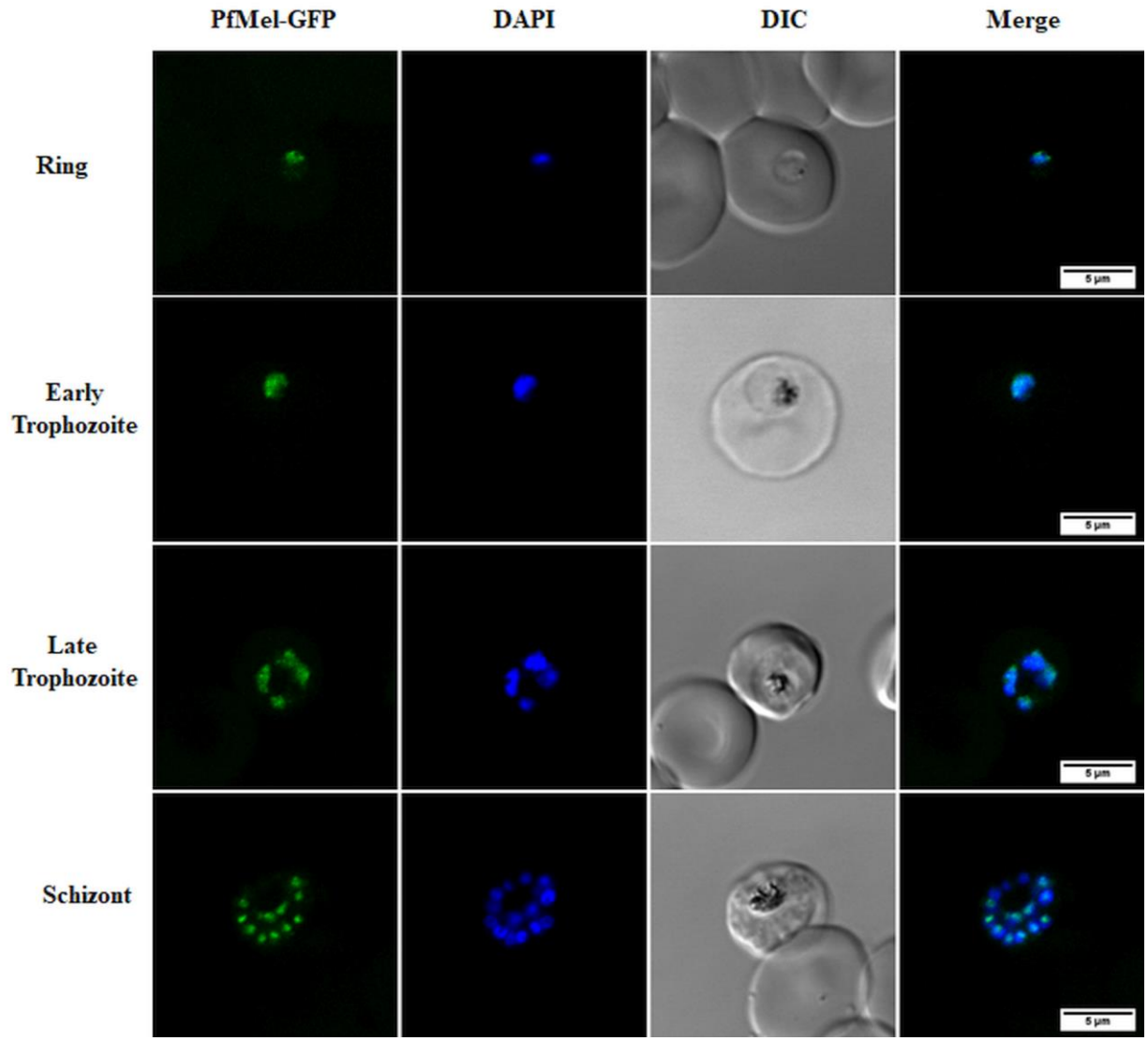

Figure 22: Confocal imaging and localization of PfMel-GFP.

Asexual rings, early-, late-trophozoites and schizonts stage parasites PfMel-GFP construct were collected and fixed. Nuclear stain DAPI was used for DNA staining and parasites were mounted on clean glass slides. Confocal images were captured and co-localization was seen.

4.2.4 Construction of PfMel gene knockdown

For studying loss of gene function, several methods are available for knocking-out or knocking-down gene expression. RNA interference (RNAi) is the most commonly used technique for attenuating expression in various model organisms but it is not applicable in *Plasmodium* species since they lack the required genes. Gene knock down is proven as a good tool to study the cell phonotype and gives better understanding of a target gene. To investigate the direct role of PfMel in *P. falciparum* asexual cycle, we used an approach with inducible ribozyme to generate a conditional knockdown system (Prommana, Uthaipibull et al. 2013, Elsworth, Matthews et al. 2014). *P. falciparum* 3D7 strain was used to develop the knockdown system and PfMel was modified by incorporating glucosamine inducible glmS ribozyme at 3' untranslated region of the gene as PfMel-HA-glmS **(Figure 23A)**. We also generated a control parasite cell line PfMel-HA **(Figure 23B)**, identical to PfMel-HA-glmS except it lacks glmS system and remains insensitive to glucosamine treatment. Transfected parasites construct PfMel-HA-glmS was then tested for the protein expression with different asexual stage parasites. Ring, trophozoite and schizont stage parasites were harvested and equal amount of protein was separated by 6% acrylamide gel. The Western blot results showed lower protein expression in ring stage while higher expression was observed in later stage of development for PfMel-HA-glmS construct **(Figure 24).** Next, we investigated the cellular localization of PfMel protein in all asexual stage parasites by confocal imaging. Immunofluorescence imaging assay was performed for both PfMel-HA **(Figure 25)** and PfMel-HA-glmS **(Fig 26)** to confirm the protein localization. We also used mitochondrial dye MitoTracker Red CMXRos along with anti-HA (rabbit) and nucleus stain DAPI. Our confocal imaging data showed that the protein is localized in the nucleus and confirmed the result obtained in Figure 21 for PfMel-GFP imaging.

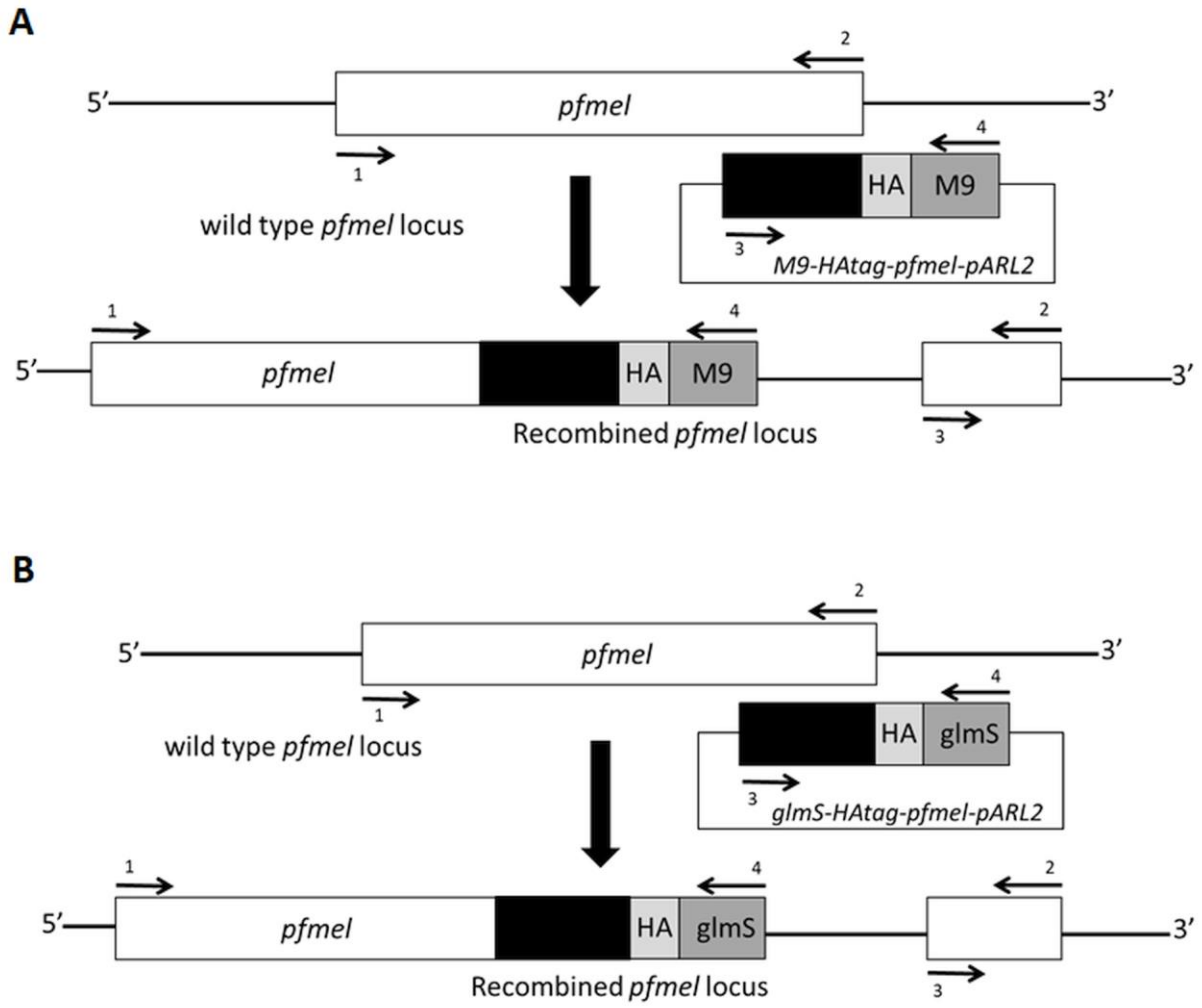

Figure 23: Schematic representation of the PfMel knockdown construction strategy.

(A) pARL2 vector containing glmS segment was used to recombine at 3' UTR region of *pfmel* to generate PfMel-HA-glmS. **(B)** Similar scheme was followed to construct PfMel-HA but pARL2-M9 empty vector that lack glmS ribozyme was recombined with *pfmel* locus. The PfMel-HA and PfMel-glmS-HA construct was prepared in Prof. Jude M. Przyborsky laboratory.

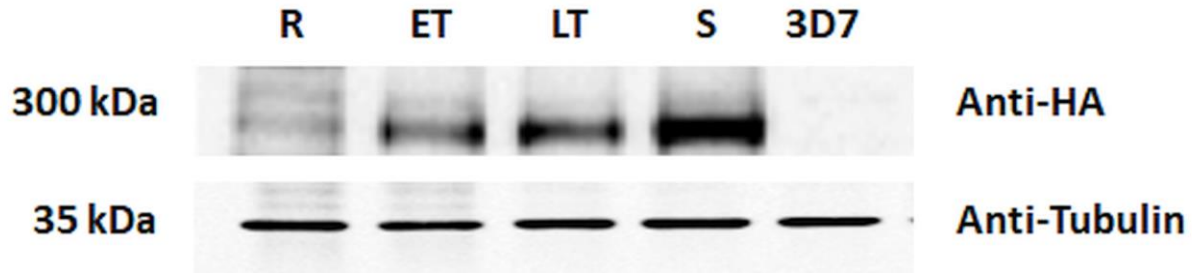

Figure 24: Expression of PfMel-HA-glmS genetic construct protein in distinct asexual stage of the parasite.

Transfected ring (R), early trophozoite (ET), late trophozoite (LT), schizont (S) and non-transfected wild type 3D7 stage parasites lysates were loaded in equal amount on 6 % polyacrylamide gel. Transferred blot was developed using anti-HA antibody and asexual stage specific protein expression of PfMel was observed.

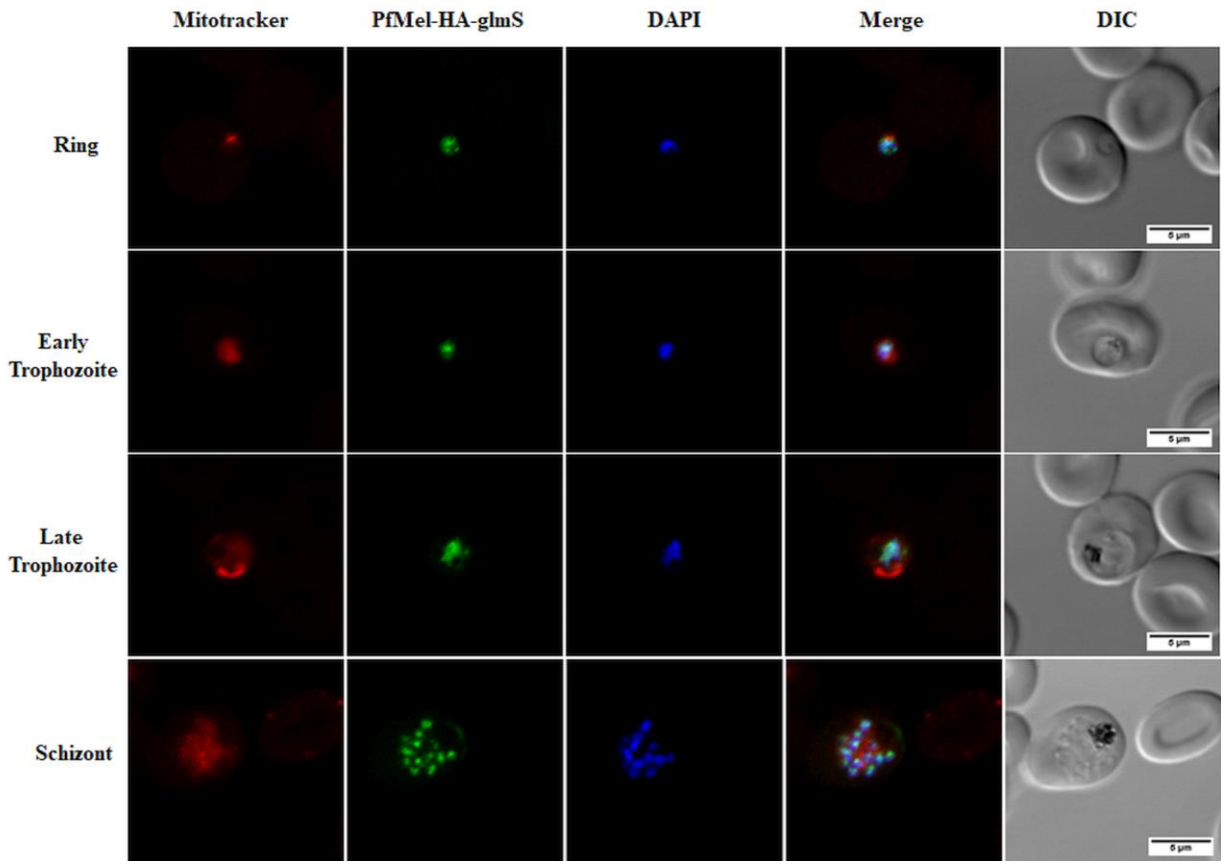

Figure 25: Immunofluorescence assay and confocal imaging of PfMel-HA-glmS.

Immunofluorescence assay and confocal microscope imaging of *P. falciparum* PfMel-HA-glmS construct. The infected erythrocytes were probed with anti-HA, mitochondrial dye mitotracker red and nuclear DNA dye DAPI to investigate subcellular localization of PfMel protein in various developmental phase. Imaging and co-localization with nucleus stain DAPI showed that PfMel localizes in nucleus.

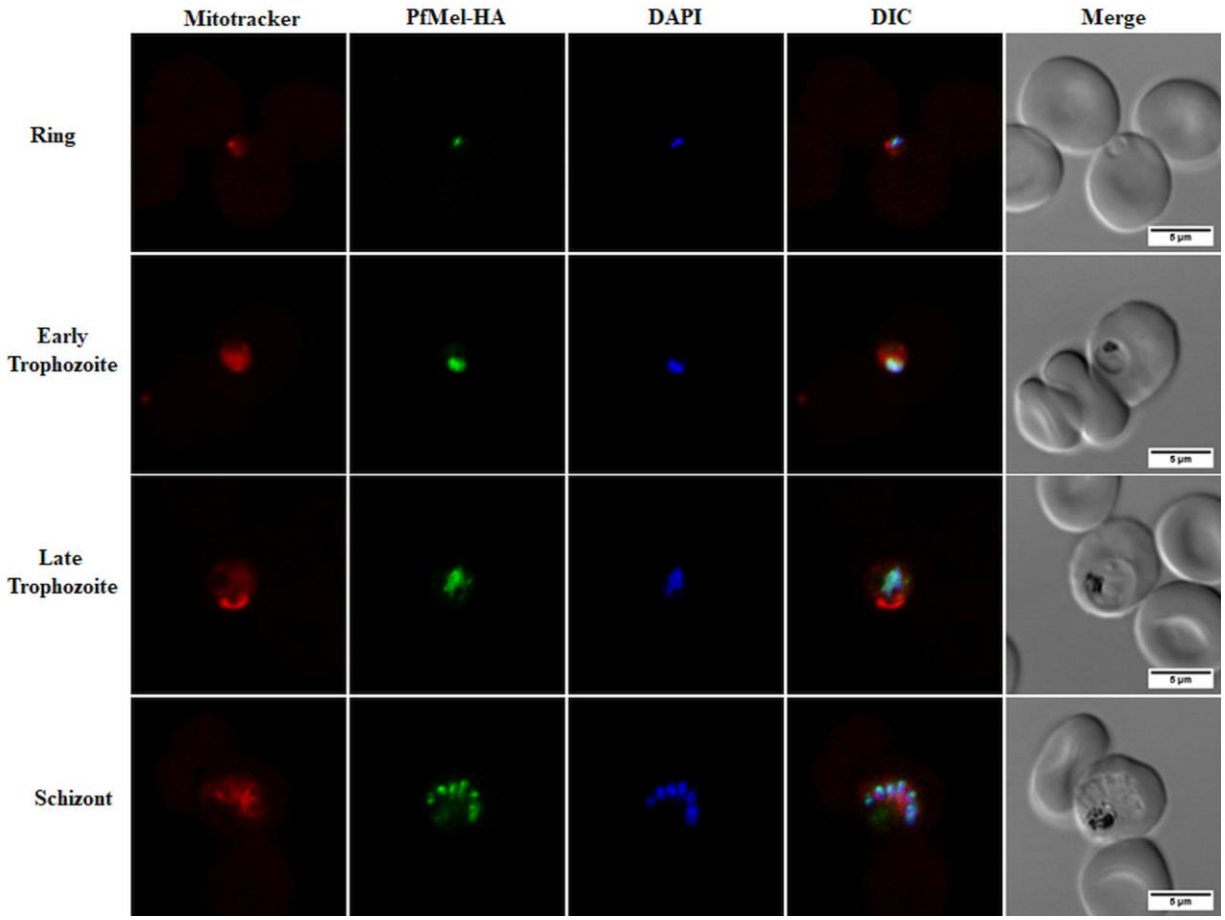

Figure 26: Immunofluorescence assay and confocal imaging of PfMel-HA.

Immunofluorescence assay and confocal microscope imaging was performed to localize PfMel-HA in *P. falciparum*-infected erythrocyte. Ring, trophozoite and schizont were stained with MitoTracker Red for mitochondria, anti-HA antibody for PfMel protein and DAPI for nuclear. Co-localization with nucleus stain DAPI shows the PfMel localizes in nucleus.

In our next study, we used the glucosamine induction of glmS ribozyme to investigate the effect of protein expression. If glucosamine addition induces the glmS ribozyme, then activated ribozyme would separate from the complete construct and digest the PfMel mRNA resulting in down regulation and lower expression of PfMel protein. To explore this possibility, *in vitro* culture of both PfMel-HA and PfMel-HA-glmS parasites were tightly synchronized and early trophozoites were incubated with 0, 0.5, 1 and 2.5 mM glucosamine. The parasites were allowed to grow until they became trophozoites in next cycle and parasite lysate was prepared. Equal amount of parasite lysate protein was resolved with SDS-PAGE and blot was developed using anti-HA (rabbit) antibody. Our Western blot data on glucosamine treatment reveals the reduction in protein level in dose dependent manner. We found more that 50 % reduction in PfMel protein expression in 2.5 mM glucosamine treated PfMel-glmS-HA parasites when compared with untreated control. However, PfMel-HA control line did not exhibit any reduction in protein level with similar dose **(Figure 27)**. Anti-tubulin (mice) was used as a positive loading control. Our Western blot data suggested that the PfMel gene is under glmS ribozyme control and indeed addition of glucosamine in *in vitro* culture affect the PfMel protein expression.

As discussed elsewhere, knockout has several morphological effects on parasites; among them one is growth progression as the cycle proceeds. In PfPK7^{-} parasites, decrease rate of asexual growth was reported as a result of lower merozoite numbers per schizont than wild type parasites and less oocyte production in mosquito vector (Dorin-Semblat, Sicard et al. 2008). Similarly, we monitored the morphological characteristics of 1468 knock down strains after glucosamine induction. We treated the PfMel knockdown parasite lines with 1 mM glucosamine at early trophozoite stage and number of merozoites per schizont was counted when majority of parasites achieved to segmented schizont in next round of growth cycle. Giemsa stained thin

smears were used for counting the merozoites number per schizont. Our result in **Figure 28A** showed that both PfMel-glmS and PfMel-HA parasites did not display any significant difference in merozoite numbers. Moreover, the number of merozoites per schizont was similar in both glucosamine treated and untreated parasites.

We have also investigated the growth pattern of knock down construct after glucosamine induction. For this assay, both PfMel-glmS-HA and PfMel-HA parasites were incubated with different concentration of glucosamine (0, 0.5, 1 and 2.5 mM) for 6 days. Thin smears were prepared every day for each concentration and parasitemia was counted every day until the completion of 3 cycles. Our data in **Figure 28B** for Pf468-glmS-HA did not exhibited any significant difference in parasite numbers when compared with control treatment. Albeit the growth of PfMel-glmS-HA parasites at 2.5 mM glucosamine concentration was marginally but not significantly slower than other lower concentration. The control strain PfMel-HA was unable to show any change in parasitemia with all tested glucosamine concentration **(Figure 28C)**.

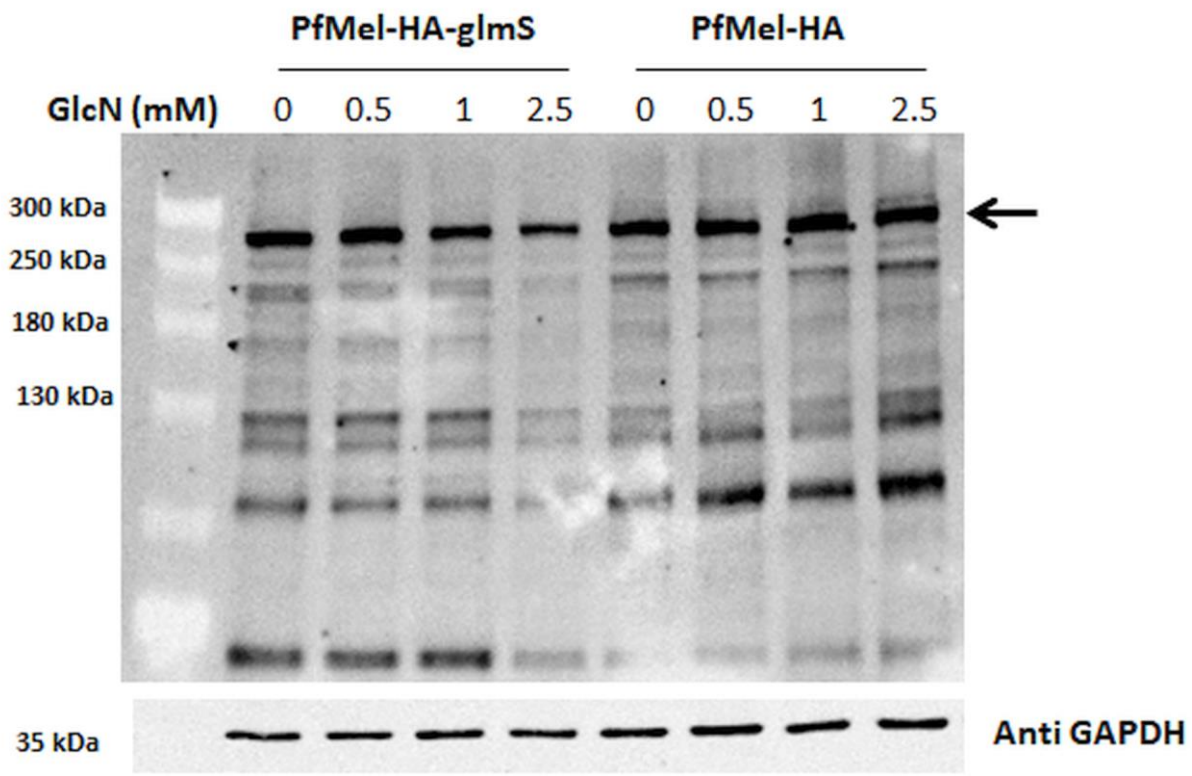

Figure 27: Analysis of the knock down of PfMel protein expression by glucosamine induction in *P. falciparum*.

Glucosamine induced knock down and control construct were resolved in 6% polyacrylamide gel. Blots were probed with anti-HA. Reduction of protein expression can be seen in PfMel-HA-glmS parasites with increased concentration of glucosamine while control strain PfMel-HA remains unaffected with glucosamine. This experiment was performed three times and single representative image is presented in the manuscript.

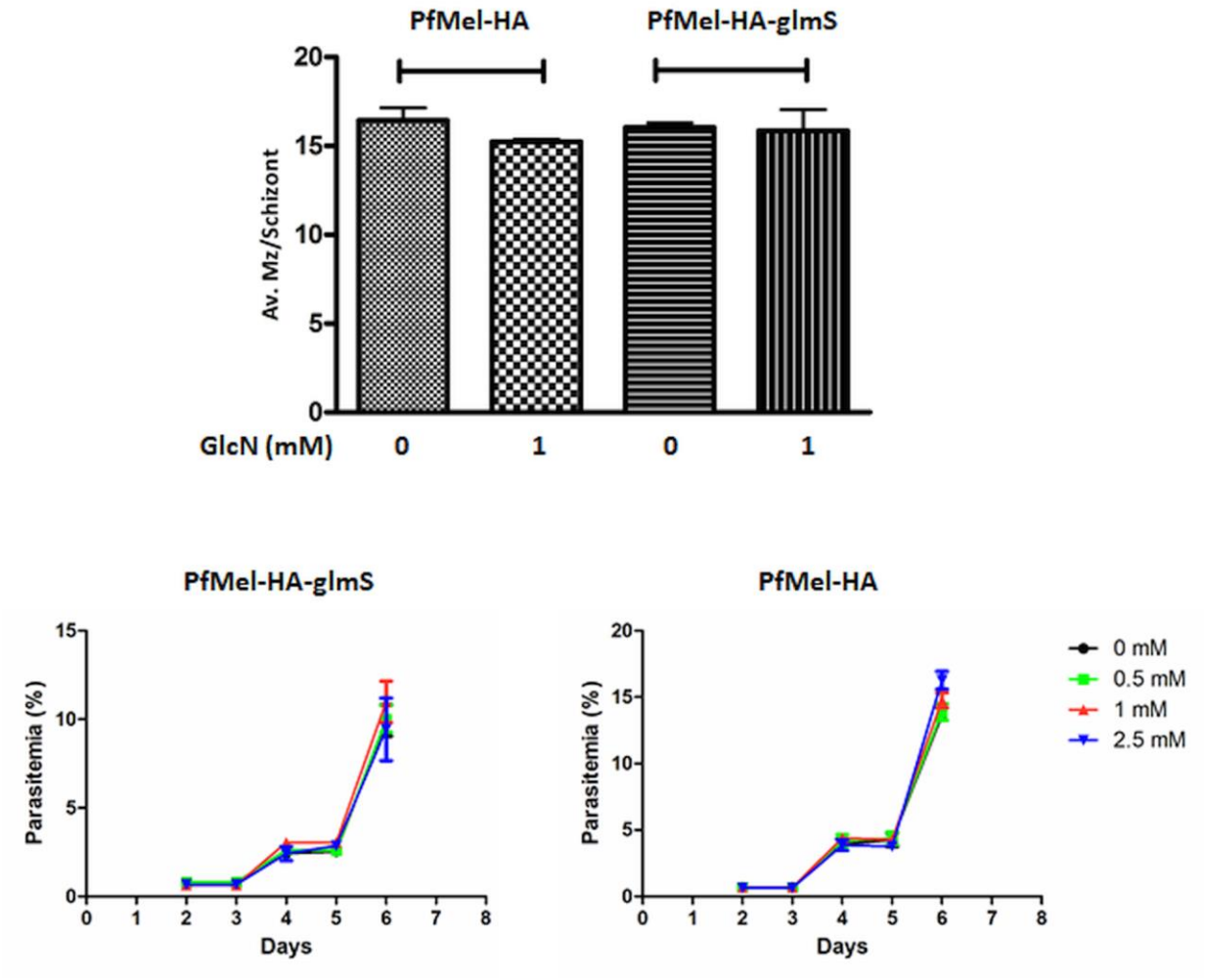

Figure 28: Evaluation of parasite growth and morphology by knocking down PfMel protein expression with glucosamine treatment.

(A) Early trophozoites were treated with 1 mM glucosamine along with control having no glucosamine. The parasites were allowed to grow till next cycle and smears were prepared when majority of parasites reached to segmented schizont. Average of merozoites per schizont in populations, were obtained by counting at least 40 parasites for each replicates. **(B)** Different concentration of glucosamine (0.5, 1 and 2.5 mM) and solvent control treated parasites were allowed to grow *in vitro* culture and parasitemia was monitored for 6 days for PfMel-HA-glmS and **(C)** PfMel-HA. No significant statistical difference was observed when unpaired t-test was performed. These experiments were performed independently at least three times in triplicate to evaluate the statistical differences. The data for this figure was generated with the help of Barbara Dias.

4.2.5 Effect of melatonin on PfMel knockdown and parasite development within asexual stages

Based on the above observations of glucosamine induced lower mRNA turnover, we hypothesized that knocking down the protein expression may have critical role in the parasite maturation process. Melatonin and related indole compounds have been shown to modulate the parasite maturation (Hotta, Gazarini et al. 2000, Schuck, Ribeiro et al. 2011). Based on this, we investigated the role of PfMel in the parasite cell cycle regulation. If PfMel does modulate the cell cycle, then knocking down the protein expression will disrupt the effect of PfMel protein and less or no effect on parasite stage will be observed. Based on this hypothesis, we incubated the asynchronous wild type 3D7, recombinant PfMel-glmS-HA and recombinant control PfMel-HA parasites with glucosamine for 48 h. After glucosamine treatment, all parasite strains were further treated with 100 nM melatonin for 24 h. These parasites were collected, fixed and stained with nuclear dye YOYO-1 iodide (Invitrogen). The stained parasites were counted by flow cytometry to determine parasite's mononucleated (ring + trophozoite) and multinucleated (schizont) distribution. Our result for wild type *P. falciparum* 3D7 in **Figure 29A** showed that the glucosamine has no effect on melatonin treatment and higher number of mature parasites were observed in either with or without glucosamine. On the other hand, the mononucleated parasite numbers were slightly but not significantly lowered. The distribution of parasite forms can also be seen for all the treatments as dot-plot in the FlowJo graphical images in (**Figure 29 B-E)**. We have found similar observation in recombinant control parasite PfMel-HA where melatonin modulated the parasite cycle irrespective of glucosamine treatment **(Figure 30A)**. Similarly, the FlowJo dot-plot graphics can be seen in (**Figure 30 B-E)** showing the distribution pattern of parasite forms. However, for PfMel-glmS-HA parasites in **Figure 31A**, which

exhibited sensitivity to glucosamine induction, have shown reduced maturation process. The number of multinucleated forms in PfMel-glmS-HA parasites has partly but not statistical difference, probably due to the ability of PfMel to restore the balance even in lower amount. The data from this experiment suggests that knocking down the PfMel protein expression does not significantly alter the acceleration towards maturation. The dot-plot distribution parasite's mononucleated ring + trophozoite and multinucleated schizont form is depicted in **(Figure 31 B-E),** where both glucosamine and melatonin treatment are marked.

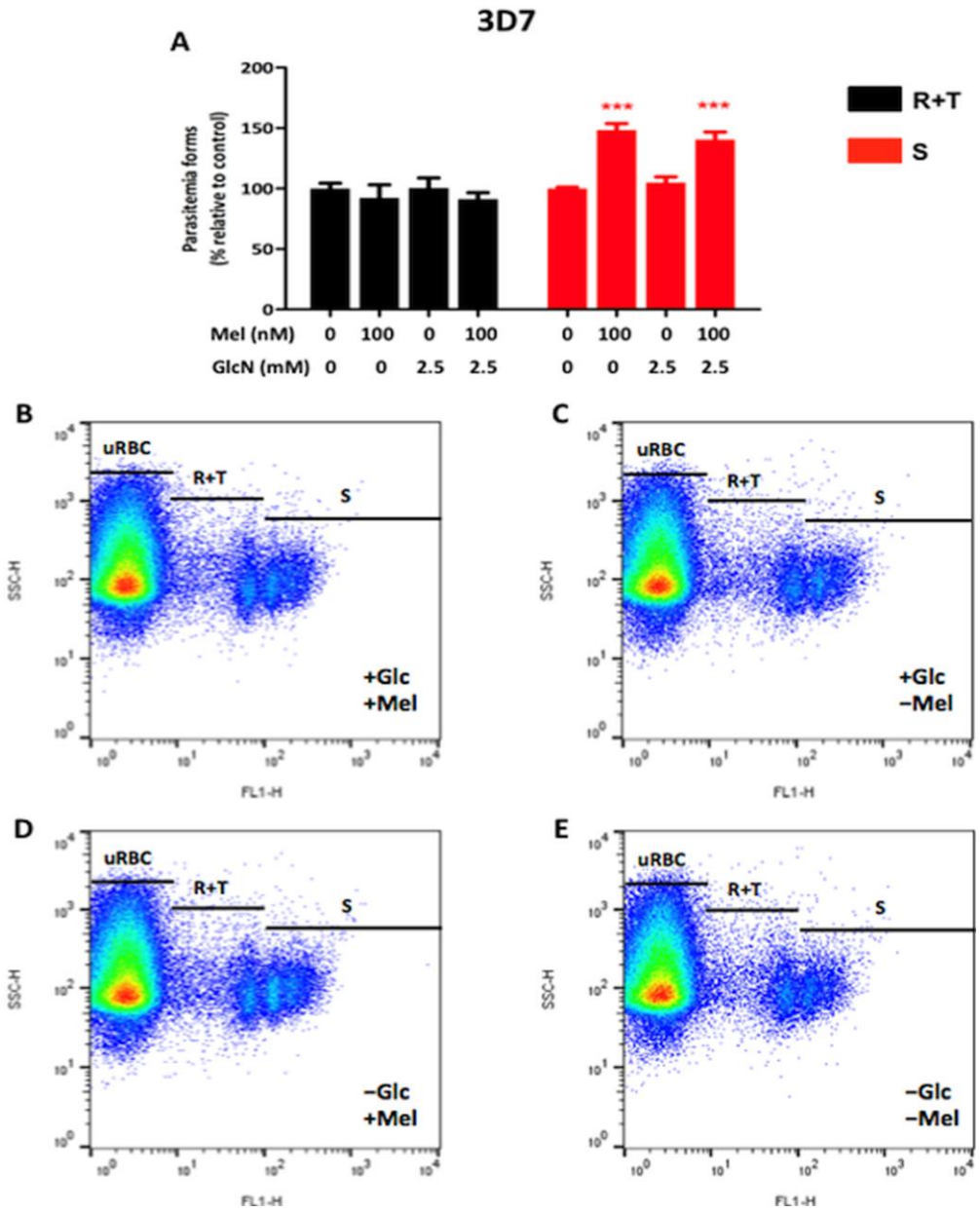

Figure 29: Positive control showing the effect of melatonin treatment in wild type 3D7 parasite cell cycle.

(A) Distinct stage of parasite forms were measured after melatonin treatment for 24 h with and without 1 mM glucosamine induction for 48 h. YOYO-1 stained parasites were counted in flow cytometer to distinguish the distribution of mononucleated rings & trophozoites to multinucleated schizonts. Graphical distribution of parasite forms distribution for **(B)** with both glucosamine & melatonin; **(C)** with glucosamine & without melatonin; **(D)** without glucosamine & with melatonin and **(E)** without both glucosamine & melatonin are depicted. All experiments were performed three times in triplicate and statistical significance with respect to control was obtained using one-way anova in GraphPad Prism V6. ***<0.001

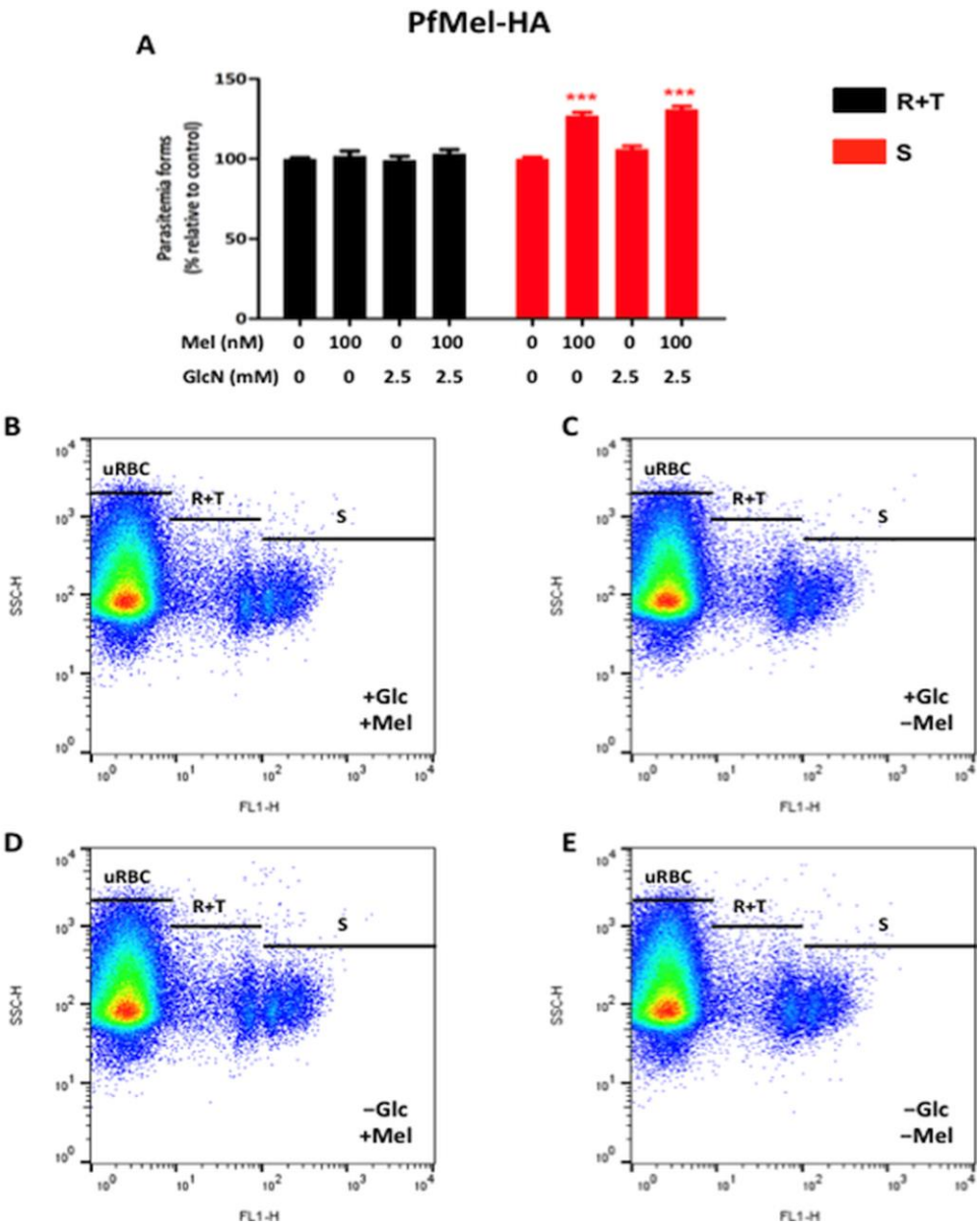

Figure 30: Effect of melatonin in PfMel-HA parasite cycle with and without glucosamine induction.

(A) Distinct stage of parasite forms were measured after melatonin treatment for 24 h with and without 1 mM glucosamine induction for 48 h. YOYO-1 stained parasites were counted in flow cytometer to distinguish the distribution of mononucleated rings & trophozoites to multinucleated schizonts. Graphical distribution of parasite forms distribution for **(B)** with both glucosamine & melatonin; **(C)** with glucosamine & without melatonin; **(D)** without glucosamine & with melatonin and **(E)** without both glucosamine & melatonin are depicted. All experiments were performed three times in triplicate and statistical significance with respect to control was obtained using one-way anova in GraphPad Prism V6. ***<0.001

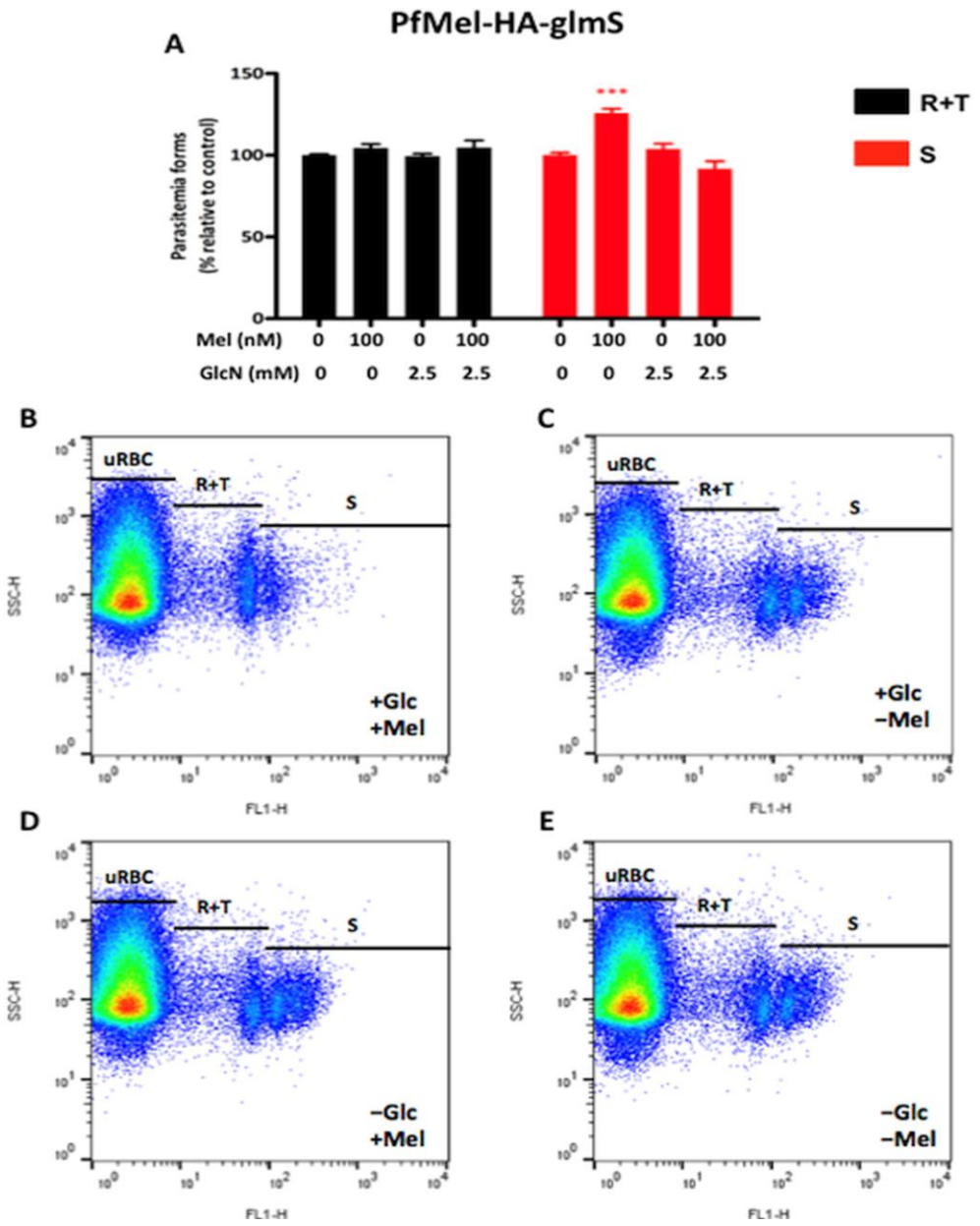

Figure 31: Effect of melatonin in PfMel-HA-glmS parasite cycle with and without glucosamine induction.

(A) Distinct stage of parasite forms were measured after melatonin treatment for 24 h with and without 1 mM glucosamine induction for 48 h. YOYO-1 stained parasites were counted in flow cytometer to distinguish the distribution of mononucleated rings & trophozoites to multinucleated schizonts. Graphical distribution of parasite forms distribution for **(B)** with both glucosamine & melatonin; **(C)** with glucosamine & without melatonin; **(D)** without glucosamine & with melatonin and **(E)** without both glucosamine & melatonin are depicted. All experiments were performed three times in triplicate and statistical significance with respect to control was obtained using one-way anova in GraphPad Prism V6. ***<0.001

4.2.6 Intracellular calcium signaling in PfMel knockdown

Previous studies from our lab have shown that melatonin and its intermediates modulate intracellular Ca^{2+} fluctuation (Hotta, Gazarini et al. 2000, Hotta, Markus et al. 2003). Blocking the unidentified melatonin receptor with either luzindol or the PLC inhibitor U73122 adversely compromised the $[Ca^{2+}]_{cyt}$ mobilization and its downstream signaling components (Beraldo, Mikoshiba et al. 2007). Altering the Ca^{2+} efflux affects the parasite asexual growth and overall fitness (Gazarini, Thomas et al. 2003). Based on our data with the PfMel, we further investigated if this protein played a role in the $[Ca^{2+}]_{cyt}$ mobilization upon melatonin addition. Therefore, our next approach was to investigate the cytosolic Ca^{2+} in both PfMel-HA and PfMel-HA-glmS parasites. In the first, we performed a control experiment with PfMel-HA parasites which was not treated with the glucosamine and monitored the $[Ca^{2+}]_{cyt}$ using a spectrofluorometer after stimulating with 100 nM melatonin. In a different set of experiment with PfMel-HA, we first treated the parasites with 2.5 mM glucosamine and then monitored the $[Ca^{2+}]_{cyt}$ against melatonin. Our results in **Figure 32A** showed that in PfMel-HA parasite, approximately same amount of the $[Ca^{2+}]_{cyt}$ mobilization irrespective of the glucosamine induction. A fluorescence difference in arbitrary units from baseline to melatonin responses were indicated as tabular form in **Figure 32B**. Similarly, kinetics of Ca^{2+} trace with melatonin challenge were also depicted in **Figure 32C-D**.

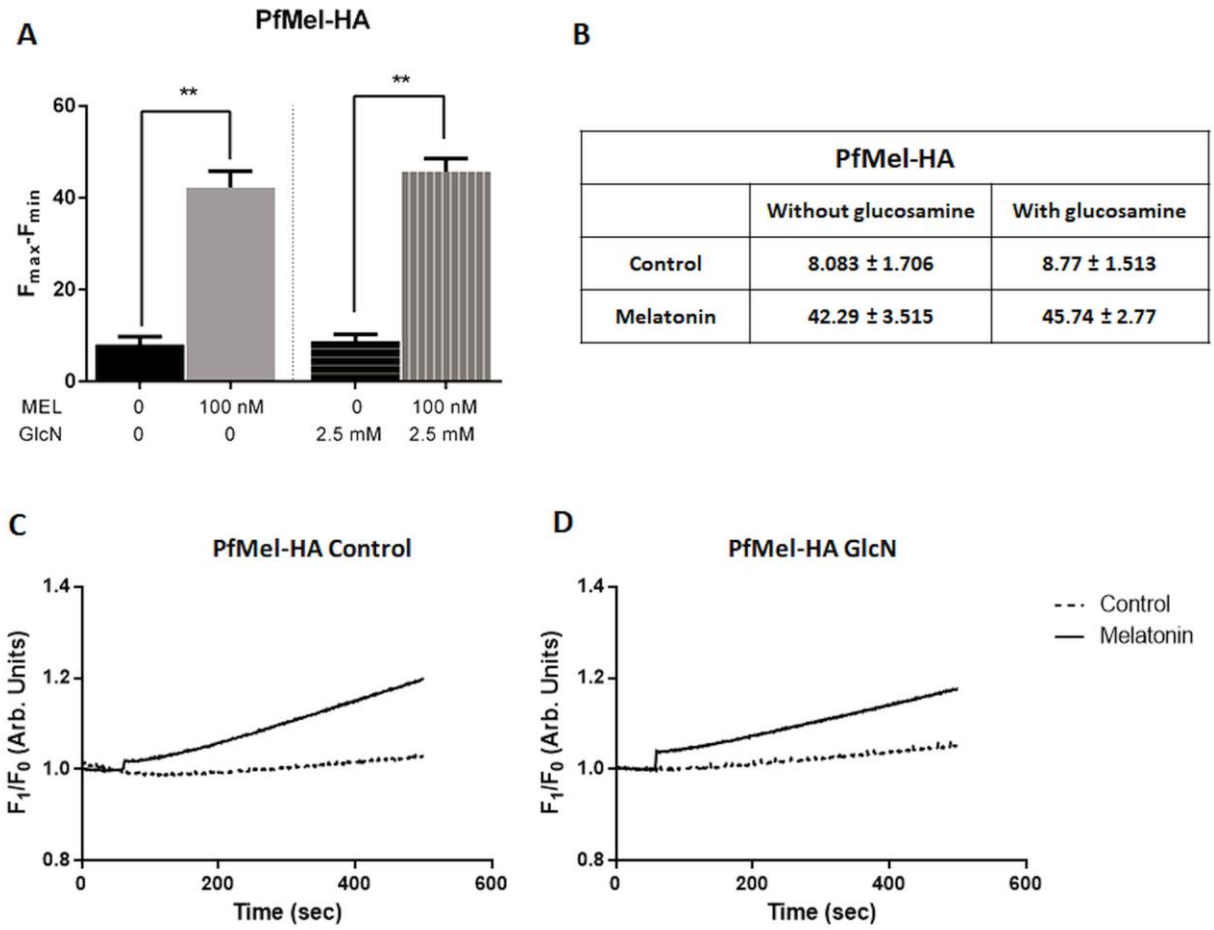

PfMel-HA		
	Without glucosamine	With glucosamine
Control	8.083 ± 1.706	8.77 ± 1.513
Melatonin	42.29 ± 3.515	45.74 ± 2.77

Figure 32: $[Ca^{2+}]_{cyt}$ mobilization in Fluo-4AM loaded PfMel-HA trophozoites.

(A) Intracellular Ca^{2+} mobilization was measured in saponin isolated live trophozoite stage parasites loaded with Ca^{2+} indicator dye Fluo-4AM with 100 nM melatonin addition without glucosamine induction. **(B)** Similar observation was seen when 2.5 mM glucosamine induction was done for 48 h. Trace of $[Ca^{2+}]_{cyt}$ efflux in case on both glucosamine non-induced **(C)** and induced **(D)** parasite is shown. These experiments were performed three times in triplicate and statistical difference was obtained by unpaired t-test. ** >0.01.

In next set of experiment, we investigated the $[Ca^{2+}]_{cyt}$ efflux in the PfMel-HA-glmS parasite line. First, the $[Ca^{2+}]_{cyt}$ influx was monitored against melatonin stimulation but without the glucosamine induction, which should respond as normal parasites where expression of PfMel is typical. Our result in **Figure 33A** for the PfMel-glmS-HA showed that the glucosamine untreated parasites exhibited similar increase of the $[Ca^{2+}]_{cyt}$ as control PfMel-HA parasites. Even the melatonin-induced Ca^{2+} increase was comparable to the PfMel-HA parasite response. However, when PfMel-glmS-HA parasites were first given glucosamine induction for 48 h and then melatonin challenge was given to monitor the Ca^{2+} release. To our surprise, we found melatonin-induced $[Ca^{2+}]_{cyt}$ efflux was partially but significantly reduced in 48 h glucosamine treated PfMel-HA-glmS parasites in comparison to non-glucosamine induced melatonin stimulated parasites. We found that approximately 50 % decrease in Ca^{2+} efflux in PfMel-glmS-HA glucosamine induced parasite when compared to the parasites without glucosamine induction **(Figure 33B)**. This result suggested that both melatonin-induced Ca^{2+} response is indeed linked and PfMel plays crucial role in $[Ca^{2+}]_{cyt}$ mobilization, which also modulate the *P. falciparum* intraerythrocytic development. The differential kinetics of free $[Ca^{2+}]_{cyt}$ trace for the melatonin challenge in both without and with glucosamine induction is presented in **Figure 33C & D**.

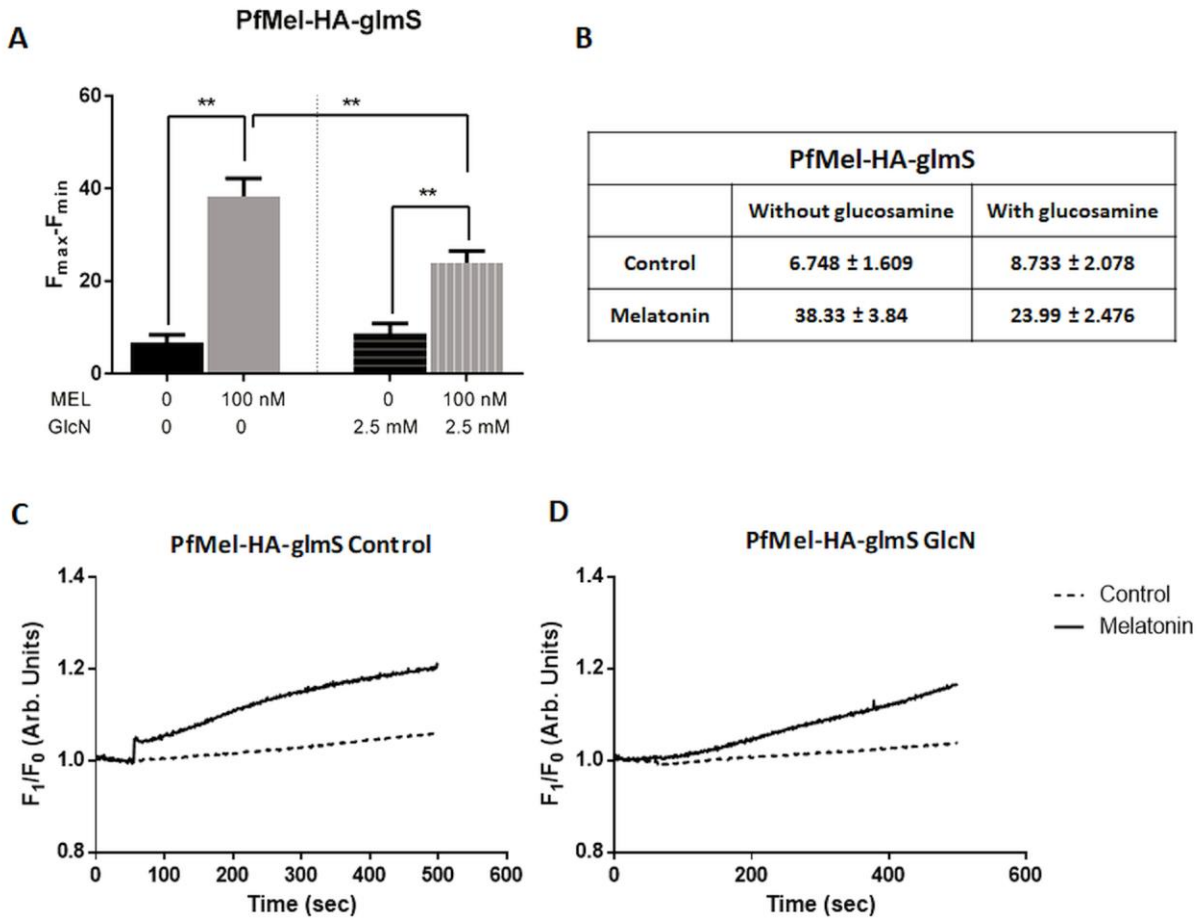

PfMel-HA-glmS		
	Without glucosamine	With glucosamine
Control	6.748 ± 1.609	8.733 ± 2.078
Melatonin	38.33 ± 3.84	23.99 ± 2.476

Figure 33: $[Ca^{2+}]_{cyt}$ mobilization in Fluo-4AM loaded PfMel-HA-glmS trophozoites.

(A) Histogram showing the trace of $[Ca^{2+}]_{cyt}$ release in isolated live trophozoite stage parasites loaded with Ca^{2+} indicator dye Fluo 4-AM showing higher Ca^{2+} efflux with 100 nM melatonin addition but in not glucosamine induced parasites. **(B)** Contrarily, 2.5 mM glucosamine treatment for 48 h partially but significantly altered the $[Ca^{2+}]_{cyt}$ in PfMel-HA-glmS. Trace of $[Ca^{2+}]_{cyt}$ efflux in case on both glucosamine non-induced **(C)** and induced **(D)** parasite is shown. These experiments were performed three times in triplicate and statistical difference was obtained by unpaired t-test. ** >0.01.

4.2.7 Co-immunoprecipitation of PfMel with anti-GFP antibody to identify its molecular partners in *P. falciparum* parasites

We next investigated the interacting partners of PfMel protein in order to gain insight into the functional mechanism of this protein within the asexual cycle. To find PfMel-interacting proteins, we performed the co-immunoprecipitation (Co-IP) technique using an anti-GFP antibody with the PfMel-GFP construct. Co-IP is a powerful technique to analyze protein–protein interactions and it works when the targeted protein involved in forming bigger complexes with other proteins. The interaction with targeted protein makes it possible to tweak various members of the complex from the solution by holding the targeted protein member with an antibody. For this purpose, we used highly synchronized PfMel-GFP trophozoite stage parasites for the co-IP study. An anti-GFP antibody was used for protein pull down that might latch to extract the entire protein complex from the parasite lysate. These proteins were then categorized from the unidentified members of the whole protein complex. To do that, trophozoite lysate samples (treatment and negative control) were pulled down with anti-GFP-Trap-A beads (ChromoTek, gta-20) antibody and resolved by SDS-PAGE and coomassie staining. Our result in **Figure 34A** showed that an approximately 300 kDa band was detected in PfMel-GFP parasites in coomassie staining while negative 3D7 control did not exhibited this band. Later, both wild type 3D7 and GFP parasite lanes were excised and subjected to mass spectrometry in CEFAP (ICB-USP). An anti-GFP pulled immunoprecipitated proteins in PfMel-GFP, which was absent in wild type 3D7 parasite were exclusively considered for potential PfMel-interacting candidates. Raw data were processed and obtained MS/MS spectra were searched against the Uniprot *Plasmodium* (isolate 3D7) (Strain: Isolate 3D7) Protein Database to identify these potential binding candidates. Our data revealed a total of 98 binding candidates specific for PfMel-GFP.

We performed further trimming by eliminating the genes having 3 or less peptide hits. The final protein numbers were reduced to 37 for which we queried Gene Ontology (GO) to elucidate their putative gene function. Pie chart distribution of GO annotation for PfMel-GFP is shown in **Figure 34B** indicating the potential binding protein properties.

The identified proteins were further divided into their diverse functional properties such as invasion, DNA transcription, RNA translation, protein folding, protein transport and others **(Table 4)**. These experiments were performed in collaboration with Prof. Giuseppe Palmisano (ICB-USP).

With GO search, we found that approximately 12 proteins have function in nucleic acid metabolism, more specifically DNA transcription, RNA splicing and RNA translation. Amino acid-tRNA ligases were also found.

Proteins belonging to parasite metabolism were also pulled down by anti-GFP antibody such as a protein in heme metabolism (protein 1), nucleotide biosynthesis (protein 13), glucose metabolism (protein 32 & 35) and others.

Proteins participating in host cell invasion and attribute to pathogenesis were also identified. These proteins were RON family proteins (protein 4 & 26), EMP2 (protein 9) and surface protein P113 (protein 19). RON family proteins play crucial role in host cell invasion by traversing across the parasite membrane and forming a complex on the erythrocyte surface to serve as the receptor for apical protein AMA1 (Tonkin, Roques et al. 2011).

Another category was belonging to protein folding and transport. These were importin-7 (protein 2), 60kDa chaperons (protein 10), T-complex protein (protein 14, 20 & 33) and EMC1 (protein 23). We also found Sec63 (protein 36) that participate in protein folding and targeting of nascent protein still attached to ribosome into ER.

Besides that, we found that 2 genes are of unknown function while there were other abundant diverse proteins that were important for various biological function. These proteins were Ca^{2+} transport (protein 12), stress response (protein 18), drug resistance (protein 25) and ubiquitination (protein 31). The detail list of identified proteins with their characteristic properties and functions are described in **Table 4.**

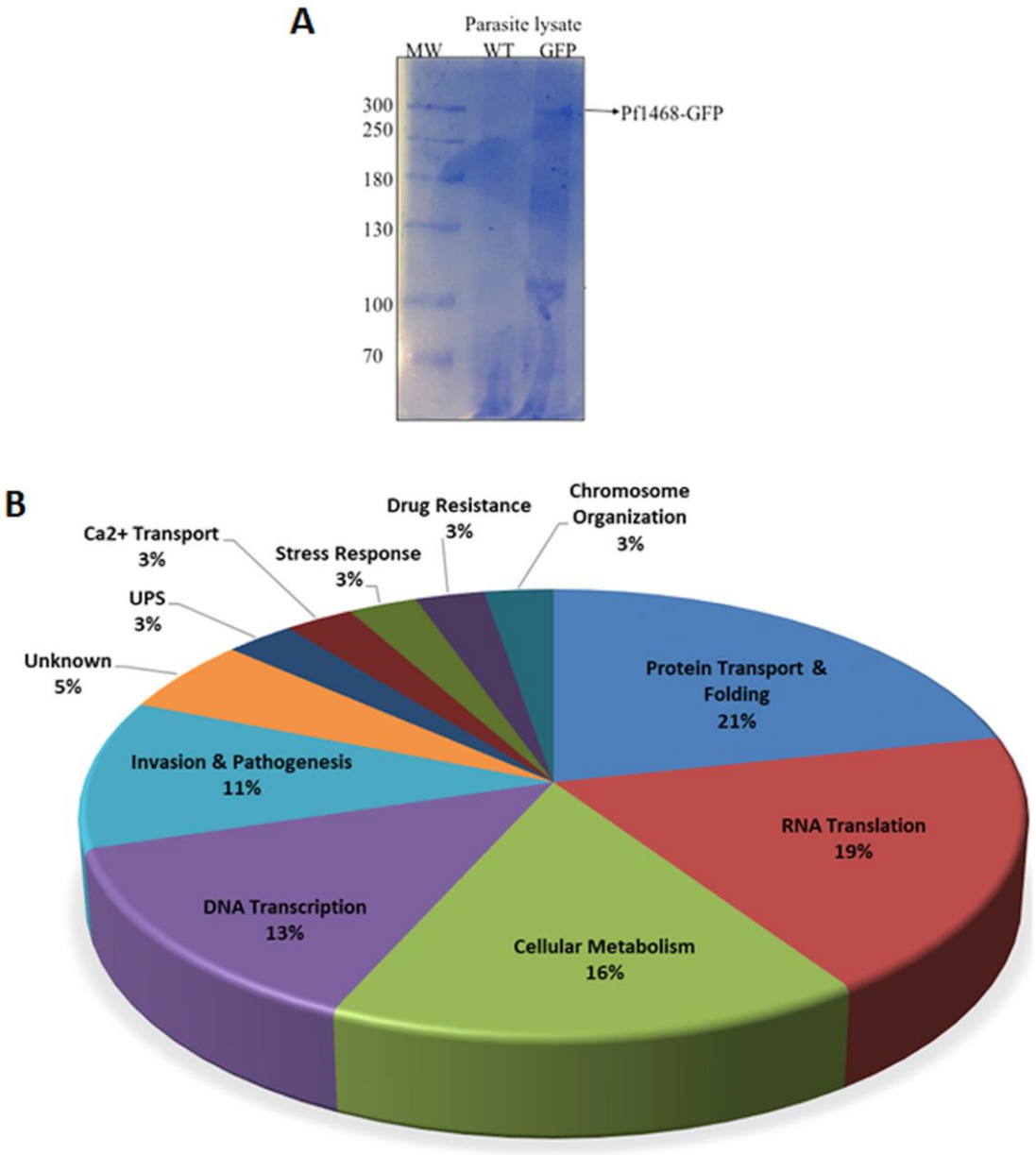

Figure 34: Immunoprecipitation of PfMel-GFP parasites

(A) Coomassie brilliant blue stained SDS-PAGE gel of PfMel lysate that was used for further immunoprecipitation study (Data was collected by Dr. Miriam Moraes). **(B)** Pie chart diagram representing that after co-immunprecipitation of PfMel-GFP parasite lysate when incubated with anti-gfp antibody. Majority of proteins recognized belongs to either protein transport or DNA/RNA metabolism.

Table 4: Selected proteins identified by crosslink followed by co-immunoprecipitation of *P. falciparum* PfMel-GFP trophozoites using anti-GFP antibody.

S.N.	Number of Peptides identified in Mass Spectrometer	PlasmDB ID	Name of the Identified Proteins	Molecular Weight (kDa)	Amino Acids	SP	Tm	Possible Function	Localization
1	16	PF3D7_1360800	Falcillycin	138.86	1193	N	N	Hemoglobin catabolism	Food Vacuole
2	16	PF3D7_0706000	Importin-7	145.51	1229	N	N	Protein transport	Cytosol / Nuclear envelope
3	16	PF3D7_0420300	AP2 domain transcription factor	400.17	3473	N	N	DNA Transcription	Nucleus
4	12	PF3D7_1252100	Rhoptry neck protein 3 (RON3)	263.15	2215	Y	Y	Host Cell Invasion	Rhoptry
5	9	PF3D7_1461900	Val-tRNA ligase	128.07	1090	N	N	RNA Translation	Cytosol
6	9	PF3D7_0215700	DNA-directed RNA polymerase II subunit RPB2	151.72	1340	N	N	DNA Transcription	Nucleus
7	9	PF3D7_1034900	Met-tRNA ligase	104.17	889	N	N	RNA Translation	Cytosol
8	9	PF3D7_0403600	Conserved Plasmodium protein	89.43	768	N	N	Unknown	Unknown
9	8	PF3D7_0500800	Erythrocyte membrane protein 2	168.29	1434	N	N	Pathogenesis	Host membrane
10	8	PF3D7_1232100	60 kDa Chaperon	81.48	718	Y	N	Protein folding	Apicoplast
11	8	PF3D7_0517700	eIF3 subunit B	84.06	716	N	N	RNA Translation	Cytosol

12	7	PF3D7_1211900	Non-SERCA-type Ca^{2+} -transporting P-ATPase	140.26	1264	N	Y	Ca^{2+} transport	Membrane
13	7	PF3D7_1308200	Carbamoyl phosphate synthetase	273.44	2375	N	N	Pyrimidine nucleotide biosynthesis	Cytosol
14	7	PF3D7_0320300	T-complex protein 1 subunit epsilon	59.17	535	N	N	Protein folding	Cytosol
15	7	PF3D7_0414000	Structural maintenance of chromosomes protein 3 (SMC3)	141.22	1193	N	N	Chromosome organization	Nucleus
16	6	PF3D7_1362200	RuvB-like helicase 3	54.63	483	N	N	DNA Transcription	Nucleus
17	6	PF3D7_1367700	Ala-tRNA ligase	165.13	1408	N	N	RNA Translation	Cytosol
18	6	PF3D7_0831700	Hsp70	75.05	679	Y	N	Stress response	J-dots
19	5	PF3D7_1420700	Surface protein P113	112.57	969	Y	Y	Host cell invasion	Membrane
20	5	PF3D7_0306800	T-complex protein 1 subunit beta	59. 2	533	N	N	Protein folding	Cytosol
21	5	PF3D7_1350100	Lys-tRNA ligase	67.59	583	N	N	RNA Translation	Cytosol
22	5	PF3D7_1234800	Splicing factor 3B subunit 3 (SF3B3)	151.81	1329	N	N	mRNA splicing	Nucleus
23	5	PF3D7_0811200	ER membrane protein complex subunit 1 (EMC1)	133.76	1133	N	Y	Protein folding	ER membrane
24	5	PF3D7_1460500	Conserved Plasmodium protein	182.72	1632	N	N	Unknown	Unknown
25	4	PF3D7_0523000	Multidrug resistance	162.25	1419	Y	N	Drug resistance	Food vacuole

			protein 1 (MDR1)						
26	4	PF3D7_1452000	Rhoptry neck protein 2 (RON2)	249.49	2189	N	Y	Host cell Invasion	Rhoptry
27	4	PF3D7_1213800	Pro-tRNA ligase	86.64	746	N	N	RNA Translation	Cytosol
28	4	PF3D7_0627700	Transportin	132.84	1147	N	N	Ribosomal protein import into nucleus	Nuclear pore
29	4	PF3D7_0802000	Glutamate dehydrogenase	160.42	1397	N	N	Urea Cycle	Mito
30	4	PF3D7_1472200	Histone deacetylase	268.92	2251	Y	N	DNA Transcription	Nucleus
31	4	PF3D7_1225800	Ubiquitin-activating enzyme E1	131.78	1140	N	N	Ubiquitination - Proteasomal Degradation	Cytosol
32	4	PF3D7_1120100	Phosphoglycerate mutase	28.77	250	N	N	Gluconeogenesis	
33	4	PF3D7_0214000	T-complex protein 1 subunit theta	60.96	542	N	N	Protein folding	Cytosol
34	4	PF3D7_1445100	His-tRNA ligase	133.67	1132	N	N	RNA Translation	Mitochondria
35	4	PF3D7_1118300	Insulinase	173.62	1488	N	N	Hydrolase activity	Unknown
36	4	PF3D7_1318800	Translocation protein SEC63	75.87	651	N	Y	Protein folding and targeting to ER	Membrane
37	4	PF3D7_0619500	Acyl-CoA synthetase	163.91	1392	N	N	Fatty acid biosynthesis	Mitochondria

SP: signal peptide; Tm: transmembrane domain

5 DISCUSSION

5.1 Ionic interplay, calcium and parasite proliferation

$[Ca^{2+}]_{cyt}$ signaling is a dynamic cellular process that controls variety of cellular function to control parasite transmission from one host to another and the vector as well (Billker, Dechamps et al. 2004). In *P. falciparum,* Ca^{2+} flux regulates the numerous functions and the most important step is the egress from the infected erythrocyte to invasion of a new one (Singh, Alam et al. 2010, Agarwal, Singh et al. 2013). Efforts have made to elucidate the molecular processes related to $[Ca^{2+}]_{cyt}$ efflux that relay downstream signaling to activate the secretion of parasite proteins. Activation of specialized apical proteins facilitates erythrocyte rupture, host-parasite interaction and invasion (Alaganan, Singh et al. 2017). However, the precise mechanism of upstream events leading to discharge of apical proteins remains elusive and requires more attention. Since erythrocyte stage parasites come in direct contact with the host immune system after egress, Ca^{2+} signaling would be a perfect target for drug development.

Before discussing our results in detail, it is important to reiterate some of the basic features of cellular K^+ homeostasis. Firstly, the K^+ concentration in the erythrocyte cytosol is much higher (~140 mM) than the extracellular blood plasma K^+ concentration (~5 mM), and this distribution is inverted for Na^+ ions. The asymmetric ionic distribution is maintained by the Na^+/K^+-ATPase ion pump, which transports two K^+ cations into the cytosol and three Na^+ cations into the extracellular milieu. Secondly, under basal conditions, the permeability of the erythrocyte plasma membranes is highest with respect to the K^+ cations and much lower for Na^+ and Ca^{2+}. Third, other passive transport systems are also necessary for vital cell functions such as

the regulation of cell volume, osmolality, pH, and the transport of nutrients (Chitnis and Staines 2013). As we discussed in **Figure 6**, as the intracellular parasites mature, the ionic balance in the RBC cytosol is shifted from high to low K^+ while parasite cytosol maintains the similar environment as blood plasma. Previous work reported that extracellular K^+ play crucial role in sensitizing the parasites to relay the apical secretion signal via PLC activation (Singh, Alam et al. 2010). To further elucidate this, we investigated the molecular mechanism undermining the Ca^{2+} signaling that may lead to Ca^{2+} flux activating various signaling pathways. In agreement with Singh et al. 2010, we have performed the experiment showing that changing the ionic microenvironment is the important factor that triggers Ca^{2+} mobilization. First, we investigated the role of ion K^+/Na^+ in $[Ca^{2+}]_{cyt}$ increase by spectrofluorometer in Fluo-4AM loaded trophozoite stage parasite. Parasites are sensitive to change in microenvironment especially from high K^+ to low K^+ that mimic the blood plasma. We have explored the effect of increasing K^+ along with Na^+ to distinguish the factor responsible for Ca^{2+} discharge. Our result in **Figure 7** suggested that Ca^{2+} could still be induced by 50 mM KCl stimulation but equimolar NaCl was unable to trigger any response. The experiment confirm that only K^+ can elicit a Ca^{2+} response but not the Na^+ ion when the parasite ruptures the RBC and sense the change in ionic fluctuation (Moraes, Budu et al. 2017).

However, the result in **Figure 7** alone was not sufficient to bridge the complete disparity between ionic interchange, so we have performed a more specific experiment using flow cytometry to avoid the K^+-free exposure to the parasites. The result in **Figure 8** suggested that parasites elicit $[Ca^{2+}]_{cyt}$ to change in high K^+ to low K^+ but vice versa did not show the Ca^{2+} change. It is important to note that all the experiment was done in the presence of extracellular Ca^{2+} that would implicate that the rise in Ca^{2+} could be the result of diffusion from the external

environment. On the other hand, experiment in **Figure 8** showed that removing extracellular Ca^{2+} had no effect in $[Ca^{2+}]_{cyt}$ release upon changing from high K^+ to low K^+ ionic milieu. Moreover, transferring the parasites from high K^+ to low K^+ buffer triggers a rise in $[Ca^{2+}]_{cyt}$ implicating the parasite's internal store as potential source of the $[Ca^{2+}]_{cyt}$ (Moraes, Budu et al. 2017). To find out the specific ionic factor responsible for evoking $[Ca^{2+}]_{cyt}$, we changed the Cl^- ion in KCl and NaCl buffer to glutamate (Na- and K-glutamate). The changed buffers had similar effect as KCl or NaCl buffer, which would prove that only K^+ is the Ca^{2+} stimulating factor and not the Cl^- ion. Results in **Figure 9** proved that a rise in Ca^{2+} was due to low K^+ environment as found in blood plasma (Moraes, Budu et al. 2017). These results lead us to another direction to investigate the source of Ca^{2+} release after parasite exposure to low K^+ buffer. We addressed this aspect in **Figure 10,** where parasites were pretreated with PLC inhibitor U73122 and its inactive analog U73343. The results in **Figure 10** showed that inhibiting PLC impairs the $[Ca^{2+}]_{cyt}$ rise but its inactive analog failed to do so. It was shown in various studies that PLC hydrolyses the PIP_2 into IP_3 that further activate the IP_3R and elicit $[Ca^{2+}]_{cyt}$. However, no IP_3R has been discovered in *Plasmodium* species but pharmacological evidences say otherwise. Based on these studies, our results indicate that blocking PLC impairs IP_3 generation thus inhibiting the $[Ca^{2+}]_{cyt}$ release. This was further confirmed in the result presented in **Figure 10C,** where parasites were treated with SERCA blocker CPA suggest that depleting $[Ca^{2+}]_{cyt}$ store of the parasites results in no difference in Ca^{2+} efflux for any of low to high or high to low K^+ change (Moraes, Budu et al. 2017).

We had conclusive evidence that parasites are able to sense the change in ionic fluctuation and that physiological low K^+ concentration triggers the $[Ca^{2+}]_{cyt}$ rise. However, the mechanism how parasites sense this change is yet to identify. Towards this end, our group has identified that

P. falciparum have four proteins (SR1, SR10, SR12 and SR25) that have the key characteristics of G-protein coupled receptors such as the presence of 7 transmembrane domains with both extra- and intra-cellular spanning domains (Madeira, Galante et al. 2008). In an attempt to identify the signaling pathway(s) governed by the *Plasmodia* GPCRs, we found that *PfSR25* is coupled with increases in $[Ca^{2+}]_{cyt}$ in response to changes in extracellular K^+ concentrations. We generated the *PfSR25* knock out (*PfSR25*$^{-}$*)* strain to study its physiological role in Ca^{2+} signaling (Moraes, Budu et al. 2017). Result in **Figure 11** shows that when *PfSR25*$^{-}$ parasites were changed from either low K^+ to high K^+ or high K^+ to low K^+ environment, no Fluo-4AM shift at x-axis was observed. These parasites failed to respond to changes in the K^+ microenvironment and had the $[Ca^{2+}]_{cyt}$ rise abrogated. The results lead to another possibility whether these parasites maintain normal Ca^{2+} store. This was confirmed by transferring the parasites from high K^+ to low K^+ buffer and a SERCA inhibitor thapsigargin was added in the buffer. An increase in the $[Ca^{2+}]_{cyt}$ was observed, demonstrating that inner Ca^{2+} stores are normally full, which is also the source of $[Ca^{2+}]_{cyt}$ rise.

By monitoring the $[Ca^{2+}]_{cyt}$ in isolated *P. falciparum*, we have provided the direct confirmation of the presence of an extracellular K^+ sensing mechanism. More precisely, we have shown that only changes in K^+ concentration are capable of altering $[Ca^{2+}]_{cyt}$ among other physiologically abundant cations. Our conclusion is in agreement with a report indicating that K^+ was able to counterbalance the Ca^{2+} signaling in the blood stages *P. falciparum* through undefined mechanisms (Singh, Alam et al. 2010). Notably, decrease in extracellular K^+ concentration causing rapid increase in the parasite $[Ca^{2+}]_{cyt}$ are within the range experienced by *Plasmodia* during their intra and extracellular life cycle in the host erythrocyte. We conclude that *Plasmodium* IP_3 sensitive organelle is the source of $[Ca^{2+}]_{cyt}$ rise activated by changes in K^+

concentration. More importantly, knocking out the *PfSR25* can eliminate K^+-dependent $[Ca^{2+}]_{cyt}$ rise. The simplest explanation for these data is *PfSR25* itself is a K^+ sensor, which is coupled via a G protein to PLC activation.

Recently, it was reported that *in vitro* blood-stage *P. falciparum* parasites are able to grow unimpeded in media having wide-ranging ionic constituents (Pillai, Addo et al. 2013). The authors have revealed that already acknowledged fluctuations in the cations of the host erythrocyte cytosol induced by developing internal parasites are not important for growth. Furthermore, their results implicate that besides the low K^+ milieu that triggers key processes such as microneme secretion and merozoite egress, there must exist other alternative signals that can control signaling processes and allow normal parasite growth in diverse ionic environments. Apart from K^+ ion, nucleotides and its cyclic components are considered most important secondary messenger molecules to transmit the signal. Interestingly, it was found that *P. falciparum* infected erythrocytes released more ATP than uninfected cells (Akkaya, Shumilina et al. 2009). Towards this end, we have previously reported that extracellular ATP stimulates the $[Ca^{2+}]_{cyt}$ rise in isolated trophozoite or schizont stage parasites. Use of purinergic receptor antagonist KN62 imparts the ATP-induced Ca^{2+} rise. More importantly, invasion assay reveals that ATP addition in *in vitro* culture increase the parasite invasion and was blocked by KN62 addition. Also, ATP hydrolyzing enzyme apyrase reduces the parasite invasion, which suggests that extracellular ATP plays crucial role in parasite development (Levano-Garcia, Dluzewski et al. 2010). Recently, it was shown that *P. falciparum* express E-NTPDase (also known as apyrase) which is important for the parasite lifecycle. Inhibition of apyrase impairs the *P. falciparum* development in red blood cells. Enzyme activity for ATPase was detected in rings, trophozoites, and schizonts stages; E-NTPDase expression was confirmed by qRT-PCR

throughout the intraerythrocytic cycle. Additionally, in an attempt to express the first 500 bp of an E-NTPDase-GFP shows that ENTPDase localizes to the endoplasmic reticulum (ER) in early stages and the digestive vacuole (DV) in late stages of the *P. falciparum* intraerythrocytic cycle (Borges-Pereira, Meissner et al. 2017). Based on these observations, we investigated the role of extracellular ATP in invasive *P. falciparum* merozoites. The merozoites were isolated by achieving very tight synchrony with maximum window of 4 h following the similar protocol described in (Singh, Alam et al. 2010). These merozoites stained with Fluo-4AM and a spectrofluorometer experiment was done to monitor the live cell $[Ca^{2+}]_{cyt}$ release after 50 µM extracellular ATP addition. Results as depicted in **Figure 12**, an increase in fluorescence was observed when compare to solvent control after extracellular ATP was added. Contrarily, addition of purinoceptor blocker KN62 (P2X7 receptor in human) prior to ATP addition severely impairs the $[Ca^{2+}]_{cyt}$ release. Additionally, we also tested the effect of ADP to Ca^{2+} rise and the result in **Figure 13** shows a similar effect as shown for ATP response. This result is interesting because previously, it was shown that ADP has minimal effect in $[Ca^{2+}]_{cyt}$ rise in trophozoite or schizont stage parasites (Levano-Garcia, Dluzewski et al. 2010). These results suggest that the coexistence of alternative signaling events modulating parasite Ca^{2+} signaling and the fact that merozoites sense ATP and induce Ca^{2+} rise promptly suggest that ATP is central for parasite to RBC invasion.

Apart from the endoplasmic reticulum, mitochondria and digestive vacuole (DV) have been shown to maintain the Ca^{2+} homeostasis and act as a Ca^{2+} storage organelles. The role of digestive vacuole, a heme degrading organelle in *Plasmodium* is less studied though another IP_3 sensitive and relatively acidic organelle is identified (Passos and Garcia 1998). In *P. falciparum,* IP_3R has not been identified but was reported in the acidic vacuole of *Trypanosoma brucei*

(Huang, Bartlett et al. 2013) and *T. cruzi* (Hashimoto, Enomoto et al. 2013). Several other studies reported two distinct Ca^{2+} storage organelles in *Plasmodium* species (Garcia 1999, Alleva and Kirk 2001, Biagini, Bray et al. 2003, Varotti, Beraldo et al. 2003). Presence of various pumps and exchanger underlines their importance in homeostasis of different ions (Docampo and Moreno 1999). Identification of Ca^{2+}-ATPases and other transporters in this organelle raise the question of its role in Ca^{2+} signaling **(Figure 14)**. In *T. gondii*, a Ca^{2+}-ATPases named *TgA1* was identified in acidocalcisome and found that a mutantion in *TgA1* caused lower invasion of the parasite with an increased and unstable basal Ca^{2+} level. Even the microneme secretion was affected in *TgA1* mutants (Luo, Ruiz et al. 2005). These studies suggest the role of the acidic compartment in Ca^{2+} mobilization during intracellular signaling.

Despite the Ca^{2+} storage and pH homeostasis, the acidic DV is the target of chloroquine, which accumulates inside this organelle and exerts an antimalarial effect by inhibiting the detoxification of heme (Martin, Marchetti et al. 2009). After invading red blood cells, the parasite uses its proteolytic machinery to cleave hemoglobin into globin for amino acid supply. Parallelly, hemoglobin breakdown also releases heme (Fe^{2+}) that oxidized quickly and tandem reaction triggered the production of free radicals and H_2O_2, which has detrimental effect on parasite. To impart this effect, the parasite converts heme into inert crystals of hemozoine. But the antimalarial effect of chloroquine is conferred by the mutant form of the chloroquine resistance transporter (PfCRT), which was identified on the digestive vacuole membrane of *P. falciparum* (Ecker, Lehane et al. 2012). PfCRT belongs to drug/metabolite transporter family having 10 transmembrane domains and its function is to efflux the antimalarial drug chloroquine from digestive vacuole (Martin and Kirk 2004). Recent studies have shown that mobilization of Ca^{2+} from this acidic compartment occurs after disrupting the proton gradient by treatment with

various ionophores (Varotti, Beraldo et al. 2003). Capability to mobilize Ca^{2+} from not only endoplasmic reticulum but also from acidic compartment by IP_3 in *P. chabaudi* provides the base that this acidic organelle might be involved in Ca^{2+} signaling (Passos and Garcia 1998). A study by (Gazarini, Sigolo et al. 2007) showed that chloroquine also contributes to alkalization by mobilizing H^+ and subsequently Ca^{2+} release. Based on the evidences it would be critical to measure the concentration of Ca^{2+} in the acidic compartment containing a genetically modified PfCRT gene, which might lead to better understanding of intracellular Ca^{2+} signaling in *P. falciparum*. In a collaborative study with Dr. David Fidock, Columbia University, USA, who provided us the PfCRT modified strains (**Table 3**). To study the Ca^{2+} efflux, we tested the modified PfCRT and monitored the Ca^{2+} mobilization pattern from DV to cytosol. For this study. two distinct traits of the parasites were used: first CQS parasites 3D7, GC03 and $Dd2^{GC03}$ and second CQR parasites Dd2 and $Dd2^{Dd2}$. Apart from that, an addition parasite with a mutation in PfCRT at position 272 amino acid (L272F) named as $Dd2^{Dd2\ L272F}$ was also tested. To test the Ca^{2+} efflux, we used the Na^+/H^+ ionophore monensin, K^+/H^+ ionophore nigericin and CQ. Monensin and nigericin are lysosomotropic carboxylic ionophores that reversibly form complexes with monovalent ions and act directly as Na^+/H^+ and K^+/H^+ exchangers to disrupt Na^+ and K^+ electrochemical gradients, respectively (Garcia, Ann et al. 1998). CQ has been shown previously to release Ca^{2+} from the DV and to act as a Zn^{2+} ionophore in human lysosomes (Alves, Bartlett et al. 2011, Ch'ng, Liew et al. 2011). Our results in **Figure 15 & 16** showed that addition of the Na^+/H^+ or K^+/H^+ ionophores monensin or nigericin respectively to Fluo-4AM-loaded trophozoites invoked $[Ca^{2+}]_{cyt}$. Additionally, addition of CQ in **Figure 17** that alkalize the DV and also mobilized $[Ca^{2+}]_{cyt}$ from the DV. In our study, we found that the *pfcrt* wild-type CQS strains 3D7 and GC03 released significantly higher Ca^{2+} than the CQR strain Dd2 and its

recombinant counterpart Dd2^{Dd2}. Ca^{2+} release was further reduced in the Dd2$^{Dd2\ L272F}$ line expressing the L272F mutation. The Ca^{2+} mobility was restored in recombinant Dd2 parasites expressing wild-type *pfcrt* (Dd2^{GC03}). These results lead us to propose that changes in PfCRT are critical for Ca^{2+} mobilization in *Plasmodium*. How these ionophores causing the distinct Ca^{2+} release from CQS and CQR parasites requires more investigation. As far as CQ is concern, it is already documented that mutation in PfCRT efflux the CQ out of DV resulting in less alkalization, hence releasing low Ca^{2+} in the cytoplasm. Our data suggest that along with the endoplasmic reticulum, the DV is fundamental for Ca^{2+} homeostasis in *P. falciparum* asexual blood stage parasites, and that disruption of Ca^{2+}-dependent signaling pathways could be a promising strategy for the development of new antimalarials.

Taken together, we propose that PfSR25 is an upstream K^+ sensing receptor expressed by *P. falciparum.* We found that shifting from a high K^+ to low K^+ concentration is the trigger to activate the PIP_2 breakdown into IP_3. Alternatively, the extracellular ATP also activates the IP_3 production by an unidentified membrane receptor. The IP_3 molecules diffuse in the cytosol and bind to an unidentified IP_3R on the surface of the ER that changes the conformation of IP_3R causing efflux of Ca^{2+} to the cytosol. Blocking PLC activity and subsequent breakdown of PIP_2 can restrict the cytosolic Ca^{2+} increase. Apart from the ER, when ionic homeostasis and proton gradient of the DV of the parasite is abruptly disturbed by ionophores, Ca^{2+} is released from the DV to cytosol to counterbalance the effect of ion changes **(Figure 35)**.

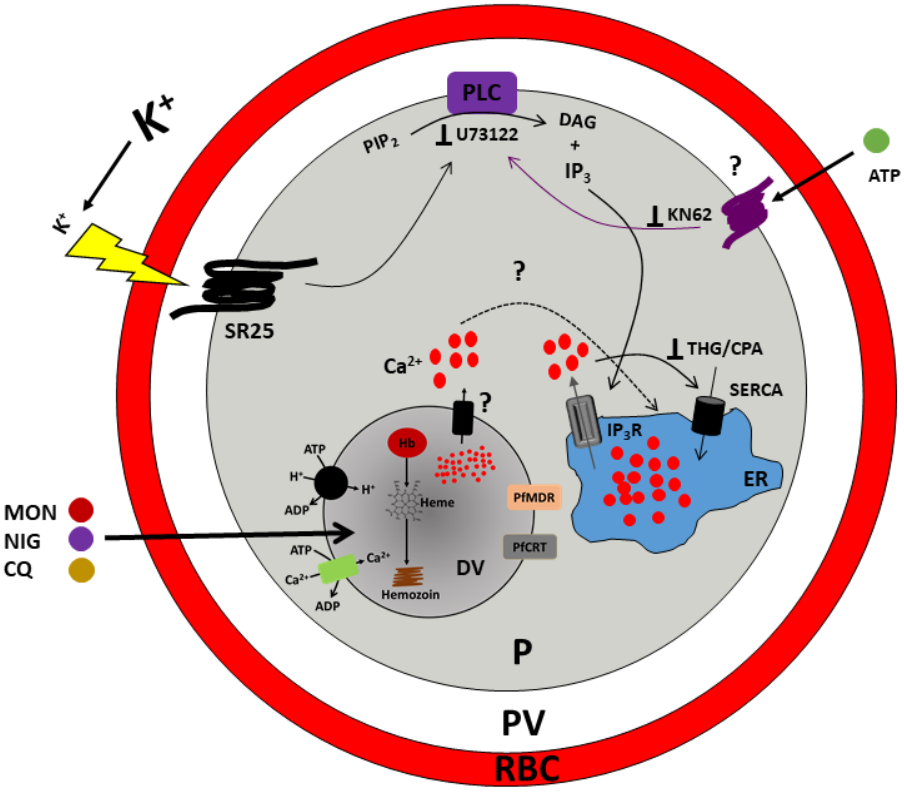

Figure 35: A schematic model representing the Ca^{2+} signaling cascades in *P. falciparum*

A schematic model of activation of PLC-IP_3 pathway downstream to K^+ sensing by PfSR25 and releasing cytosolic Ca^{2+} from the ER is shown. Alternatively, an unknown purinergic receptor is stimulated by the ATP molecules and triggers the ER-mediated Ca^{2+} release. The cytosolic Ca^{2+} is restored back to the ER by the SERCA pump. In a distinct pathway, when the ionic homeostasis is disrupted by the ionophores or CQ, Ca^{2+} is released from the DV. RBC: Red blood cell; PV: Parasitophorous vacuole; P: Parasite; Ca^{2+}: Calcium; ER: Endoplasmic reticulum; DV: Digestive vacuole; MON: Monensin; NIG: Nigericin; CQ: Chloroquine; PLC: Phospholipase C; CPA: Cyclopiazonic acid; THG: Thapsigargin

5.2 Identification of PfMel gene in P. falciparum that regulate melatonin signaling and cell cycle

The most striking feature of the malaria parasite is the coordinated rupture in host cell that follow a systematic periodicity of multiple of 24 hours. Remarkably, the synchrony is lost in *in vitro* culture and researchers often use other artificial ways such as sorbitol or heparin treatment

to achieve synchronous culture (Lambros and Vanderberg 1979, Ranford-Cartwright, Sinha et al. 2010, Kobayashi and Kato 2016). It was found that host circadian clock plays crucial role in parasite proliferation and has control over cell cycle synchrony of the parasites inside the host cell. Supplementing melatonin in *in vitro* culture has positive effect on parasite maturation and shift towards synchrony. On the other hand surgically removed pineal gland, which secrets melatonin, severely affects the parasite synchrony in the *P. chabaudi* infected mouse (Hotta, Gazarini et al. 2000). It is important to mention that the simultaneous rupture of schizonts provides the evolutionary advantage to parasites thus creating a challenging task for the immune system to deal with the rapid burst of merozoites inside the host bloodstream. Interference in the circadian rhythm of the host has a strong perturbing effect in parasite fitness for production of both replicating and transmission stages (O'Donnell, Schneider et al. 2011). Despite these evidences, the molecular basis of signaling mechanism and factors that relay melatonin message remains elucidated. In the eukaryotic system, two melatonin receptors MT1 and MT2 were identified and characterized as GPCR (Reppert 1997, Sugden, Davidson et al. 2004). Later, a third receptor MT3 has been identified in Syrian hamster kidney cells but more interestingly, it was characterized as homologue of the human quinone reductase 2 (QR2) (Nosjean, Ferro et al. 2000). However, such receptors are yet to identify in *Plasmodium* despite the fact that pharmacological evidence suggest the presence of a hypothetical melatonin receptor (Hotta, Gazarini et al. 2000, Beraldo, Almeida et al. 2005, Beraldo and Garcia 2005). Despite the availability of *P. falciparum* genome sequence, more than 60% genes are yet to be characterized, majorly due to non-homologous nature of these genes with known eukaryotic genes.

In this section, we tried to identify and characterize the molecular effector that may involve in cell cycle modulation by melatonin. Dr Luciana Madeira from our group has started this

project in search of possible melatonin receptor from *P. falciparum* extracts using Mel-Aga resins. Interestingly, two potential candidates were identified but unfortunately, none of them has any topological property of either a GPCR or a eukaryotic melatonin receptor. For further characterization, we have selected PfMel genes and investigate its role in parasite life cycle. In **Figure 18 & 19,** we have shown the protein domain organization and gene expression data from PlasmoDB server that shows that the expression of PfMel is constitutive in asexual stages and that mature parasites show a higher expression. When bioinformatics tools were applied to explore the domain organization, we found the presence of a kelch motif along with histidine kinase ATPase. Kelch is a 50-aa residue motif, first discovered as a six-fold tandem element in *Drosophila*, in which Kelch-mutant females lay sterile, cup-shaped eggs and affect cytoplasmic transport (Xue and Cooley 1993). The kelch motif largely present as a set of 5-7 kelch repeats (β-sheet blade) forming a β-propeller tertiary structure, for example 6-bladed β-propeller in the Drosophila egg-chamber. A kelch motif was also discovered in a multiple inositol-polyphosphate phosphatase (MIPP) – a mouse protein and in the poxvirus. Additionally, kelch repeats have also been recognized in an actin-cross-linking protein (scruin) of Limulus sperm (Way, Sanders et al. 1995) and in galactose oxidase of *Dactylium dendroides* (Ito, Phillips et al. 1991). β-propellers of kelch repeats are often involved in protein–protein interactions and kelch-like proteins are identified as substrate adaptors for Cullin 3 ubiquitin ligases (Pintard, Willems et al. 2004). Various functions are reported for kelch-containing proteins, which are largely dynamic: galactose oxidase catalyses the oxidation of the OH-group in D-galactose; scruin is an actin cross-linking protein; neuraminidase hydrolyses sialic acid residues from glycoproteins (Adams, Kelso et al. 2000). Kelch may also have a cytoskeletal function and appear to regulate the microtubule and microfilament networks.

The second domain was identified as histidine kinase like ATPase (HKATPase) domain. Interestingly, signaling components comprising histidine kinase (HK) are found in nearly all bacteria whose genome is available (Capra and Laub 2012). This domain is of great importance in bacteria and facilitates the response to a broad range of stimuli such as nutrients, cellular redox state, changes in osmolarity, quorum sensing and antibiotics (Laub and Goulian 2007). It was reported that HK involves a two-component signal transduction in bacteria via autophosphorylation at a conserved histidine residue with subsequent transfer of the phosphoryl group to a cognate response regulator (Capra and Laub 2012). Two-component pathways often involved in DNA binding so the cells can able to sense and then respond to the stimuli by inducing changes in transcription (Laub and Goulian 2007). However, the presence of HKATPase domain in PfMel suggests that *P. falciparum* may have functions in sensing extracellular signals.

When we performed the quantitative real time PCR for rings, trophozoites and schizonts, we found the constitutive presence of the PfMel transcript throughout the asexual cycle. More than a 2.5-fold increase with respect to ring parasites was seen in **Figure 20A,** which suggests a function of PfMel protein at late stages. To test the further synergistic role, we have performed the quantitative RT-PCR for PfMel expression in wild type 3D7 and *P. falciparum* orphan protein kinase PfPK7. The results in **Figure 20B** shows that in 3D7 parasites, 5 h melatonin treatment did not result in any change however; small but significant increase in PfPK7^{-} and PfPK7 complement parasites was seen. Moreover, a 17 h treatment resulted in an approximately 2-fold increase in PfMel transcript in 3D7 parasites. Our data shows that, PfPK7^{-} parasites displayed significant decrease while complementing PfPK7 vector to PfPK7^{-} somewhat decrease this difference but not as 3D7 **(Figure 20C)**. The different effect in 3D7 and PfPK7 parasites

may be due to differences in the promoter sequence upstream to the endogenous gene. It is important to note that up-regulation of melatonin induced UPS components were abolished in PfPK7^{-} when a comparative study was done with wild type *P. falciparum*. Unable to change in the asexual parasite development ratio and to induce $[Ca^{2+}]_{cyt}$ was other factors associated with PfPK7^{-} parasites. These effects were partially restored by complementing a functional copy of the PfPK7 gene in the PfPK7^{-} parasites (Koyama, Ribeiro et al. 2012). A differential gene expression pattern was seen when 3D7 trophozoites were treated with melatonin but PfPK7^{-} parasites were unable to replicate this profile, suggesting that PfPK7^{-} may positively affect the gene expression pattern.

In a study, when approximately 300 amino acids residues from C-terminal PF14_0649 (aka Pf1468 or PfMel) was transfected in yeast, it localizes both in cytosol and at the plasma membrane (Jeffress and Fields 2005). In this study, the authors have also suggested the PfMel function in drug resistance. They have shown that the antimalarial mefloquine treatment upregulated the PfMel expression in both CQS and CQR parasites, thus suggesting it may also involve in drug metabolism. However, no direct experiment was performed to elucidate the subcellular localization of PfMel in *P. falciparum*. In our next experiment, we have collaborated with Prof. Jude M. Przyborsky, Marburg University, Germany, to fuse various tags with PfMel to conduct more studies. First, we investigated the subcellular localization of PfMel and integrated green fluorescent biosensor GFP at 3'-UTR region of PfMel. Our immunofluorescent confocal imaging with ring, trophozoite and schizont parasites stained with the nuclear dye DAPI in **Figure 22** confirmed the nuclear localization in all forms of the parasites in the intraerythrocytic cycle. This leads us to investigate the possible direct role of PfMel in various physiological and morphological changes in the parasite. We followed a novel inducible gene

knock down approach over conventional reverse genetics approach to develop PfMel-HA and PfMel-HA-glmS parasite lines in collaboration with Dr. Jude Przyborsky, University of Marburg, Germany. The glmS ribozyme is a first known natural riboswitch RNA identified in Gram-positive bacteria and it encodes for an enzyme glutamine-fructose-6-phosphate amidotransferase that catalyzes the formation of glucosamine-6-phosphate (GlcN6P) (Barrick, Corbino et al. 2004). When present at physiologic concentration, glucosamine binds to the glmS ribozyme and uncovers a latent self-cleavage activity that ultimately leads to the degradation of the mRNA (Ferre-D'Amare 2010). The glmS ribozyme was inserted at 3'-UTR region of PfMel endogenous locus. Parallelly, an empty M9 vector lacking glmS ribozyme was also inserted as control parasite. The Western blot of recombinant parasite clones was shown in **Figure 24** suggesting the successful knock down parasite line. These constructs were tested for protein expression in asexual stages, which indicated that the protein expression is constitutive but became increased when parasite growth progressed to maturity confirming the expression profile of PlasmoDB and RT-PCR data. We also perform the immunofluorescent confocal imaging to investigate the subcellular localization using anti-HA (rabbit, Cell Signaling) antibody. Our imaging data in **Figure 25 & 25** was in agreement with PfMel-GFP imaging and in all asexual stages described, it co-localized with the nuclear stain DAPI, while the mitochondrial dye Mitotracker Red used as addition control that did not co-localized with PfMel.

Once the glmS-inducible recombinant strains were obtained, we tested the ability of glucosamine to activate the ribozyme to down-regulate the gene expression and subsequently intracellular protein production. Sorbitol synchronized young trophozoites were induced without and with 0.5, 1, 2.5 mM glucosamine for approximately 48 h when parasites became trophozoites in the subsequent cycle. Isolated parasites were resolved by SDS-PAGE and probed

with anti-HA antibody. Our result in **Figure 27** clearly illustrated the dose dependent protein reduction in PfMel-HA-glmS parasites while PfMel-HA control parasites were insensitive to glucosamine treatment. Our Western blot assay validates the knock down constructs and the correct band size (approximately 295 kDa) proved that PfMel is indeed under glmS ribozyme control.

Next, we investigated the morphological feature of recombinant parasites after glucosamine treatment. As **Figure 28** suggests, we performed two different sets of experiments. First, we counted the number of merozoites per schizont with and without glucosamine induction. These results did not exhibit any significant difference in merozoite numbers suggesting that the DNA replication and cell division is normal even after glucosamine induction **(Figure 28A)**. In other experiment, we investigated the growth pattern of PfMel knockdown parasites for three successive asexual cycles with and without glucosamine induction. We found normal PfMel-HA-glmS parasite growth in each glucosamine concentration, although there was a marginal but not significant decrease in parasitemia at 2.5 mM glucosamine suggesting that the less PfMel is not detrimental for the parasite **(Figure 28B)**. This leads us to explore other possible physiological effects since PfMel is sensitive to melatonin treatment. Therefore, we monitored the parasite maturation process after glucosamine induction in the PfMel construct. Wild type 3D7 was used as an additional control. Previously, we have shown that melatonin and its derivatives modulate parasite cycle by accelerating the maturation process (Hotta, Markus et al. 2003, Beraldo and Garcia 2005). Asynchronous parasites were first induced with glucosamine for 48 h followed by melatonin treatment for 24 h and asexual parasite distribution was monitored by flow cytometry. Our data in **Figure 29-31** clearly demonstrated that glucosamine induction abolished the parasite maturation in PfMel-HA-glmS parasites while 3D7 and PfMel-

HA remains responsive to melatonin where more matured parasites were detected. This result suggests that PfMel did not affect the number of mature parasite in schizonts but it can modulate the synchrony and hence may have functional role in the parasite rhythm.

It was also shown that melatonin based cell cycle modulation is also involved in $[Ca^{2+}]_{cyt}$ signaling and blocking Ca^{2+} has a detrimental effect on parasites (Hotta, Gazarini et al. 2000, Gazarini, Thomas et al. 2003, Beraldo, Almeida et al. 2005). Since our target gene was partly able to modulate the parasite cycle, so it would be important to test if it has any role in $[Ca^{2+}]_{cyt}$. To test this possibility, we treated the parasite construct with and without glucosamine and monitor the Ca^{2+} simulation upon melatonin stimulation. As per our expectation, the PfMel-HA control strain did not alter Ca^{2+} response in either cases however, in PfMel-HA-glmS strain, 2.5 mM glucosamine reduce the Ca^{2+} mobilization when compared to the control as seen in **Figure 32 & 33**. This result is very interesting and indicated the involvement of PfMel in cell cycle modulation; however, we do not know how this protein located in the nucleus could affect the Ca^{2+} mobilization by melatonin. However, it is worth to mention that in mammalian systems, the melatonin-exerted effect can be (i) binding with melatonin receptor on plasma membrane, (ii) binding to cytosolic proteins, and (iii) binding to unknown nuclear receptors (Emet, Ozcan et al. 2016). It was already shown that in the cell cytosol, melatonin interacts with Ca^{2+} binding proteins such as calmodulin and calreticulin to modulate various physiological processes (Benitez-King and Anton-Tay 1993, Macias, Escames et al. 2003). It was also shown that *P. falciparum* genome encodes various calmodulin-containing proteins that play crucial role in parasite growth and proliferation via cytosolic Ca^{2+} fluctuation (Budu, Gomes et al. 2016, Gomes Smaul, Budu et al. 2018). It might possible that melatonin interaction to either cytosolic proteins

or nuclear receptor is the key trigger to $[Ca^{2+}]_{cyt}$ release as well as different parasite form distribution. This hypothesis may be true but it requires further investigation.

To identify proteins that interact with PfMel, Co-IP in combination of mass-spectrometry was performed. In MS-based proteomics, the protein itself is used as an affinity reagent to isolate its binding partners. The primary advantages over previous technologies (specifically yeast-two hybrid) are that the protein is used in its fully processed form, the interactions are in the native environment of the protein, and multicomponent complexes may be isolated in a single step. Therefore, we investigated the interactome of PfMel in trophozoite stages by immunoprecipitation of PfMel from PfMel-GFP parasite lysates using anti-GFP antibodies and identify the proteins that had been affinity purified by mass-spectrometry. The obtained results are shown as pie chart diagram in **Figure 34** where we categorized them based on their basic functional properties using GO annotation. Among 37 identified proteins, two remained unidentified while majority of identified proteins belong to protein transport and protein folding **(Table 4)**. Other proteins that participate in cell metabolism, DNA/RNA metabolism, UPS and stress related proteins were also identified. Interestingly, a protein with high peptide hits was AP2 domain transcription factor. The ApiAp2 family protein PfAP2-I was shown to associate with bromodomain protein-1 (PfBDP-1) along with many chromatin-associated proteins and this complex formation is associated with transcriptional regulation for key invasive proteins (Josling and Llinas 2015, Santos, Josling et al. 2017).

Taken together, we have identified a new putative *P. falciparum* gene that localized in nucleus and play crucial role in melatonin-dependent cell signaling. Disrupting parasites cell-cycle may open new avenues for the development of antimalarial drugs. However, full characterization of PfMel requires further detail study.

6 CONCLUSIONS

In this study, we have performed various experiments and reached to the following goals:

1- We have investigated the role of a novel *P. falciparum* GPCR-like protein PfSR25 in asexual life cycle and found that this protein senses the change in extracellular potassium. In wild type parasites, sensing extracellular leads to change in $[Ca^{2+}]_{cyt}$, however knocking out the PfSR25 alter the sensing capability of the parasites. GPCRs are involved in several human diseases and are potential drug target for approximately 35% available drugs in the market. Finding GPCRs in *Plasmodium* and characterization of these GPCR-like receptor may open the new avenues to drug development to eliminate malaria.

2- Further, we also studied the role of extracellular ATP in cytosoloic Ca^{2+} mobilization. Addition of ATP to the parasites loaded with Ca^{2+} indicator dye reveals the change in Ca^{2+} flux. However, pretreatment of parasites with purinergic receptor antagonist KN62 ablate the Ca^{2+} change indicating multiple pathways in parasite Ca^{2+} signaling activation. It also suggests that, egress and invasion process is redundant and may harness $[Ca^{2+}]_{cyt}$ changes by alternate means.

3- Our studies on Ca^{2+} efflux by digestive vacuole suggest that mutation in chloroquine resistant transporter (PfCRT) is critical for the Ca^{2+} efflux. We also found that the chloroquine sensitive parasites 3D7, GC03 and $Dd2^{GC03}$ are more susceptible to either ionophore monensin & nigericin or antimalarial drug chloroquine treatment and released higher Ca^{2+} than resistant parasites Dd2 and $Dd2^{Dd2}$. Interestingly, introduction of new mutation in Dd2 parasite ($Dd2^{Dd2\ L272F}$) partially revert the Dd2 from CQ resistance to

partly sensitive however, the Ca^{2+} efflux was lower than the both CQS and CQR parasites.

4- In the last part of the study, we have for the first time, characterized a novel *P. falciparum* protein. Base on its melatonin sensitivity we named it PfMel. The expression of PfMel is throughout the asexual stages however, expression became relatively high in late stages. Our subcellular co-localization study revealed that PfMel is present in the nucleus. Knocking down the PfMel affects the parasite maturation to some extent as well as the $[Ca^{2+}]_{cyt}$ efflux. It is still unclear how PfMel modulate the parasite morphology and to some extent $[Ca^{2+}]_{cyt}$ efflux while residing in nucleus. It is possible that PfMel might be the part of nuclear protein complex that regulate the upstream genes or transcription factors necessary for parasite development.

REFERENCES

Adams, J., R. Kelso and L. Cooley (2000). "The kelch repeat superfamily of proteins: propellers of cell function." Trends Cell Biol **10**(1): 17-24.

Agarwal, S., M. K. Singh, S. Garg, C. E. Chitnis and S. Singh (2013). "Ca(2+) -mediated exocytosis of subtilisin-like protease 1: a key step in egress of Plasmodium falciparum merozoites." Cell Microbiol **15**(6): 910-921.

Akkaya, C., E. Shumilina, D. Bobballa, V. B. Brand, H. Mahmud, F. Lang and S. M. Huber (2009). "The Plasmodium falciparum-induced anion channel of human erythrocytes is an ATP-release pathway." Pflugers Arch **457**(5): 1035-1047.

Alaganan, A., P. Singh and C. E. Chitnis (2017). "Molecular mechanisms that mediate invasion and egress of malaria parasites from red blood cells." Curr Opin Hematol **24**(3): 208-214.

Alleva, L. M. and K. Kirk (2001). "Calcium regulation in the intraerythrocytic malaria parasite Plasmodium falciparum." Mol Biochem Parasitol **117**(2): 121-128.

Alves, E., P. J. Bartlett, C. R. Garcia and A. P. Thomas (2011). "Melatonin and IP3-induced Ca2+ release from intracellular stores in the malaria parasite Plasmodium falciparum within infected red blood cells." J Biol Chem **286**(7): 5905-5912.

Aly, A. S. and K. Matuschewski (2005). "A malarial cysteine protease is necessary for Plasmodium sporozoite egress from oocysts." J Exp Med **202**(2): 225-230.

Amino, R., D. Giovannini, S. Thiberge, P. Gueirard, B. Boisson, J. F. Dubremetz, M. C. Prevost, T. Ishino, M. Yuda and R. Menard (2008). "Host cell traversal is important for progression of the malaria parasite through the dermis to the liver." Cell Host Microbe **3**(2): 88-96.

Arrizabalaga, G. and J. C. Boothroyd (2004). "Role of calcium during Toxoplasma gondii invasion and egress." Int J Parasitol **34**(3): 361-368.

Ashley, E. A., M. Dhorda, R. M. Fairhurst, C. Amaratunga, P. Lim, S. Suon, S. Sreng, J. M. Anderson, S. Mao, B. Sam, C. Sopha, C. M. Chuor, C. Nguon, S. Sovannaroth, S. Pukrittayakamee, P. Jittamala, K. Chotivanich, K. Chutasmit, C. Suchatsoonthorn, R. Runcharoen, T. T. Hien, N. T. Thuy-Nhien, N. V. Thanh, N. H. Phu, Y. Htut, K. T. Han, K. H. Aye, O. A. Mokuolu, R. R. Olaosebikan, O. O. Folaranmi, M. Mayxay, M. Khanthavong, B. Hongvanthong, P. N. Newton, M. A. Onyamboko, C. I. Fanello, A. K. Tshefu, N. Mishra, N. Valecha, A. P. Phyo, F. Nosten, P. Yi, R. Tripura, S. Borrmann, M. Bashraheil, J. Peshu, M. A. Faiz, A. Ghose, M. A. Hossain, R. Samad, M. R. Rahman, M. M. Hasan, A. Islam, O. Miotto, R. Amato, B. MacInnis, J. Stalker, D. P. Kwiatkowski, Z. Bozdech, A. Jeeyapant, P. Y. Cheah, T. Sakulthaew, J. Chalk, B. Intharabut, K. Silamut, S. J. Lee, B. Vihokhern, C. Kunasol, M. Imwong, J. Tarning, W. J. Taylor, S. Yeung, C. J. Woodrow, J. A. Flegg, D. Das, J. Smith, M. Venkatesan, C. V. Plowe, K. Stepniewska, P. J. Guerin, A. M. Dondorp, N. P. Day, N. J. White

and C. Tracking Resistance to Artemisinin (2014). "Spread of artemisinin resistance in Plasmodium falciparum malaria." N Engl J Med **371**(5): 411-423.

Baldauf, S. L. (2003). "The deep roots of eukaryotes." Science **300**(5626): 1703-1706.

Bannister, L. and G. Mitchell (2003). "The ins, outs and roundabouts of malaria." Trends Parasitol **19**(5): 209-213.

Bannister, L. H., J. M. Hopkins, R. E. Fowler, S. Krishna and G. H. Mitchell (2000). "A brief illustrated guide to the ultrastructure of Plasmodium falciparum asexual blood stages." Parasitol Today **16**(10): 427-433.

Barrick, J. E., K. A. Corbino, W. C. Winkler, A. Nahvi, M. Mandal, J. Collins, M. Lee, A. Roth, N. Sudarsan, I. Jona, J. K. Wickiser and R. R. Breaker (2004). "New RNA motifs suggest an expanded scope for riboswitches in bacterial genetic control." Proc Natl Acad Sci U S A **101**(17): 6421-6426.

Benitez-King, G. and F. Anton-Tay (1993). "Calmodulin mediates melatonin cytoskeletal effects." Experientia **49**(8): 635-641.

Beraldo, F. H., F. M. Almeida, A. M. da Silva and C. R. Garcia (2005). "Cyclic AMP and calcium interplay as second messengers in melatonin-dependent regulation of Plasmodium falciparum cell cycle." J Cell Biol **170**(4): 551-557.

Beraldo, F. H. and C. R. Garcia (2005). "Products of tryptophan catabolism induce Ca2+ release and modulate the cell cycle of Plasmodium falciparum malaria parasites." J Pineal Res **39**(3): 224-230.

Beraldo, F. H., K. Mikoshiba and C. R. Garcia (2007). "Human malarial parasite, Plasmodium falciparum, displays capacitative calcium entry: 2-aminoethyl diphenylborinate blocks the signal transduction pathway of melatonin action on the P. falciparum cell cycle." J Pineal Res **43**(4): 360-364.

Berridge, M. J., P. Lipp and M. D. Bootman (2000). "The versatility and universality of calcium signalling." Nat Rev Mol Cell Biol **1**(1): 11-21.

Biagini, G. A., P. G. Bray, D. G. Spiller, M. R. White and S. A. Ward (2003). "The digestive food vacuole of the malaria parasite is a dynamic intracellular Ca2+ store." J Biol Chem **278**(30): 27910-27915.

Billker, O., S. Dechamps, R. Tewari, G. Wenig, B. Franke-Fayard and V. Brinkmann (2004). "Calcium and a calcium-dependent protein kinase regulate gamete formation and mosquito transmission in a malaria parasite." Cell **117**(4): 503-514.

Billker, O., V. Lindo, M. Panico, A. E. Etienne, T. Paxton, A. Dell, M. Rogers, R. E. Sinden and H. R. Morris (1998). "Identification of xanthurenic acid as the putative inducer of malaria development in the mosquito." Nature **392**(6673): 289-292.

Billker, O., M. K. Shaw, G. Margos and R. E. Sinden (1997). "The roles of temperature, pH and mosquito factors as triggers of male and female gametogenesis of Plasmodium berghei in vitro." Parasitology **115 (Pt 1)**: 1-7.

Bloland, P. B. (2001). "Drug resistance in malaria." World Health Organization.

Borges-Pereira, L., K. A. Meissner, C. Wrenger and C. R. Garcia (2017). "Plasmodium falciparum GFP-E-NTPDase expression at the intraerythrocytic stages and its inhibition blocks the development of the human malaria parasite." Purinergic Signal.

Brancucci, N. M. B., N. L. Bertschi, L. Zhu, I. Niederwieser, W. H. Chin, R. Wampfler, C. Freymond, M. Rottmann, I. Felger, Z. Bozdech and T. S. Voss (2014). "Heterochromatin protein 1 secures survival and transmission of malaria parasites." Cell Host Microbe **16**(2): 165-176.

Brancucci, N. M. B., J. P. Gerdt, C. Wang, M. De Niz, N. Philip, S. R. Adapa, M. Zhang, E. Hitz, I. Niederwieser, S. D. Boltryk, M. C. Laffitte, M. A. Clark, C. Gruring, D. Ravel, A. Blancke Soares, A. Demas, S. Bopp, B. Rubio-Ruiz, A. Conejo-Garcia, D. F. Wirth, E. Gendaszewska-Darmach, M. T. Duraisingh, J. H. Adams, T. S. Voss, A. P. Waters, R. H. Y. Jiang, J. Clardy and M. Marti (2017). "Lysophosphatidylcholine Regulates Sexual Stage Differentiation in the Human Malaria Parasite Plasmodium falciparum." Cell **171**(7): 1532-1544 e1515.

Budu, A., M. M. Gomes, P. M. Melo, S. El Chamy Maluf, P. Bagnaresi, M. F. Azevedo, A. K. Carmona and M. L. Gazarini (2016). "Calmidazolium evokes high calcium fluctuations in Plasmodium falciparum." Cell Signal **28**(3): 125-135.

Budu, A., R. Peres, V. B. Bueno, L. H. Catalani and C. R. Garcia (2007). "N1-acetyl-N2-formyl-5-methoxykynuramine modulates the cell cycle of malaria parasites." J Pineal Res **42**(3): 261-266.

Capra, E. J. and M. T. Laub (2012). "Evolution of two-component signal transduction systems." Annu Rev Microbiol **66**: 325-347.

Carey, A. F., M. Singer, D. Bargieri, S. Thiberge, F. Frischknecht, R. Menard and R. Amino (2014). "Calcium dynamics of Plasmodium berghei sporozoite motility." Cell Microbiol **16**(5): 768-783.

Carter, R. and L. H. Miller (1979). "Evidence for environmental modulation of gametocytogenesis in Plasmodium falciparum in continuous culture." Bull World Health Organ **57 Suppl 1**: 37-52.

Cassone, V. M. and A. K. Natesan (1997). "Time and time again: the phylogeny of melatonin as a transducer of biological time." J Biol Rhythms **12**(6): 489-497.

Ch'ng, J. H., K. Liew, A. S. Goh, E. Sidhartha and K. S. Tan (2011). "Drug-induced permeabilization of parasite's digestive vacuole is a key trigger of programmed cell death in Plasmodium falciparum." Cell Death Dis **2**: e216.

Chakravorty, S. J., K. R. Hughes and A. G. Craig (2008). "Host response to cytoadherence in Plasmodium falciparum." Biochem Soc Trans **36**(Pt 2): 221-228.

Chaves, Y. O., A. G. da Costa, M. L. Pereira, M. V. de Lacerda, J. G. Coelho-Dos-Reis, O. A. Martins-Filho, A. Teixeira-Carvalho, A. Malheiro, W. M. Monteiro, P. P. Orlandi, C. R. Marinho and P. A. Nogueira (2016). "Immune response pattern in recurrent Plasmodium vivax malaria." Malar J **15**(1): 445.

Chitnis, C. E. and H. M. Staines (2013). "Dealing with change: the different microenvironments faced by the malarial parasite." Mol Microbiol **88**(1): 1-4.

Cho, J. W., C. W. Kim and K. S. Lee (2007). "Modification of gene expression by melatonin in UVB-irradiated HaCaT keratinocyte cell lines using a cDNA microarray." Oncol Rep **17**(3): 573-577.

Clapham, D. E. (2007). "Calcium signaling." Cell **131**(6): 1047-1058.

Coleman, B. I., K. M. Skillman, R. H. Y. Jiang, L. M. Childs, L. M. Altenhofen, M. Ganter, Y. Leung, I. Goldowitz, B. F. C. Kafsack, M. Marti, M. Llinas, C. O. Buckee and M. T. Duraisingh (2014). "A Plasmodium falciparum histone deacetylase regulates antigenic variation and gametocyte conversion." Cell Host Microbe **16**(2): 177-186.

Collins, C. R., F. Hackett, M. Strath, M. Penzo, C. Withers-Martinez, D. A. Baker and M. J. Blackman (2013). "Malaria parasite cGMP-dependent protein kinase regulates blood stage merozoite secretory organelle discharge and egress." PLoS Pathog **9**(5): e1003344.

Collins, W. E. and G. M. Jeffery (2007). "Plasmodium malariae: parasite and disease." Clin Microbiol Rev **20**(4): 579-592.

Cowman, A. F., D. Berry and J. Baum (2012). "The cellular and molecular basis for malaria parasite invasion of the human red blood cell." J Cell Biol **198**(6): 961-971.

Cowman, A. F., J. Healer, D. Marapana and K. Marsh (2016). "Malaria: Biology and Disease." Cell **167**(3): 610-624.

Cox, F. E. (2002). "History of human parasitology." Clin Microbiol Rev **15**(4): 595-612.

Craig, A. G., M. F. Khairul and P. R. Patil (2012). "Cytoadherence and severe malaria." Malays J Med Sci **19**(2): 5-18.

Cruz, L. N., Y. Wu, H. Ulrich, A. G. Craig and C. R. Garcia (2016). "Tumor necrosis factor reduces Plasmodium falciparum growth and activates calcium signaling in human malaria parasites." Biochim Biophys Acta **1860**(7): 1489-1497.

Cui, L., S. Mharakurwa, D. Ndiaye, P. K. Rathod and P. J. Rosenthal (2015). "Antimalarial Drug Resistance: Literature Review and Activities and Findings of the ICEMR Network." Am J Trop Med Hyg **93**(3 Suppl): 57-68.

Dobson, S., T. May, M. Berriman, C. Del Vecchio, A. H. Fairlamb, D. Chakrabarti and S. Barik (1999). "Characterization of protein Ser/Thr phosphatases of the malaria parasite, Plasmodium falciparum: inhibition of the parasitic calcineurin by cyclophilin-cyclosporin complex." Mol Biochem Parasitol **99**(2): 167-181.

Docampo, R. and S. N. Moreno (1999). "Acidocalcisome: A novel Ca2+ storage compartment in trypanosomatids and apicomplexan parasites." Parasitol Today **15**(11): 443-448.

Doerig, C., D. Baker, O. Billker, M. J. Blackman, C. Chitnis, S. Dhar Kumar, V. Heussler, A. A. Holder, C. Kocken, S. Krishna, G. Langsley, E. Lasonder, R. Menard, M. Meissner, G. Pradel, L. Ranford-Cartwright, A. Sharma, P. Sharma, T. Tardieux, U. Tatu and P. Alano (2009). "Signalling in malaria parasites. The MALSIG consortium." Parasite **16**(3): 169-182.

Dondorp, A. M., T. T. Chau, N. H. Phu, N. T. Mai, P. P. Loc, L. V. Chuong, D. X. Sinh, A. Taylor, T. T. Hien, N. J. White and N. P. Day (2004). "Unidentified acids of strong prognostic significance in severe malaria." Crit Care Med **32**(8): 1683-1688.

Dorin, D., J. P. Semblat, P. Poullet, P. Alano, J. P. Goldring, C. Whittle, S. Patterson, D. Chakrabarti and C. Doerig (2005). "PfPK7, an atypical MEK-related protein kinase, reflects the absence of classical three-component MAPK pathways in the human malaria parasite Plasmodium falciparum." Mol Microbiol **55**(1): 184-196.

Dorin-Semblat, D., A. Sicard, C. Doerig, L. Ranford-Cartwright and C. Doerig (2008). "Disruption of the PfPK7 gene impairs schizogony and sporogony in the human malaria parasite Plasmodium falciparum." Eukaryot Cell **7**(2): 279-285.

Dubocovich, M. L. and M. Markowska (2005). "Functional MT1 and MT2 melatonin receptors in mammals." Endocrine **27**(2): 101-110.

Dvorak, J. A., L. H. Miller, W. C. Whitehouse and T. Shiroishi (1975). "Invasion of erythrocytes by malaria merozoites." Science **187**(4178): 748-750.

Dvorin, J. D., D. C. Martyn, S. D. Patel, J. S. Grimley, C. R. Collins, C. S. Hopp, A. T. Bright, S. Westenberger, E. Winzeler, M. J. Blackman, D. A. Baker, T. J. Wandless and M. T. Duraisingh (2010). "A plant-like kinase in Plasmodium falciparum regulates parasite egress from erythrocytes." Science **328**(5980): 910-912.

Ecker, A., A. M. Lehane, J. Clain and D. A. Fidock (2012). "PfCRT and its role in antimalarial drug resistance." Trends Parasitol **28**(11): 504-514.

Eckstein-Ludwig, U., R. J. Webb, I. D. Van Goethem, J. M. East, A. G. Lee, M. Kimura, P. M. O'Neill, P. G. Bray, S. A. Ward and S. Krishna (2003). "Artemisinins target the SERCA of Plasmodium falciparum." Nature **424**(6951): 957-961.

Edgar, R. S., E. W. Green, Y. Zhao, G. van Ooijen, M. Olmedo, X. Qin, Y. Xu, M. Pan, U. K. Valekunja, K. A. Feeney, E. S. Maywood, M. H. Hastings, N. S. Baliga, M. Merrow, A. J.

Millar, C. H. Johnson, C. P. Kyriacou, J. S. O'Neill and A. B. Reddy (2012). "Peroxiredoxins are conserved markers of circadian rhythms." Nature **485**(7399): 459-464.

Elsworth, B., K. Matthews, C. Q. Nie, M. Kalanon, S. C. Charnaud, P. R. Sanders, S. A. Chisholm, N. A. Counihan, P. J. Shaw, P. Pino, J. A. Chan, M. F. Azevedo, S. J. Rogerson, J. G. Beeson, B. S. Crabb, P. R. Gilson and T. F. de Koning-Ward (2014). "PTEX is an essential nexus for protein export in malaria parasites." Nature **511**(7511): 587-591.

Emet, M., H. Ozcan, L. Ozel, M. Yayla, Z. Halici and A. Hacimuftuoglu (2016). "A Review of Melatonin, Its Receptors and Drugs." Eurasian J Med **48**(2): 135-141.

Farrell, A., S. Thirugnanam, A. Lorestani, J. D. Dvorin, K. P. Eidell, D. J. Ferguson, B. R. Anderson-White, M. T. Duraisingh, G. T. Marth and M. J. Gubbels (2012). "A DOC2 protein identified by mutational profiling is essential for apicomplexan parasite exocytosis." Science **335**(6065): 218-221.

Ferre-D'Amare, A. R. (2010). "The glmS ribozyme: use of a small molecule coenzyme by a gene-regulatory RNA." Q Rev Biophys **43**(4): 423-447.

Fidock, D. A., T. Nomura, A. K. Talley, R. A. Cooper, S. M. Dzekunov, M. T. Ferdig, L. M. Ursos, A. B. Sidhu, B. Naude, K. W. Deitsch, X. Z. Su, J. C. Wootton, P. D. Roepe and T. E. Wellems (2000). "Mutations in the P. falciparum digestive vacuole transmembrane protein PfCRT and evidence for their role in chloroquine resistance." Mol Cell **6**(4): 861-871.

Frevert, U., P. Sinnis, C. Cerami, W. Shreffler, B. Takacs and V. Nussenzweig (1993). "Malaria circumsporozoite protein binds to heparan sulfate proteoglycans associated with the surface membrane of hepatocytes." J Exp Med **177**(5): 1287-1298.

Galinski, M. R. and J. W. Barnwell (2008). "Plasmodium vivax: who cares?" Malar J **7 Suppl 1**: S9.

Gantt, S., C. Persson, K. Rose, A. J. Birkett, R. Abagyan and V. Nussenzweig (2000). "Antibodies against thrombospondin-related anonymous protein do not inhibit Plasmodium sporozoite infectivity in vivo." Infect Immun **68**(6): 3667-3673.

Garcia, C. R. (1999). "Calcium homeostasis and signaling in the blood-stage malaria parasite." Parasitol Today **15**(12): 488-491.

Garcia, C. R., S. E. Ann, E. S. Tavares, A. R. Dluzewski, W. T. Mason and F. B. Paiva (1998). "Acidic calcium pools in intraerythrocytic malaria parasites." Eur J Cell Biol **76**(2): 133-138.

Garcia, C. R., M. F. de Azevedo, G. Wunderlich, A. Budu, J. A. Young and L. Bannister (2008). "Plasmodium in the postgenomic era: new insights into the molecular cell biology of malaria parasites." Int Rev Cell Mol Biol **266**: 85-156.

Garcia, C. R. S., E. Alves, P. H. S. Pereira, P. J. Bartlett, A. P. Thomas, K. Mikoshiba, H. Plattner and L. D. Sibley (2017). "InsP3 Signaling in Apicomplexan Parasites." Curr Top Med Chem **17**(19): 2158-2165.

Gardner, M. J., N. Hall, E. Fung, O. White, M. Berriman, R. W. Hyman, J. M. Carlton, A. Pain, K. E. Nelson, S. Bowman, I. T. Paulsen, K. James, J. A. Eisen, K. Rutherford, S. L. Salzberg, A. Craig, S. Kyes, M. S. Chan, V. Nene, S. J. Shallom, B. Suh, J. Peterson, S. Angiuoli, M. Pertea, J. Allen, J. Selengut, D. Haft, M. W. Mather, A. B. Vaidya, D. M. Martin, A. H. Fairlamb, M. J. Fraunholz, D. S. Roos, S. A. Ralph, G. I. McFadden, L. M. Cummings, G. M. Subramanian, C. Mungall, J. C. Venter, D. J. Carucci, S. L. Hoffman, C. Newbold, R. W. Davis, C. M. Fraser and B. Barrell (2002). "Genome sequence of the human malaria parasite Plasmodium falciparum." Nature **419**(6906): 498-511.

Garg, S., S. Agarwal, S. Kumar, S. S. Yazdani, C. E. Chitnis and S. Singh (2013). "Calcium-dependent permeabilization of erythrocytes by a perforin-like protein during egress of malaria parasites." Nat Commun **4**: 1736.

Gazarini, M. L. and C. R. Garcia (2004). "The malaria parasite mitochondrion senses cytosolic Ca2+ fluctuations." Biochem Biophys Res Commun **321**(1): 138-144.

Gazarini, M. L., C. A. Sigolo, R. P. Markus, A. P. Thomas and C. R. Garcia (2007). "Antimalarial drugs disrupt ion homeostasis in malarial parasites." Mem Inst Oswaldo Cruz **102**(3): 329-334.

Gazarini, M. L., A. P. Thomas, T. Pozzan and C. R. Garcia (2003). "Calcium signaling in a low calcium environment: how the intracellular malaria parasite solves the problem." J Cell Biol **161**(1): 103-110.

Ginsburg, H., M. Krugliak, O. Eidelman and Z. I. Cabantchik (1983). "New permeability pathways induced in membranes of Plasmodium falciparum infected erythrocytes." Mol Biochem Parasitol **8**(2): 177-190.

Glushakova, S., V. Lizunov, P. S. Blank, K. Melikov, G. Humphrey and J. Zimmerberg (2013). "Cytoplasmic free Ca2+ is essential for multiple steps in malaria parasite egress from infected erythrocytes." Malar J **12**: 41.

Gomes Smaul, M. M., A. Budu, G. N. Montagna, T. Fernanda da Silva Ferrara, S. El Chamy Maluf, P. Bagnaresi, M. M. Ferreira Machado, F. Bronze Dos Santos, M. Ferreira de Azevedo, A. K. Carmona and M. L. Gazarini (2018). "Plasmodium falciparum histidine triad protein and calmodulin modulates calcium homeostasis and intracellular proteolysis." Biochem Biophys Res Commun.

Grau, G. E., P. F. Piguet, P. Vassalli and P. H. Lambert (1989). "Involvement of tumour necrosis factor and other cytokines in immune-mediated vascular pathology." Int Arch Allergy Appl Immunol **88**(1-2): 34-39.

Grau, G. E., T. E. Taylor, M. E. Molyneux, J. J. Wirima, P. Vassalli, M. Hommel and P. H. Lambert (1989). "Tumor necrosis factor and disease severity in children with falciparum malaria." N Engl J Med **320**(24): 1586-1591.

Green, J. L., R. R. Rees-Channer, S. A. Howell, S. R. Martin, E. Knuepfer, H. M. Taylor, M. Grainger and A. A. Holder (2008). "The motor complex of Plasmodium falciparum: phosphorylation by a calcium-dependent protein kinase." J Biol Chem **283**(45): 30980-30989.

Hashimoto, M., M. Enomoto, J. Morales, N. Kurebayashi, T. Sakurai, T. Hashimoto, T. Nara and K. Mikoshiba (2013). "Inositol 1,4,5-trisphosphate receptor regulates replication, differentiation, infectivity and virulence of the parasitic protist Trypanosoma cruzi." Mol Microbiol **87**(6): 1133-1150.

Hojo-Souza, N. S., D. B. Pereira, T. A. Mendes, L. S. Passos, A. C. Gazzinelli-Guimaraes, P. H. Gazzinelli-Guimaraes, M. S. Tada, G. M. Zanini, D. C. Bartholomeu, R. T. Fujiwara and L. L. Bueno (2015). "CD4+ T cells apoptosis in Plasmodium vivax infection is mediated by activation of both intrinsic and extrinsic pathways." Malar J **14**: 5.

Hotta, C. T., M. L. Gazarini, F. H. Beraldo, F. P. Varotti, C. Lopes, R. P. Markus, T. Pozzan and C. R. Garcia (2000). "Calcium-dependent modulation by melatonin of the circadian rhythm in malarial parasites." Nat Cell Biol **2**(7): 466-468.

Hotta, C. T., R. P. Markus and C. R. Garcia (2003). "Melatonin and N-acetyl-serotonin cross the red blood cell membrane and evoke calcium mobilization in malarial parasites." Braz J Med Biol Res **36**(11): 1583-1587.

Huang, G., P. J. Bartlett, A. P. Thomas, S. N. Moreno and R. Docampo (2013). "Acidocalcisomes of Trypanosoma brucei have an inositol 1,4,5-trisphosphate receptor that is required for growth and infectivity." Proc Natl Acad Sci U S A **110**(5): 1887-1892.

Ito, N., S. E. Phillips, C. Stevens, Z. B. Ogel, M. J. McPherson, J. N. Keen, K. D. Yadav and P. F. Knowles (1991). "Novel thioether bond revealed by a 1.7 A crystal structure of galactose oxidase." Nature **350**(6313): 87-90.

Jeffress, M. and S. Fields (2005). "Identification of putative Plasmodium falciparum mefloquine resistance genes." Mol Biochem Parasitol **139**(2): 133-139.

Jones, M. L., C. Cottingham and J. C. Rayner (2009). "Effects of calcium signaling on Plasmodium falciparum erythrocyte invasion and post-translational modification of gliding-associated protein 45 (PfGAP45)." Mol Biochem Parasitol **168**(1): 55-62.

Josling, G. A. and M. Llinas (2015). "Sexual development in Plasmodium parasites: knowing when it's time to commit." Nat Rev Microbiol **13**(9): 573-587.

Kafsack, B. F., N. Rovira-Graells, T. G. Clark, C. Bancells, V. M. Crowley, S. G. Campino, A. E. Williams, L. G. Drought, D. P. Kwiatkowski, D. A. Baker, A. Cortes and M. Llinas (2014).

"A transcriptional switch underlies commitment to sexual development in malaria parasites." Nature **507**(7491): 248-252.

Kapishnikov, S., A. Weiner, E. Shimoni, G. Schneider, M. Elbaum and L. Leiserowitz (2013). "Digestive vacuole membrane in Plasmodium falciparum-infected erythrocytes: relevance to templated nucleation of hemozoin." Langmuir **29**(47): 14595-14602.

Kariu, T., M. Yuda, K. Yano and Y. Chinzei (2002). "MAEBL is essential for malarial sporozoite infection of the mosquito salivary gland." J Exp Med **195**(10): 1317-1323.

Karunaweera, N. D., G. E. Grau, P. Gamage, R. Carter and K. N. Mendis (1992). "Dynamics of fever and serum levels of tumor necrosis factor are closely associated during clinical paroxysms in Plasmodium vivax malaria." Proc Natl Acad Sci U S A **89**(8): 3200-3203.

Kirk, K., H. A. Horner, B. C. Elford, J. C. Ellory and C. I. Newbold (1994). "Transport of diverse substrates into malaria-infected erythrocytes via a pathway showing functional characteristics of a chloride channel." J Biol Chem **269**(5): 3339-3347.

Kobayashi, K. and K. Kato (2016). "Evaluating the use of heparin for synchronization of in vitro culture of Plasmodium falciparum." Parasitol Int **65**(5 Pt B): 549-551.

Kojin, B. B., A. L. Costa-da-Silva, C. Maciel, D. A. Henriques, D. O. Carvalho, K. Martin, O. Marinotti, A. A. James, M. C. Bonaldo and M. L. Capurro (2016). "Endogenously-expressed NH2-terminus of circumsporozoite protein interferes with sporozoite invasion of mosquito salivary glands." Malar J **15**: 153.

Koyama, F. C., R. Y. Ribeiro, J. L. Garcia, M. F. Azevedo, D. Chakrabarti and C. R. Garcia (2012). "Ubiquitin proteasome system and the atypical kinase PfPK7 are involved in melatonin signaling in Plasmodium falciparum." J Pineal Res **53**(2): 147-153.

Krishna, S. and L. L. Ng (1989). "Cation metabolism in malaria-infected red cells." Exp Parasitol **69**(4): 402-406.

Krishna, S., C. Woodrow, R. Webb, J. Penny, K. Takeyasu, M. Kimura and J. M. East (2001). "Expression and functional characterization of a Plasmodium falciparum Ca2+-ATPase (PfATP4) belonging to a subclass unique to apicomplexan organisms." J Biol Chem **276**(14): 10782-10787.

Kumar, K. A., C. R. Garcia, V. R. Chandran, N. Van Rooijen, Y. Zhou, E. Winzeler and V. Nussenzweig (2007). "Exposure of Plasmodium sporozoites to the intracellular concentration of potassium enhances infectivity and reduces cell passage activity." Mol Biochem Parasitol **156**(1): 32-40.

Kumar, R., A. Musiyenko, A. Oldenburg, B. Adams and S. Barik (2004). "Post-translational generation of constitutively active cores from larger phosphatases in the malaria parasite, Plasmodium falciparum: implications for proteomics." BMC Mol Biol **5**: 6.

Lambros, C. and J. P. Vanderberg (1979). "Synchronization of Plasmodium falciparum erythrocytic stages in culture." J Parasitol **65**(3): 418-420.

Laub, M. T. and M. Goulian (2007). "Specificity in two-component signal transduction pathways." Annu Rev Genet **41**: 121-145.

Lerner, A. B., J. D. Case, W. Mori and M. R. Wright (1959). "Melatonin in peripheral nerve." Nature **183**: 1821.

Levano-Garcia, J., A. R. Dluzewski, R. P. Markus and C. R. Garcia (2010). "Purinergic signalling is involved in the malaria parasite Plasmodium falciparum invasion to red blood cells." Purinergic Signal **6**(4): 365-372.

Lima, W. R., G. Tessarin-Almeida, A. Rozanski, K. S. Parreira, M. S. Moraes, D. C. Martins, R. F. Hashimoto, P. A. F. Galante and C. R. S. Garcia (2016). "Signaling transcript profile of the asexual intraerythrocytic development cycle of Plasmodium falciparum induced by melatonin and cAMP." Genes Cancer **7**(9-10): 323-339.

Liu, W., Y. Li, G. H. Learn, R. S. Rudicell, J. D. Robertson, B. F. Keele, J. B. Ndjango, C. M. Sanz, D. B. Morgan, S. Locatelli, M. K. Gonder, P. J. Kranzusch, P. D. Walsh, E. Delaporte, E. Mpoudi-Ngole, A. V. Georgiev, M. N. Muller, G. M. Shaw, M. Peeters, P. M. Sharp, J. C. Rayner and B. H. Hahn (2010). "Origin of the human malaria parasite Plasmodium falciparum in gorillas." Nature **467**(7314): 420-425.

Liu, W., Y. Li, K. S. Shaw, G. H. Learn, L. J. Plenderleith, J. A. Malenke, S. A. Sundararaman, M. A. Ramirez, P. A. Crystal, A. G. Smith, F. Bibollet-Ruche, A. Ayouba, S. Locatelli, A. Esteban, F. Mouacha, E. Guichet, C. Butel, S. Ahuka-Mundeke, B. I. Inogwabini, J. B. Ndjango, S. Speede, C. M. Sanz, D. B. Morgan, M. K. Gonder, P. J. Kranzusch, P. D. Walsh, A. V. Georgiev, M. N. Muller, A. K. Piel, F. A. Stewart, M. L. Wilson, A. E. Pusey, L. Cui, Z. Wang, A. Farnert, C. J. Sutherland, D. Nolder, J. A. Hart, T. B. Hart, P. Bertolani, A. Gillis, M. LeBreton, B. Tafon, J. Kiyang, C. F. Djoko, B. S. Schneider, N. D. Wolfe, E. Mpoudi-Ngole, E. Delaporte, R. Carter, R. L. Culleton, G. M. Shaw, J. C. Rayner, M. Peeters, B. H. Hahn and P. M. Sharp (2014). "African origin of the malaria parasite Plasmodium vivax." Nat Commun **5**: 3346.

Luo, S., F. A. Ruiz and S. N. Moreno (2005). "The acidocalcisome Ca2+-ATPase (TgA1) of Toxoplasma gondii is required for polyphosphate storage, intracellular calcium homeostasis and virulence." Mol Microbiol **55**(4): 1034-1045.

Macias, M., G. Escames, J. Leon, A. Coto, Y. Sbihi, A. Osuna and D. Acuna-Castroviejo (2003). "Calreticulin-melatonin. An unexpected relationship." Eur J Biochem **270**(5): 832-840.

Mackintosh, C. L., J. G. Beeson and K. Marsh (2004). "Clinical features and pathogenesis of severe malaria." Trends Parasitol **20**(12): 597-603.

Madeira, L., P. A. Galante, A. Budu, M. F. Azevedo, B. Malnic and C. R. Garcia (2008). "Genome-wide detection of serpentine receptor-like proteins in malaria parasites." PLoS One **3**(3): e1889.

Martin, R. E. and K. Kirk (2004). "The malaria parasite's chloroquine resistance transporter is a member of the drug/metabolite transporter superfamily." Mol Biol Evol **21**(10): 1938-1949.

Martin, R. E., R. V. Marchetti, A. I. Cowan, S. M. Howitt, S. Broer and K. Kirk (2009). "Chloroquine transport via the malaria parasite's chloroquine resistance transporter." Science **325**(5948): 1680-1682.

McClung, C. R. (2006). "Plant circadian rhythms." Plant Cell **18**(4): 792-803.

Mendonca, V. R., L. C. Souza, G. C. Garcia, B. M. Magalhaes, M. V. Lacerda, B. B. Andrade, M. S. Goncalves and M. Barral-Netto (2014). "DDX39B (BAT1), TNF and IL6 gene polymorphisms and association with clinical outcomes of patients with Plasmodium vivax malaria." Malar J **13**: 278.

Mideo, N., S. E. Reece, A. L. Smith and C. J. Metcalf (2013). "The Cinderella syndrome: why do malaria-infected cells burst at midnight?" Trends Parasitol **29**(1): 10-16.

Moraes, M. S., A. Budu, M. K. Singh, L. Borges-Pereira, J. Levano-Garcia, C. Currà, L. Picci, T. Pace, M. Ponzi, T. Pozzan and C. R. S. Garcia (2017). "Plasmodium falciparum GPCR-like receptor SR25 mediates extracellular K+ sensing coupled to Ca2+ signaling and stress survival." Scientific Reports **7**(1): 9545.

Moudy, R., T. J. Manning and C. J. Beckers (2001). "The loss of cytoplasmic potassium upon host cell breakdown triggers egress of Toxoplasma gondii." J Biol Chem **276**(44): 41492-41501.

Mullis, K., F. Faloona, S. Scharf, R. Saiki, G. Horn and H. Erlich (1986). "Specific enzymatic amplification of DNA in vitro: the polymerase chain reaction." Cold Spring Harb Symp Quant Biol **51 Pt 1**: 263-273.

Nadjm, B. and R. H. Behrens (2012). "Malaria: an update for physicians." Infect Dis Clin North Am **26**(2): 243-259.

Nagamune, K., L. M. Hicks, B. Fux, F. Brossier, E. N. Chini and L. D. Sibley (2008). "Abscisic acid controls calcium-dependent egress and development in Toxoplasma gondii." Nature **451**(7175): 207-210.

Nagamune, K., S. N. Moreno, E. N. Chini and L. D. Sibley (2008). "Calcium regulation and signaling in apicomplexan parasites." Subcell Biochem **47**: 70-81.

Nagamune, K. and L. D. Sibley (2006). "Comparative genomic and phylogenetic analyses of calcium ATPases and calcium-regulated proteins in the apicomplexa." Mol Biol Evol **23**(8): 1613-1627.

Nijhout, M. M. and R. Carter (1978). "Gamete development in malaria parasites: bicarbonate-dependent stimulation by pH in vitro." Parasitology **76**(1): 39-53.

Nosjean, O., M. Ferro, F. Coge, P. Beauverger, J. M. Henlin, F. Lefoulon, J. L. Fauchere, P. Delagrange, E. Canet and J. A. Boutin (2000). "Identification of the melatonin-binding site MT3 as the quinone reductase 2." J Biol Chem **275**(40): 31311-31317.

O'Donnell, A. J., P. Schneider, H. G. McWatters and S. E. Reece (2011). "Fitness costs of disrupting circadian rhythms in malaria parasites." Proc Biol Sci **278**(1717): 2429-2436.

Ono, T., L. Cabrita-Santos, R. Leitao, E. Bettiol, L. A. Purcell, O. Diaz-Pulido, L. B. Andrews, T. Tadakuma, P. Bhanot, M. M. Mota and A. Rodriguez (2008). "Adenylyl cyclase alpha and cAMP signaling mediate Plasmodium sporozoite apical regulated exocytosis and hepatocyte infection." PLoS Pathog **4**(2): e1000008.

Paredes, S. D., A. Korkmaz, L. C. Manchester, D. X. Tan and R. J. Reiter (2009). "Phytomelatonin: a review." J Exp Bot **60**(1): 57-69.

Passos, A. P. and C. R. Garcia (1998). "Inositol 1,4,5-trisphosphate induced Ca2+ release from chloroquine-sensitive and -insensitive intracellular stores in the intraerythrocytic stage of the malaria parasite P. chabaudi." Biochem Biophys Res Commun **245**(1): 155-160.

Paul, A. S., S. Saha, K. Engelberg, R. H. Jiang, B. I. Coleman, A. L. Kosber, C. T. Chen, M. Ganter, N. Espy, T. W. Gilberger, M. J. Gubbels and M. T. Duraisingh (2015). "Parasite Calcineurin Regulates Host Cell Recognition and Attachment by Apicomplexans." Cell Host Microbe **18**(1): 49-60.

Pillai, A. D., R. Addo, P. Sharma, W. Nguitragool, P. Srinivasan and S. A. Desai (2013). "Malaria parasites tolerate a broad range of ionic environments and do not require host cation remodelling." Mol Microbiol **88**(1): 20-34.

Pingret, L., J. M. Millot, S. Sharonov, A. Bonhomme, M. Manfait and J. M. Pinon (1996). "Relationship between intracellular free calcium concentrations and the intracellular development of Toxoplasma gondii." J Histochem Cytochem **44**(10): 1123-1129.

Pintard, L., A. Willems and M. Peter (2004). "Cullin-based ubiquitin ligases: Cul3-BTB complexes join the family." EMBO J **23**(8): 1681-1687.

Poinar, G., Jr. (2005). "Plasmodium dominicana n. sp. (Plasmodiidae: Haemospororida) from Tertiary Dominican amber." Syst Parasitol **61**(1): 47-52.

Prole, D. L. and C. W. Taylor (2011). "Identification of intracellular and plasma membrane calcium channel homologues in pathogenic parasites." PLoS One **6**(10): e26218.

Prommana, P., C. Uthaipibull, C. Wongsombat, S. Kamchonwongpaisan, Y. Yuthavong, E. Knuepfer, A. A. Holder and P. J. Shaw (2013). "Inducible knockdown of Plasmodium gene expression using the glmS ribozyme." PLoS One **8**(8): e73783.

Raabe, A. C., K. Wengelnik, O. Billker and H. J. Vial (2011). "Multiple roles for Plasmodium berghei phosphoinositide-specific phospholipase C in regulating gametocyte activation and differentiation." Cell Microbiol **13**(7): 955-966.

Ranford-Cartwright, L. C., A. Sinha, G. S. Humphreys and J. M. Mwangi (2010). "New synchronization method for Plasmodium falciparum." Malar J **9**: 170.

Recht, J., A. M. Siqueira, W. M. Monteiro, S. M. Herrera, S. Herrera and M. V. G. Lacerda (2017). "Malaria in Brazil, Colombia, Peru and Venezuela: current challenges in malaria control and elimination." Malar J **16**(1): 273.

Reiter, R. J. (1993). "The melatonin rhythm: both a clock and a calendar." Experientia **49**(8): 654-664.

Reppert, S. M. (1997). "Melatonin receptors: molecular biology of a new family of G protein-coupled receptors." J Biol Rhythms **12**(6): 528-531.

Ridley, R. G. (2002). "Medical need, scientific opportunity and the drive for antimalarial drugs." Nature **415**(6872): 686-693.

Rivkees, S. A., R. W. Conron, Jr. and S. M. Reppert (1990). "Solubilization and purification of melatonin receptors from lizard brain." Endocrinology **127**(3): 1206-1214.

Robson, K. J., U. Frevert, I. Reckmann, G. Cowan, J. Beier, I. G. Scragg, K. Takehara, D. H. Bishop, G. Pradel, R. Sinden and et al. (1995). "Thrombospondin-related adhesive protein (TRAP) of Plasmodium falciparum: expression during sporozoite ontogeny and binding to human hepatocytes." EMBO J **14**(16): 3883-3894.

Rodrigues, C. D., M. Hannus, M. Prudencio, C. Martin, L. A. Goncalves, S. Portugal, S. Epiphanio, A. Akinc, P. Hadwiger, K. Jahn-Hofmann, I. Rohl, G. J. van Gemert, J. F. Franetich, A. J. Luty, R. Sauerwein, D. Mazier, V. Koteliansky, H. P. Vornlocher, C. J. Echeverri and M. M. Mota (2008). "Host scavenger receptor SR-BI plays a dual role in the establishment of malaria parasite liver infection." Cell Host Microbe **4**(3): 271-282.

Rodriguez-Naranjo, M. I., M. J. Torija, A. Mas, E. Cantos-Villar and C. Garcia-Parrilla Mdel (2012). "Production of melatonin by Saccharomyces strains under growth and fermentation conditions." J Pineal Res **53**(3): 219-224.

Roopin, M. and O. Levy (2012). "Melatonin distribution reveals clues to its biological significance in basal metazoans." PLoS One **7**(12): e52266.

Santos, J. M., G. Josling, P. Ross, P. Joshi, L. Orchard, T. Campbell, A. Schieler, I. M. Cristea and M. Llinas (2017). "Red Blood Cell Invasion by the Malaria Parasite Is Coordinated by the PfAP2-I Transcription Factor." Cell Host Microbe **21**(6): 731-741 e710.

Schuck, D. C., S. B. Ferreira, L. N. Cruz, D. R. da Rocha, M. S. Moraes, M. Nakabashi, P. J. Rosenthal, V. F. Ferreira and C. R. Garcia (2013). "Biological evaluation of hydroxynaphthoquinones as anti-malarials." Malar J **12**: 234.

Schuck, D. C., R. Y. Ribeiro, A. A. Nery, H. Ulrich and C. R. Garcia (2011). "Flow cytometry as a tool for analyzing changes in Plasmodium falciparum cell cycle following treatment with indol compounds." Cytometry A **79**(11): 959-964.

Sharma, A., I. O. Santos, P. Gaur, V. F. Ferreira, C. R. Garcia and D. R. da Rocha (2013). "Addition of thiols to o-quinone methide: new 2-hydroxy-3-phenylsulfanylmethyl[1,4]naphthoquinones and their activity against the human malaria parasite Plasmodium falciparum (3D7)." Eur J Med Chem **59**: 48-53.

Sibley, L. D., A. Khan, J. W. Ajioka and B. M. Rosenthal (2009). "Genetic diversity of Toxoplasma gondii in animals and humans." Philos Trans R Soc Lond B Biol Sci **364**(1530): 2749-2761.

Silvestri, M. and G. A. Rossi (2013). "Melatonin: its possible role in the management of viral infections--a brief review." Ital J Pediatr **39**: 61.

Sinden, R. E. (1983). "The cell biology of sexual development in plasmodium." Parasitology **86 (Pt 4)**: 7-28.

Singh, S., M. M. Alam, I. Pal-Bhowmick, J. A. Brzostowski and C. E. Chitnis (2010). "Distinct external signals trigger sequential release of apical organelles during erythrocyte invasion by malaria parasites." PLoS Pathog **6**(2): e1000746.

Siqueira, A. M., O. Mesones-Lapouble, P. Marchesini, V. S. Sampaio, P. Brasil, P. L. Tauil, C. J. Fontes, F. T. Costa, C. T. Daniel-Ribeiro, M. V. Lacerda, C. P. Damasceno and A. C. Santelli (2016). "Plasmodium vivax Landscape in Brazil: Scenario and Challenges." Am J Trop Med Hyg **95**(6 Suppl): 87-96.

Smith, J. D., C. E. Chitnis, A. G. Craig, D. J. Roberts, D. E. Hudson-Taylor, D. S. Peterson, R. Pinches, C. I. Newbold and L. H. Miller (1995). "Switches in expression of Plasmodium falciparum var genes correlate with changes in antigenic and cytoadherent phenotypes of infected erythrocytes." Cell **82**(1): 101-110.

Staines, H. M., T. Powell, S. L. Thomas and J. C. Ellory (2004). "Plasmodium falciparum-induced channels." Int J Parasitol **34**(6): 665-673.

Storch, K. F., O. Lipan, I. Leykin, N. Viswanathan, F. C. Davis, W. H. Wong and C. J. Weitz (2002). "Extensive and divergent circadian gene expression in liver and heart." Nature **417**(6884): 78-83.

Sturm, A., R. Amino, C. van de Sand, T. Regen, S. Retzlaff, A. Rennenberg, A. Krueger, J. M. Pollok, R. Menard and V. T. Heussler (2006). "Manipulation of host hepatocytes by the malaria parasite for delivery into liver sinusoids." Science **313**(5791): 1287-1290.

Sugden, D., K. Davidson, K. A. Hough and M. T. Teh (2004). "Melatonin, melatonin receptors and melanophores: a moving story." Pigment Cell Res **17**(5): 454-460.

Sung, J. H., E. H. Cho, M. O. Kim and P. O. Koh (2009). "Identification of proteins differentially expressed by melatonin treatment in cerebral ischemic injury--a proteomics approach." J Pineal Res **46**(3): 300-306.

Taylor, C. J., L. McRobert and D. A. Baker (2008). "Disruption of a Plasmodium falciparum cyclic nucleotide phosphodiesterase gene causes aberrant gametogenesis." Mol Microbiol **69**(1): 110-118.

Tonkin, C. J., G. G. van Dooren, T. P. Spurck, N. S. Struck, R. T. Good, E. Handman, A. F. Cowman and G. I. McFadden (2004). "Localization of organellar proteins in Plasmodium falciparum using a novel set of transfection vectors and a new immunofluorescence fixation method." Mol Biochem Parasitol **137**(1): 13-21.

Tonkin, M. L., M. Roques, M. H. Lamarque, M. Pugniere, D. Douguet, J. Crawford, M. Lebrun and M. J. Boulanger (2011). "Host cell invasion by apicomplexan parasites: insights from the co-structure of AMA1 with a RON2 peptide." Science **333**(6041): 463-467.

Trager, W. and J. B. Jensen (1976). "Human malaria parasites in continuous culture." Science **193**(4254): 673-675.

Udeinya, I. J., J. A. Schmidt, M. Aikawa, L. H. Miller and I. Green (1981). "Falciparum malaria-infected erythrocytes specifically bind to cultured human endothelial cells." Science **213**(4507): 555-557.

Udomsangpetch, R., B. Wahlin, J. Carlson, K. Berzins, M. Torii, M. Aikawa, P. Perlmann and M. Wahlgren (1989). "Plasmodium falciparum-infected erythrocytes form spontaneous erythrocyte rosettes." J Exp Med **169**(5): 1835-1840.

Vaid, A., D. C. Thomas and P. Sharma (2008). "Role of Ca2+/calmodulin-PfPKB signaling pathway in erythrocyte invasion by Plasmodium falciparum." J Biol Chem **283**(9): 5589-5597.

Varotti, F. P., F. H. Beraldo, M. L. Gazarini and C. R. Garcia (2003). "Plasmodium falciparum malaria parasites display a THG-sensitive Ca2+ pool." Cell Calcium **33**(2): 137-144.

Veiga, M. I., S. K. Dhingra, P. P. Henrich, J. Straimer, N. Gnadig, A. C. Uhlemann, R. E. Martin, A. M. Lehane and D. A. Fidock (2016). "Globally prevalent PfMDR1 mutations modulate Plasmodium falciparum susceptibility to artemisinin-based combination therapies." Nat Commun **7**: 11553.

Wassmer, S. C., G. J. Cianciolo, V. Combes and G. E. Grau (2006). "[LMP-420, a new therapeutic approach for cerebral malaria?]." Med Sci (Paris) **22**(4): 343-345.

Way, M., M. Sanders, C. Garcia, J. Sakai and P. Matsudaira (1995). "Sequence and domain organization of scruin, an actin-cross-linking protein in the acrosomal process of Limulus sperm." J Cell Biol **128**(1-2): 51-60.

Weiss, G. E., P. R. Gilson, T. Taechalertpaisarn, W. H. Tham, N. W. de Jong, K. L. Harvey, F. J. Fowkes, P. N. Barlow, J. C. Rayner, G. J. Wright, A. F. Cowman and B. S. Crabb (2015). "Revealing the sequence and resulting cellular morphology of receptor-ligand interactions during Plasmodium falciparum invasion of erythrocytes." PLoS Pathog **11**(2): e1004670.

Wellems, T. E., L. J. Panton, I. Y. Gluzman, V. E. do Rosario, R. W. Gwadz, A. Walker-Jonah and D. J. Krogstad (1990). "Chloroquine resistance not linked to mdr-like genes in a Plasmodium falciparum cross." Nature **345**(6272): 253-255.

White, N. J., S. Pukrittayakamee, T. T. Hien, M. A. Faiz, O. A. Mokuolu and A. M. Dondorp (2014). "Malaria." Lancet **383**(9918): 723-735.

Wurtman, R. J., J. Axelrod and L. S. Phillips (1963). "Melatonin Synthesis in the Pineal Gland: Control by Light." Science **142**(3595): 1071-1073.

Xue, F. and L. Cooley (1993). "kelch encodes a component of intercellular bridges in Drosophila egg chambers." Cell **72**(5): 681-693.

Yeoh, S., R. A. O'Donnell, K. Koussis, A. R. Dluzewski, K. H. Ansell, S. A. Osborne, F. Hackett, C. Withers-Martinez, G. H. Mitchell, L. H. Bannister, J. S. Bryans, C. A. Kettleborough and M. J. Blackman (2007). "Subcellular discharge of a serine protease mediates release of invasive malaria parasites from host erythrocytes." Cell **131**(6): 1072-1083.

APPENDIX